Volume 36 No. 2 | JNSChE Sept/Oct 2021 | ISSN 0794-6759

DOI: 10.51975/EFSD2591

JOURNAL OF THE NIGERIAN SOCIETY OF CHEMICAL ENGINEERS

Published by,
THE NIGERIAN SOCIETY OF CHEMICAL ENGINEERS
National Secretariat: Infinite Grace House, Plot 4, Oyetubo Street,
Off Obafemi Awolowo Way, Ikeja, Lagos State, Nigeria.
E-mail: nationalhqtrs@nsche.org, nsche_headquarters@yahoo.com
Website: https://www.nsche.org.ng; Journal URL: https://journal.nsche.org.ng
Submission of Manuscripts: nschejournal@yahoo.com and copy: stevmomoh@yahoo.com

JOURNAL OF THE NIGERIAN SOCIETY OF CHEMICAL ENGINEERS
A Publication on the Science and Technology of Chemical Engineering

EDITORIAL BOARD

2021 BOARD OF DIRECTORS AND OFFICIALS

INTERNAL AUDITORS

SUBSCRIPTION

a.	**Individual Member**	₦3,000.00
b.	**Overseas Subscribers**	US$100.00
c.	**Institution, Libraries, etc**	₦5,000.00

CHAPTER CHAIRMEN

DOI:10.51975/21360201.som
Journal of the Nigerian Society of Chemical Engineers, 36(2), 2021

OVAT DEGRADATION ANALYSIS OF METHYLENE BLUE USING RICE HUSK ASH (AGRO-WASTE) BASED CATALYST IN SOLAR IRRADIATION

Okeniyi, O.O.[1], Adekunle, O.A[1], Ajayi, O.A[1], Bello, T.K. [1], Okeniyi, S.O.[2] and *Sani, Y.M[1]

[1]Department of Chemical Engineering, Ahmadu Bello University, 870001 Zaria, Nigeria
[2]Department of Chemistry, Nigerian Defence Academy, Kaduna
*Corresponding author Tel.: +234 903 965 4787
e-mail: ymsani@abu.edu.ng; abaa.sumayyaah@gmail.com (Y.M. Sani).
Co-authors: segeaj@gmail.com (O.A. Ajayi), funtookeniyi1@gmail. com (O.O. Okeniyi)
adekunleojo2010@yahoo.com (O.A. Adekunle), tjbello27@gmail.com (T.K. Bello) and
drokeniyisok@gmail.com (S.O. Okeniyi)

ABSTRACT

This study investigated the degradation of methylene blue dye with ZnO-CuO/RHA, a synthesised agro waste-based photocatalyst under solar irradiation at ambient temperature. Preliminary screening of the methylene blue degradation facilitated the selection of the best ZnO-CuO/RHA combination. The photocatalytic degradation was done by taking varying weights of catalyst in 100 mL of dissolved 10-30 ppm MB solutions. The sample was magnetically stirred at 500 rpm in darkness before being exposed to sunlight irradiation. The suspension was magnetically stirred continuously and 5 ml was withdrawn intermittently, centrifuged and analysed with UV-Vis spectrophotometer. The effect of catalyst dosage, initial concentration and irradiation time on the photodegradation were studied using the one-variable-at-a-time method. The result showed that the degradation percentages of the catalyst with 1, 2, 3, 4, and 5 wt. % of RHA were 80.31%, 88.23%, 99.94%, 91.06 % and 81.12% respectively after 180 minutes. These results showed that degradation percentage was directly proportional to the irradiation time up to 3 wt. % thereafter, there was a decline in the percentage degradation. Hence, as the irradiation time increases, there was a significant increase in the degradation of methylene blue dye. ZnO-CuO/RHA catalyst was found to possess a higher photocatalytic activity in the presence of sunlight in comparison to bare ZnO-CuO since using RHA as a base for ZnO-CuO increased the surface area resulting in more active sites under visible light irradiation. ZnO-CuO/RHA may serve as an efficient-photocatalyst for industrial applications with excellent prospects.

Keywords: *Photocatalytic degradation, Sunlight irradiation, One-variable-at-a-time*

1. INTRODUCTION

Industrial and domestic wastewater or effluents generally comprises of pollutants in the form of organic and inorganic materials which should be destroyed or removed before disposal into the environment or water bodies. If untreated, these contaminants are retained in the various water bodies i.e. ground and surface waters and causes lasting and irremediable damages to all forms and aspects of the environment (Gajbhiye, 2012). In recent times, heavy and uncontrolled chemical disposal from different industries are major causes of water pollution. The use of dyes and pigments are prevalent in many industries for imparting color to materials such as paper, textiles, plastics, leather, food and cosmetics industries (Mohabansi *et al.*, 2011). A lot of industries utilize dyes for colour impartation on products and the discharge of the generated wastewater containing dye to the ocean, rivers and streams causes severe hazards due to the toxic nature of the pollutants. This makes the treatment of dye wastewater an important issue in solving environmental problems present today (Katheresan *et al.*, 2018).

Methylene blue (MB) dye with molecular formula $C_{16}H_{18}N_3ClS$ is a heterocyclic aromatic chemical compound with a dark green colour that changes to blue when dissolved in water at ambient temperature. MB is commonly used in industries for dyeing cotton, paper stocks, wood, and silk and in the field of medicine and laboratory science (Viswanathan, 2017). Extreme exposure of humans to methylene blue causes the release of aromatic amines such as benzedrine and methylene which has carcinogenic tendencies, and may lead to vomiting, shock, cyanosis and tissue necrosis. The presence of methylene blue is visible and has effect on aquatic life and the biosphere as a whole due to the

increase in the biochemical oxygen demand (BOD) level (Ehrampoush *et al.,* 2011). It is toxic to aquatic microbiota and humans, as a teratogenic substance and inhibits light penetration needed for photosynthesis. (Amini and Ashrafi, 2016).

There are various methods/techniques available for treating dye effluents (Iracà and Romero, 2017). These methods include "biological, chemical, physical and electrochemical methods" as shown in Figure 1.

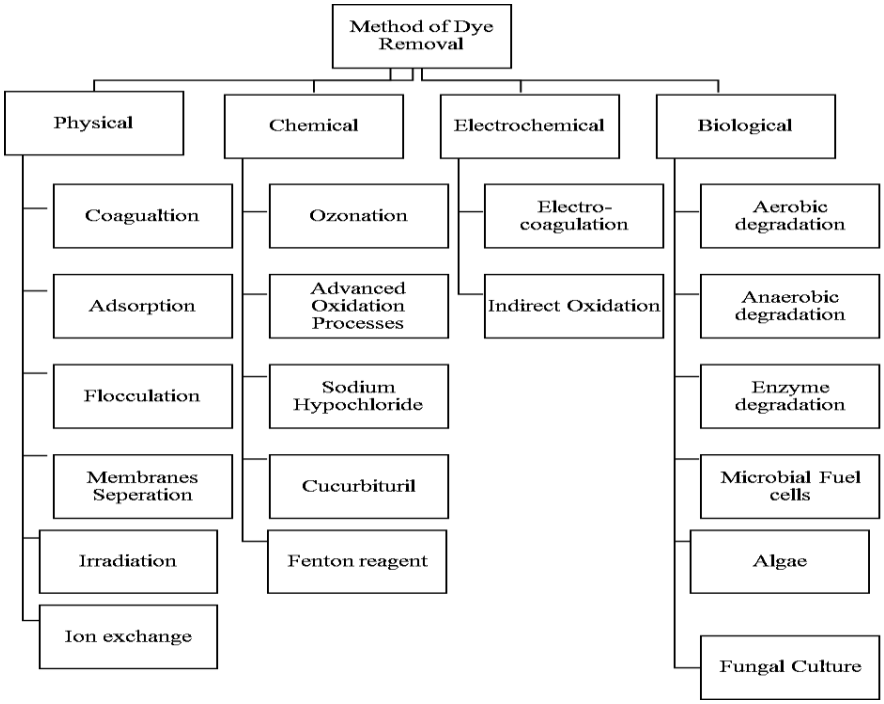

Figure 1: Techniques for waste water treatment (Iracà and Romero, 2017)

Photocatalysis, a technique employed in dye degradation, involves a "catalysis driven light-induced reaction" where the dyes are oxidized or broken down into smaller molecules like water, carbon dioxide, and other mineral byproducts (Mardikar *et. al.,*2018). This reaction takes place under photon or light and thermal condition, where hydroxyl radicals that react with organic material for degradation to occur are generated in the presence of higher oxidation metal ion complexes (Saravanan *et al.*, 2017). The reactions are usually initialized when catalyst absorbs light energy or photons that have a greater energy than the band gap energy from the illumination. The photo-induced electron on the surface of the photocatalyst is transferred from the valence band (VB) to the conduction band (CB), to form hole (h_{VB}^{+}) and electron (e_{CB}^{-}). The general photocatalytic reaction according to Saravanan *et al.,* (2017) is given in Eqn 1 - 10 as;

$$\text{Photocatalyst} + \text{Light Energy} \rightarrow \text{Photocatalyst}\,(e_{CB}^{-} + h_{VB}^{+}) \quad (1)$$

$$\text{Dye} + \text{Photocatalyst}(h_{VB}^{+}) \rightarrow \text{Oxidation process} \quad (2)$$

$$\text{Photocatalyst}\,(h_{VB}^{+}) + H_2O \rightarrow \text{Photocatalyst} + H^{+} + OH^{\bullet} \quad (3)$$

$$\text{Photocatalyst}\,(h_{VB}^{+}) + OH^{-} \rightarrow \text{Photocatalyst} + OH^{\bullet} \quad (4)$$

$$\text{Dye} + \text{Photocatalyst}(e_{CB}^{-}) \rightarrow \text{Reduction process} \quad (5)$$

$$\text{Photocatalyst}\,(e_{CB}^{-}) + O_2 \rightarrow \text{Photocatalyst} + O_2^{\bullet -} \quad (6)$$

$$O_2^{\bullet -} + H^{+} \rightarrow HO_2^{\bullet} \quad (7)$$

$$HO_2^{\bullet} + HO_2^{\bullet} \rightarrow H_2O_2 + O_2 \quad (8)$$

$$H_2O_2 + O_2^{\bullet -} \rightarrow OH^{\bullet} + OH^{-} + O_2 \quad (9)$$

$$\text{Dye} + OH^{\bullet} \rightarrow \text{Degraded products} \quad (10)$$

Sunlight powered photocatalytic degradation has been studied extensively by various researchers with distinct advantages like sustainability, non-toxicity and cost effectiveness (Foletto *et al.,* 2012; Kant, 2012; Das *et al.,* 2018; Mardikar *et al.,* 2018; Villarrubia *et al.,* 2018). However, the process is one in which the efficiency is highly dependent on properties of the catalyst and the photocatalytic reaction conditions. This implies that great attention has to be placed on the catalyst to enhance the photocatalytic performance as optimal composition of the process conditions and material to obtain high degradation percentage are necessary. Rice

husk ash is an agricultural waste which contains high silica content of amorphous silica with a large surface area and serves as a suitable support material for the ZnO-CuO metal oxide. CuO based catalysts are prone to rapid deactivation (Poreddy *et al.*, 2015) which can be avoided by providing a support to aid the distribution of the copper oxide particles (Chang *et al.*, 2003). ZnO possesses a smaller pore volume and surface area leading to low adsorption of organic pollutants in on the catalyst system hence it is important to increase or enlarge the specific surface area and adsorption capacity of the catalyst. The use of semiconductor photocatalyst in the removal of pollutants has the advantage of total decomposition & mineralization without waste generation, a feat not feasible with other treatment methods. However, in order to maximize the catalyst and increase the activity, we set out to apply rice husk ash/ZnO-CuO photocatalyst in degrading MB. There is no known report on use of agro-waste in band gap adjustment to facilitate sunlight degradation or as a component in photocatalyst.

2. EXPERIMENTAL

2.1 Materials

The agro based ZnO-CuO/RHA photocatalyst was synthesised using the modified sol-gel method adopted from Widiarti *et al*, (2017) while methylene blue ($C_{16}H_{18}ClN_3S{\cdot}2H_2O$) dissolved in distilled water was the simulated pollutant evaluated to determine the photocatalytic efficiency of the synthesized catalyst. The sunlight irradiation intensity was measured using the Hukseflux pyranometer software during the photocatalysis experiment at a 1-hour interval and a 752S UV- Vis spectrophotometer was used to measure the absorbance for all experiment.

2.2 Methods

2.2.1 Calibration of UV- spectrophotometer

The spectrophotometer was calibrated in order to determine the peak wavelength of methylene blue. 50 mg/l of methylene blue dye served as the stock solution which was diluted into a serial dilution of 30 mg/l, 25 mg/l, 20 mg/l, 15 mg/l, 10 mg/l, and 5 to 1 mg/l. The blank solution used was distilled water and the wavelength was varied from 450 µm to 700 µm to determine the relevant peak and obtain a standard absorbance - concentration curve.

2.2.2 General procedure for the photocatalytic degradation

The photocatalytic activity of ZnO-CuO/RHA for the degradation of methylene blue was conducted under sunlight irradiation at ambient temperature. The experiment was conducted in a beaker with continuous magnetic stirring at 500 rpm for varying reaction time. The reactants (methylene blue and ZnO-CuO/RHA catalyst) were stirred in darkness for 30 minutes to establish equilibrium for adsorption-desorption between the surface of the photocatalyst and the dye under ambient conditions after which it was exposed to sunlight irradiation with intensity of 78.56 kW/m^2 to aid the photocatalytic degradation. During the experiments 5 ml of the sample was withdrawn from the beaker at a 30 minutes interval and centrifuged at 2500 rpm for 20 minutes to be analysed by a UV-Vis spectrophotometer to obtain final concentration. The same procedure was used for every experiment. The percentage of photocatalytic degradation was calculated using equation 11.

$$Degradation = \left(\frac{C_o - C_t}{C_o}\right) * 100 \quad (11)$$

Where C_0 = Initial concentration of methylene blue
C_t = Final concentration of methylene blue after irradiation.

Figure 2 presents a schematic diagram of the experimental setup used to conduct the Photocatalysis in the presence of sunlight.

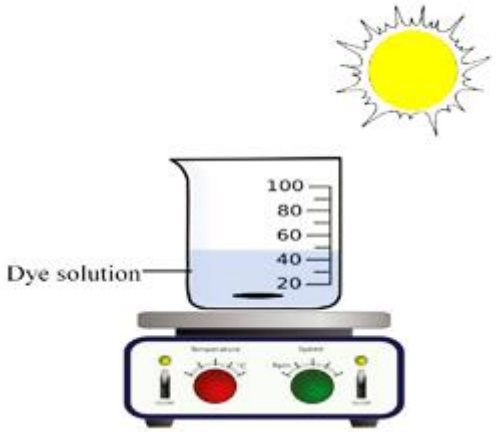

Figure 2: Experimental set up for Photocatalysis

2.2.3 Preliminary screening and Comparative degradation efficiency

The 5 different synthesized ZnO-CuO/RHA catalysts were analyzed under the same conditions of catalyst dosage 0.1 g, in 100 mL of 15 ppm MB concentration for 3 hours (180 minutes) and the catalyst that consistently gave the highest percentage of degradation was selected as the choice catalyst for the process. The photocatalytic degradation was conducted using control catalysts (ZnO, CuO, RHA and a blank sample) to perform a comparative analysis with the selected best catalyst.

2.2.4 Photocatalytic Degradation (One-Variable-at-a-Time)

The catalyst dosage of ZnO-CuO/RHA was varied from 0.1 g to 0.3 g in 100 mL of varied concentration of Methylene blue from 10 to 30 ppm at different time intervals.

To investigate the effect of catalyst dosage, different weights of the ZnO-CuO/RHA photocatalyst varying from 0.05 g- 0.20 g were added to 100 ml of methylene blue dye with dye concentration of 5 ppm. The reaction was done in 270 minutes under sunlight irradiation being magnetically stirred (500 rpm).

For the effect of initial concentration, varied concentrations of MB were used with fixed photocatalyst dosage of 0.2 g at different initial concentration of methylene blue ranging from 5 to 30 mg/l (ppm) as prepared from the stock solution. The effect of time was also observed following these experiments.

3. RESULTS AND DISCUSSION

3.1 Calibration of UV-Spectrophotometer

Figure 3 gives the calibration curve of methylene blue with the maximum absorption peaks wavelength of MB at λ_{max} = 664 um. The spectral absorption curve measurement of dyes during the process of photodegradation is a means providing evidence of the structural changes of dyes and determining reaction rates (Jassim, 2017). As absorptivity is an intrinsic property of dyes, the degradation of the dyes is usually accompanied by a color change (wavelength shift) of the solution hence, the color change was monitored by the UV-Vis spectrophotometer to provide more information about the photodegradation. The decrease in the maximum absorbance of MB dye was observed and a linearly dependent relationship was noted between the absorbance and the concentration of methylene blue.

Figure 3 gives the calibration curve which was used to determine the peak wavelength of the methylene blue solution and the standard curve which is a plot of pollutant concentration versus absorbance used for the determination of dye concentration in the prepared solution at different absorbance value. After each measurement at the peak wavelength, the MB concentration was calculated using the model equation given in figure 3b with R^2 = 0.9971 given as:

y = 0.0619x + 0.11; where y = absorbance and x = concentration

3.2 Preliminary Screening

The photodegradation efficiency of ZnO-CuO/RHA on 15 mg/l of methylene blue having varied weights of rice husk ash (RHA) were analyzed. As shown in figure 4, the degradation percentage of the ZCR catalyst with 1, 2, 3, 4, and 5 wt.% of RHA were obtained to be 80.31%, 88.23%, 99.94%, 91.06 % and 81.12% respectively after 180 minutes. Upon increasing the weight of rice husk ash incorporated into the matrix at 4 grams and 5 grams the degradation efficiency decreased to 91.06% and 81.12% respectively, this may be attributed to the accumulation of RHA on the surface of ZnO-CuO that causes a reduction in the light being penetrated unto the active sites of the photocatalyst. With higher RHA weight, activated molecules are deactivated due to the collision with the molecules in the ground state which dominates the reaction, thereby slowing down the reaction rate and increasing time required for degradation. The photocatalytic activity against irradiation time given in figure 5 shows that the catalysts give a linear relationship with increase in time. Hence, the ZnO-CuO with 3 g of RHA was selected as the best catalyst composition for the photodegradation process.

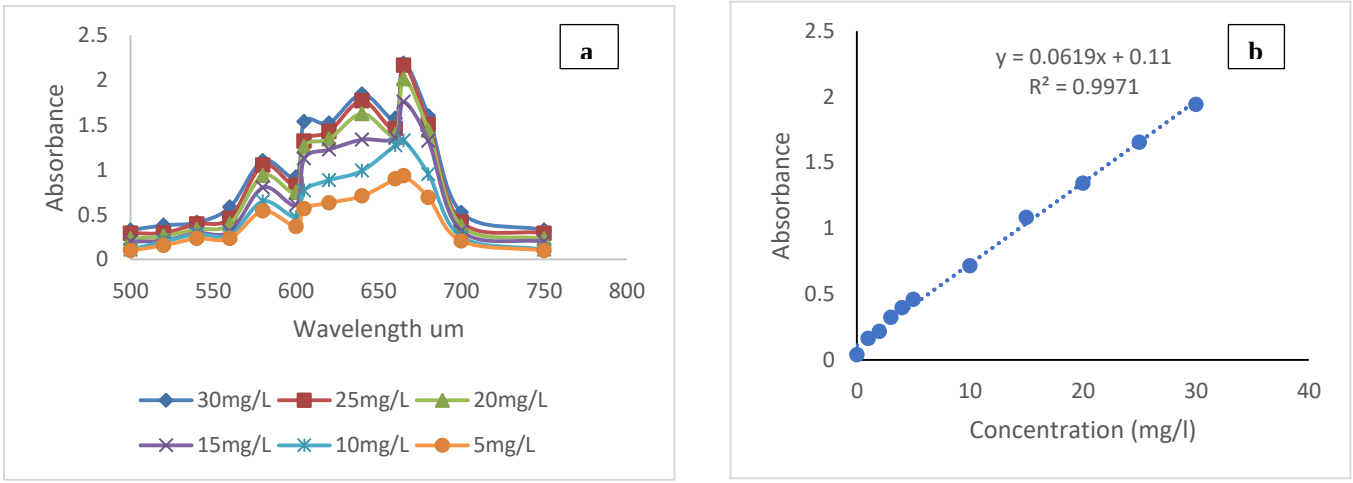

Figure 3: (a) Calibration Curve (b): The Spectrophotometer calibration curve of Methylene Blue dye at λ= 664 um

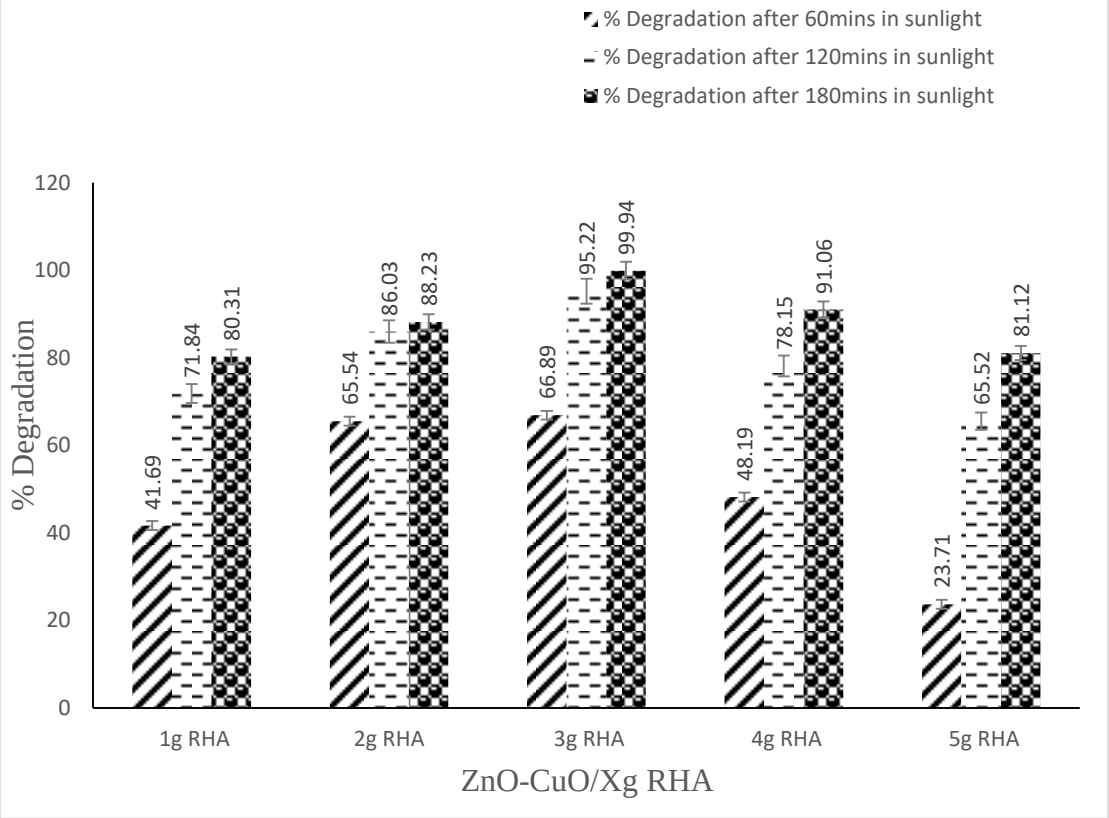

Figure 4: Catalytic activity of different RHA wt. % (ZnO-CuO/RHA) on the photodegradation of MB

3.3 Comparative degradation efficiency

ZnO, CuO, and RHA were tested as a form of control for the process of photocatalytic gradation of MB.

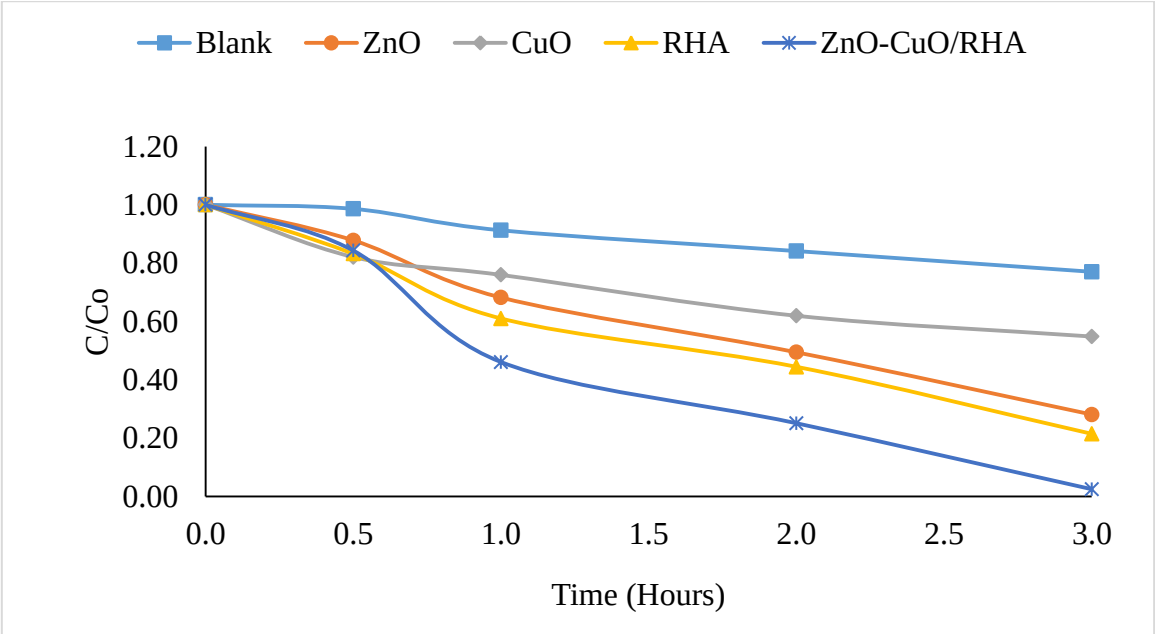

Figure 5a: Plot of concentration ratio versus time using the different catalyst

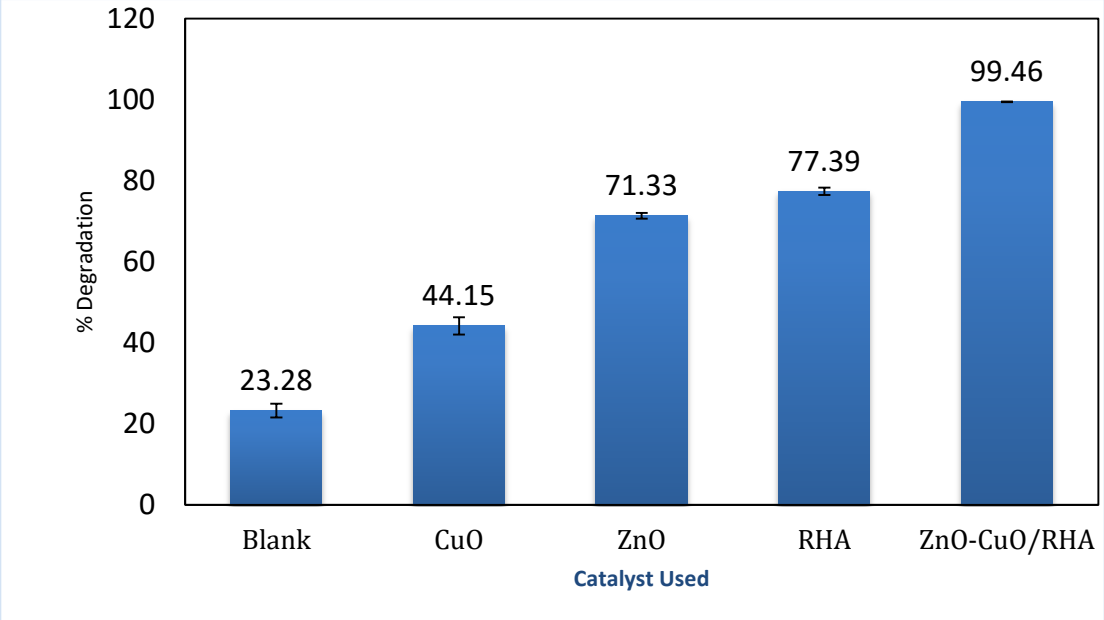

Figure 5b: Photocatalytic Activity of MB using Control Catalyst

The degradation of MB with a blank solution (no catalyst), with ZnO, CuO, RHA and the ZnO-CuO/RHA catalyst was conducted using the same conditions as the preliminary screen and the result is shown in figure 5b to be 23.28%, 44.15%, 71.33%, 77.39% and 99.46 % respectively after 3 hours. From figure 5a, the concentration ratio against time was given and it was observed that there is no remarkable degradation with the blank samples, this is due to the absence of a catalyst. The plot in 5a shows a notable increase in the photocatalytic activity of the synthesized catalyst, this implies that the catalyst synthesized has higher degradation activity for the degradation of methylene blue when compared with the singular control catalyst.

Probable reasons for this is the resultant increase in the surface area of the synthesized catalyst after coupling with rice husk ash an agricultural waste with high surface area Shu-Ting *et al.* (2014) which enables the ZnO-CuO/RHA catalyst to have a more active site leading to faster and higher degradation of the dye. According to Zaman *et al.* (2012) , the reactants that aid degradation of organic dyes includes free radicals like the hydroxyl radicals and super oxide anions generated when hydrogen peroxide (H_2O_2) is broken down. It was observed from figure 5b that the ZnO-CuO/RHA catalysts has higher degradation in the presence of sunlight when compared with zinc oxide, copper (II) oxide and rice husk ash individually, likely due to reduction in bandgap energy levels by tuning the valence bands of ZnO with CuO and the higher surface area of the catalyst.

3.4 Effect of Catalyst Dosage

During the process of photocatalytic degradation, the catalyst dosage or loading is an important factor to determine the cost of the photocatalyst. Figure 6 shows the plot of the percentage degradation with respect to the catalyst dosage to observe the effect of catalyst dosage over time.

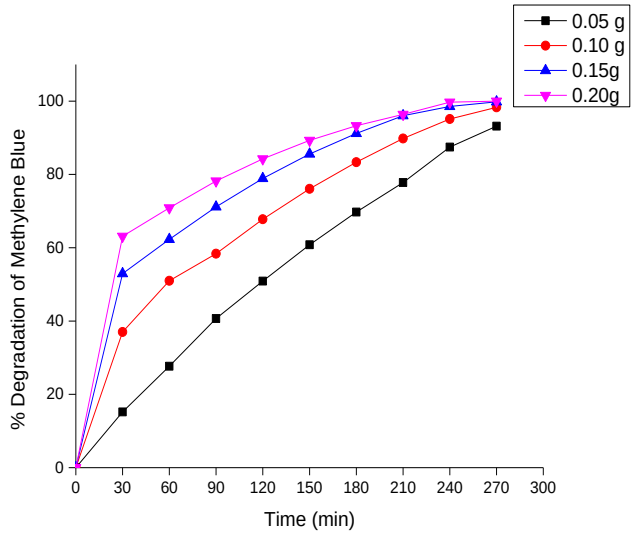

Figure 6: Plot showing the effect of catalyst dosage

A plot of percentage degradation of methylene blue dye for various catalyst dosage against time is given in figure 6. It was observed that an increase in the photocatalyst dosage resulted in an increase in the percentage (%) degradation and rate of reaction as degradation occurred faster as catalyst dosage increases.

As catalyst dosage increased the number of active sites available on the surface of the catalyst also increased. However, it was observed for 0.15 and 0.2 grams that after 240 min there is no significant increase in the degradation. This implies that using a higher catalyst dosage reduces the time required but if it is too high it can lead to ineffective degradation and wasting of resources.

3.5 Effect of Initial Concentration

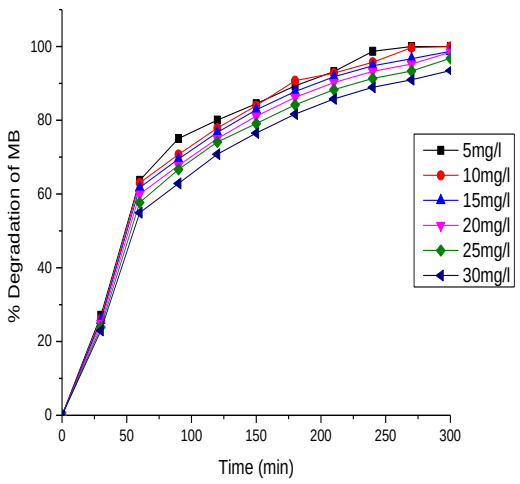

Figure 7: Plot showing the effect of initial concentration

The Photocatalytic degradation of MB solution with an initial concentration of 5 to 30 mg/L resulted in a degradation rate that exceeded 97% at 3 hours, as shown in Figure 7 with the plot of the percentage degradation versus time for different initial concentrations. From this plot a sharp inclination is observed in the first 30 minutes this is because during the process of achieving adsorption-desorption equilibrium in the absence of sunlight, part of the dye was absorbed on the surface of the photocatalyst and as the reaction proceeds, the percentage degradation decreased as initial concentration of the dye increased. As the initial concentration increased, the quantity of reactants and the reaction intermediates adsorbed on the photocatalyst surface increased forming a layer over the surface that leads to reduction in hydroxyl radicals' formation because active sites available for formation of hydroxyl ion reduces as light penetration needed to activate the photocatalyst is reduced (Zhao *et al.*, 2017). The highest % degradation obtained was at 5 mg/l initial concentration of methylene blue because it had the lowest dye concentration. As the initial concentration increased, the photocatalytic efficiency decreased and this is attributed to decrease in solution transmittance which affects photon absorption in the system. The high concentration of methylene blue causes an excessive absorption of dye molecules on the surface of the catalysts.

3.6 Effect of Time

To observe and investigate the effect of time on the photocatalytic degradation process, different concentrations of MB and catalyst dosages were tested and is shown in figure 8.

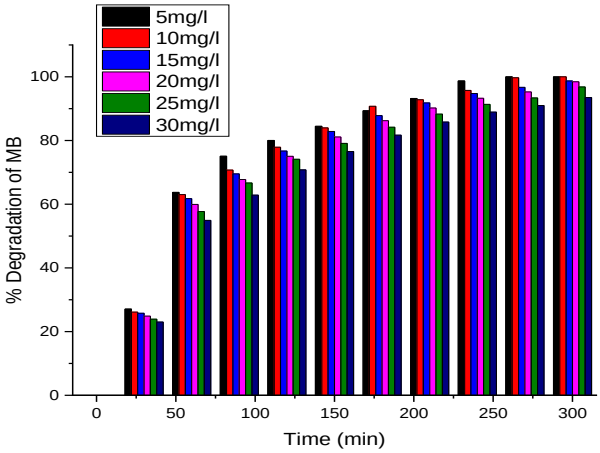

Figure 8: Plot showing the effect of initial concentration

The effect of time on the degradation of different concentration of methylene is given in figure 8 and it was observed that as the reaction time increased, the degradation percentage also increased. For each experiment remarkable increase in degradation percentage was observed as time of reaction increases. This tallies with what was reported by (Bharati *et al.*, 2017; Mardikar *et al.*, 2018) in the photocatalytic degradation of MB and certifies that the time of reaction or exposure to sunlight is directly proportional to the degradation of methylene blue.

4. CONCLUSIONS

The photocatalytic degradation of methylene blue with ZnO-CuO/RHA catalyst was conducted. ZnO-CuO/RHA was found to possess a higher photocatalytic activity when compared with ZnO-CuO. This was premised by the increased surface area that RHA base provided to ZnO-CuO/RHA. This resulted in more active sites under visible light irradiation for high photocatalytic efficiency. The effect of process parameters, dye concentration, catalyst dosage and irradiation time were explored studying one variable at a time. As catalyst dosage increased the number of active

sites available on the surface of the catalyst also increased and a higher catalyst dosage reduces the time required but if it is too high may lead to ineffective degradation and wasting of resources. As concentration increases, the active sites available for formation of hydroxyl ion reduces as light penetration needed to activate the photocatalyst is reduced. The highest % degradation obtained was at 5 mg/l initial concentration of methylene blue because it had the lowest dye concentration. This provided the advantage of determining the percentage linear removal of dye MB as it increases with increasing irradiation time. ZnO-CuO/RHA may be used as an efficient photocatalyst in the treatment of industrial wastewater.

5. REFERENCES

Amini, M. and Ashrafi, M. (2016) 'Photocatalytic degradation of some organic dyes under solar light irradiation using TiO 2 and ZnO nanoparticles', *Nano. Chem. Res*, 1(1), pp. 79–86. doi: 10.7508/ncr.2016.01.010.

Bharati, B. *et al.* (2017) 'Enhanced photocatalytic degradation of dyes under sunlight using biocompatible TiO 2 nanoparticles', *Materials Research Express*, 4(8). doi: 10.1088/2053-1591/aa6a36.

Chang, F. W., Kuo, W. Y. and Lee, K. C. (2003) 'Dehydrogenation of ethanol over copper catalysts on rice husk ash prepared by incipient wetness impregnation', *Applied Catalysis A: General*, 246(2), pp. 253–264. doi: 10.1016/S0926-860X(03)00050-4.

Das, S. *et al.* (2018) 'Sunlight assisted photocatalytic degradation of ciprofloxacin in water using fe doped zno nanoparticles for potential public health applications', *International Journal of Environmental Research and Public Health*, 15(11). doi: 10.3390/ijerph15112440.

Ehrampoush, M. H. *et al.* (2011) *J. Environ. Health. Sci. Eng*.

Foletto, E. L. *et al.* (2012) 'Removal Of Methylene Blue Dye from Textile Simulated Sample Using Tubular Reactor And TiO_2/Uv- Photocatalytic Process,Degradation of leather dye using CeO2-SnO2 nanocomposite as photocatalyst under sunlight', *Water, Air, and Soil Pollution*, 223(9), pp. 5773–5779. doi: 10.1007/s11270-012-1313-3.

Gajbhiye, S. B. (2012) 'Photocatalytic Degradation Study of Methylene Blue Solutions and Its Application to Dye Industry Effluent', *International Journal of Modern Engineering Research (IJMER)*, 2(3), pp. 1204–1208.

H. A. Jassim, A. K. and A. A.-A. (2017) 'Photovoltaic Degradation of Methylene Blue Dye Using CuO Nanoparticles Prepared by SOL-GEL Method', *International Journal of Computation and Applied Sciences IJOCAAS*, 2(2).

Iracà, F. and Romero, M. (2017) *Abstract review on: Current treatment technologies and practical approaches on textile wastewater Dyes Removal*. Available at: www.pantareiwater.com.

Kant, R. (2012) 'Textile dyeing industry an environmental hazard', *Natural Science*, 04(01), pp. 22–26. doi: 10.4236/ns.2012.41004.

Katheresan, V., Kansedo, J. and Lau, S. Y. (2018) 'Efficiency of various recent wastewater dye removal methods: A review', *Journal of Environmental Chemical Engineering*. Elsevier Ltd, pp. 4676–4697. doi: 10.1016/j.jece.2018.06.060.

Mardikar, S. P., Kulkarni, S. and Adhyapak, P. V. (2018) 'Sunlight driven highly efficient degradation of methylene blue by CuO-ZnO nanoflowers', *Journal of Environmental Chemical Engineering*. doi: 10.1016/j.jece.2018.11.033.

Mohabansi, N. P., Patil, V. B. and Yenkie, N. (2011) 'A Comparative Study on Photo Degradation of Methylene Blue Dye Effluent by Advanced Oxidation Process by Using TiO2/ZnO Photocatalyst.', *Rasayan Journal Chem.*, 4(4), pp. 814–819. Available at: http://www.rasayanjournal.com.

Poreddy, R., Engelbrekt, C. and Riisager, A. (2015) 'Copper oxide as efficient catalyst for oxidative dehydrogenation of alcohols with air', *Catalysis Science and Technology*, 5(4), pp. 2467–2477. doi: 10.1039/c4cy01622j.

Saravanan, R., Gracia, F. and Stephen, A. (2017) 'Basic Principles, Mechanism, and Challenges of Photocatalysis', in, pp. 19–40. doi: 10.1007/978-3-319-62446-4_2.

Shu-Ting Liu, Xue-Gang Chen, Ao-Bo Zhang, Kang-Kang Yan, Y. Y. (2014) 'Electromagnetic Performance of Rice Husk Ash', *BioResources*, 9(2), pp. 2328–2340. doi: 10.15376/biores.9.2.2328-2340.

Villarrubia, G. *et al.* (2018) 'Artificial neural networks used in optimization problems', *Neurocomputing*, 272, pp. 10–16. doi: 10.1016/j.neucom.2017.04.075.

Viswanathan, B. (2017) 'Photocatalytic Degradation of

Dyes: An Overview', *Current Catalysis*, 7(2), pp. 99–121. doi: 10.2174/2211544707666171219161846.

Widiarti, N., Sae, J. K. and Wahyuni, S. (2017) 'Synthesis CuO-ZnO nanocomposite and its application as an antibacterial agent', in *IOP Conference Series: Materials Science and Engineering*. Institute of Physics Publishing. doi: 10.1088/1757-899X/172/1/012036.

Zaman, S. *et al.* (2012) 'Efficient catalytic effect of CuO nanostructures on the degradation of organic dyes', *Journal of Physics and Chemistry of Solids*, 73(11), pp. 1320–1325. doi: 10.1016/j.jpcs.2012.07.005.

Zhao, T. *et al.* (2017) 'Photocatalytic degradation of methylene blue solution by diphenylanthrazoline compounds', *Journal of Physical Organic Chemistry*, 30(12), pp. 1–11. doi: 10.1002/poc.3712.

DOI: 10.51975/21360202.som
Journal of the Nigerian Society of Chemical Engineers, 36(2), 2021

THERMAL AND EMISSION CHARACTERISTICS OF CARBONISED AND UNCARBONISED RICE HUSK BRIQUETTE, A COMPARATIVE APPROACH

***Ejikeme, E. M., Enemuo, M.S., and Ejikeme, P.C.N**
Department of Chemical Engineering,
Enugu State University of Science and Technology, Enugu, Nigeria
*ebemoca@yahoo.com

ABSTRACT

Production of briquettes from carbonized and uncarbonized rice husk using a locally fabricated hydraulic press was studied. Proximate and Fourier Transform Infrared Spectroscopy (FTIR) analyses, thermal characteristics, and emission properties of the briquettes were determined. Thermal and emission characteristics were determined in real-time measurements during Water Boiling Test (WBT) using Laboratory Emissions Monitoring System (LEMS) equipment. The burning rates of the uncarbonized and carbonized briquettes were 14.35541g/min and 6.478456g/min respectively. The specific fuel consumptions of the briquettes were 96.5502g/L and 80.12107g/L for uncarbonized and carbonized respectively.The energy consumption rate of uncarbonized briquette was 203.4046KJ/min while that of carbonized was 157.6007KJ/min. It took uncarbonized sample average cooking power of 1.598235KW and 0.543518KW for thecarbonized briquette. High power particulate matter of uncarbonized briquette was 13.20391mg/MJ while that of carbonized was 0.510256mg/MJ. High power carbonmonoxide of uncarbonized and carbonized briquette were 0.443276g/MJ and -0.00964g/MJ respectively. Both briquettes were categorized as tier four in line with the International Workshop Agreement (IWA), International Organization for Standardization (ISO) standard specification for stove testing.

***Keywords**: Briquette, Carbon Monoxide, Carbonization, Cassava Starch, Rice Husk*

1.0. INTRODUCTION

The limitations of fossil fuels and the attendant pollution problems associated with the consequential effect on health have ignited the interest of researchers towards the search for alternative energy resources for domestic and industrial purposes. This search found abundant solutions in the energy benefits of biomass as a renewable energy resource. This choice is large because it is biodegradable, significantly available, environmentally friendly, and sustainable. The need for sustainable energy is rapidly increasing in the world.To this end, renewable energy has been identified as a veritable alternative to fossil fuels in a sustainable and environmentally friendly manner (Chukwueyem etal., 2015). Renewable energy is clean or inexhaustible energy like hydrogen energy and nuclear energy and it can reduce environmental pollution (Siti-Farhana, 2011).It is interesting to note that this biomass is mainly products of agricultural processing activities which may require that they are consigned to agricultural wastes bins, hence constituting environmental pollution. Solving the problem of environmental pollution can be very expensive, cumbersome, and herculean, therefore reducing the occurrence of thorough biomass processing and utilization remains the best available option.

In Nigeria rice husk which is a form of biomass is abundant from rice processing. Disposal of this husk is very difficult and has constituted a lot of environmental problems to the public. During burning a lot of smoke is released to the environment and this can lead to death when inhaled or to an accident due to blurred vision on highways. Other emissions like particulate matter constitute health hazards to the inhabitants. Hence channeling the biomass to useful purposes contributes significantly to the biomass indirect disposal methods. Biomass is the fourth largest source of energy worldwide and provides basic energy requirements for cooking and heating of rural households in developing countries (Bhattacharya and Salam 2002).

The rice husk can be directly applied for energy generation. It can also be modified for the same purpose. However, various techniques have been applied for the biomass modification process and all aimed at improving the energy generation capacity of the biomass and reduce possible thermal emissions from the product. A known form for biomass modification is the production of briquettes. One of the promising technologies by which biomass could be converted to

energy is briquette technology (Oladeji 2011).The biomass that was not useful due to low density was collected and compressed into solid fuel for convenient use and handling.This can be burned in the same way as wood or charcoal(Adekoya 1989); (Ajit etal., 2017). In this way, a briquette can be produced. Briquetting increases the bulk and energy densities of the biomass material, which in turn reduces transport costs. These make it easier for the end-user to handle. Agricultural residues are difficult to handle especially in their raw state because they are bulky and when burnt is very smoky and they also burn very fast (UNEP 2007).There is a remarkable improvement in the combustion characteristics of compressed biomass when compared with the loose one (Husain et.al., 2002).

The densification of biomass materials for energy generation can be achieved through hydraulic compaction of the biomass or a combination of it with an additive for an improved briquette product. These briquettes are used for the generation of energy for domestic uses like cooking and lighting or for industrial uses in generating energy for turbines and heat exchangers. In the course of their use, these briquettes exhibit certain characteristics. Therefore, evaluation of the burning, thermal, and combustion characteristics of these briquettes is considered very imperative and apt. These characteristics define the burning, thermal, and combustion profile of the briquettes and accordingly position them in the purity chart of the briquettes.

The characteristics of the briquettes to be evaluated include but are not limited to the ignition time, boiling time, burning rate, particulate matter, carbon monoxide, and carbon dioxide emissions, and thermal efficiency. These emissions are capable of causing deaths if inhaled in large quantities. The World Health Organization (WHO) estimates that more than 1.5 million people die annually due to smoke from the combustion of solid fuel (WHO 2006).Nigeria experiences one of the highest numbers of smoke-related deaths in the world. It is therefore eloquently important to establish the levels consistent with the produced rice husk briquettes to assign positions to them in the comity of commercially available briquettes through the process of characterization of the briquettes

This study is therefore intended to evaluate the thermal and combustion characteristics of rice husk briquette for purposes of determining their thermal and combustion integrity as a viable alternative for domestic energy supply.

2.0. MATERIALS AND METHOD

All materials used were sourced locally. They include the following:

Risk husk: The rice husk sample was collected from Adani in Uzo-Uwani LGA of Enugu State, Southeast Nigeria.

Cassava starch: Cassava Starch sample which was used as a binder was procured from the Abakpa Nike market in Enugu, Enugu State, South Eastern Nigeria.

2.1. Briquette production method

The Carbonization of the biomass sample was carried out at a temperature of 400^0C using a muffle furnace. After allowing it to cool to room temperature the biomass sample was weighed using a digital weighing balance. The corresponding weight of the binder was also determined with the same weighing balance. The binder mixed with 50ml of water was heated in a heater with a magnetic stirrer until it gelled. Another 50ml of water was added to ensure proper mixing of binder and biomass. The biomass-binder mixture was transferred into the mold of a locally fabricated hydraulic press briquette machine (Figure 1)and compacted to form a briquette. The briquette was removed after 20minutes of dwelling time. After the ejection of the briquette from the mold cavity, it was allowed to dry until a constant weight was achieved.

Figure1. LocallyFabricated Hydraulic Press Briquette Machine

2.2. Proximate analysis of biomass and briquette

The method of Akouwah et al (Akouwah et. al., 2012) was employed for the proximate analysis of the samples

2.3. Determination of Thermal properties

The ignition time, boiling time, burning rate, thermal fuel efficiency, and other emission characteristics of the briquette during combustion were determined in real-time measurements during the Water Boiling Test (WBT) using the Laboratory Emissions Monitoring System(LEMS) equipment (ARC, Oragon U.S.A) set up (Figure2) at the National Stove Eligibility Laboratory in the National Centre for Energy Research and Development (NCERD), University of Nigeria Nsukka (UNN).

Figure 2 Laboratory Emissions Monitoring System (LEMS)

2.4. Water boiling test using LEMS.

A modified Water Boiling Test (WBT) was carried out where a standard stove and standard pot with provision for temperature probe were used and the fuel (briquettes) varied. One liter of water was used. The pot was weighed first after which the pot and water were weighed to determine the weight of water used. The LEMS start-up process was initiated and allowed to acclimatize with the environment.20g of briquette was introduced into the standard stove and lit up. When the ignition was complete, the pot with a measured weight of water was kept on the stove and both immediately lifted into the hood of the LEMS. Real-time monitoring of the briquette combustion process was done by the computer-controlled LEMS and real-time data generated.

2.5. Calorific Value Determination

The calorific value was measured using a bomb calorimeter available at the National Centre for Energy Research and Development, University of Nigeria Nsukka. A standard method was adopted usinga bomb calorimeter (model XRY-1A, make: Shanghai Changji, China)(AOAC 1975). It involves igniting the sample under the influence of high pressure of oxygen gas in an oxygen bomb calorimeter. Consequently, there was a release of very high energy that was absorbed by the surrounding water inside the bomb Calorimeter. The temperature of the water showed great increase and this was used to estimate the energy value of the sample. One gram of the sample was molded into pellets and burnt in the oxygen bomb calorimeter. The calculated heat of combustion represented gross energy.

2.6. Fourier transformed Infrared Spectroscopy (FTIR)

The surface functional groups and structure were studied using Fourier Transform Infrared Spectroscopy [Buck 530 IR] England. The FTIR spectra of the carbonized and uncarbonized samples were scanned at a wavelength of 600–4000nm. This was done at Ahmadu Bello University Zaria.

3.0. RESULTS AND DISCUSSION

3.1. Proximate And Ultimate Analysis

Table 1 shows the results of the proximate and ultimate analysis of uncarbonized rice husk, carbonized rice husk, uncarbonized rice husk briquette, and carbonized rice husk briquette.

Moisture content is one of the main parameters that determine briquette quality (Aina etal., 2009). Briquettes with lower moisture content have higher calorific values (Akowuah etal., 2012). The moisture content of the briquettes produced from both carbonized and uncarbonized rice husks was lower than that of the loose sample. This low moisture content suggested good storability and the combustibility of the briquettes. The volatile matter content of the carbonized briquette was lower than the uncarbonized one. The higher volatile matter content of the uncarbonized one is an indication of the quick ignition period of the briquette and commensurate rise in the length of the produced flame (Deepak and Jnanesh 2015). The carbonized briquette though may not ignite so fast as that of the uncarbonized one but will give out fewer emissions in the course of their combustion. The fixed carbon is high for the carbonized briquettes. Fixed carbon is the percentage of carbon (solid fuel) accessible for char combustion after distilling off volatile matter. It showed that the

carbonized briquette has a higher heating value compared to the uncarbonized one.

Table 1:Proximate and Ultimate Analysis of The Samples

Parameter	UCR	CR	UCRB	CRB
Moisture (%)	8.2	1.3	8.4	2.6
Ash (%)	15.1	6.8	15.8	3.8
Volatile matter (%)	67.0	32.9	65.5	22.5
Fixed carbon (%)	9.7	5.9	20.3	71.1
Bulk density	0.2941	0.462 1	-	-
Carbon (%)	51.0	27.5	60.8	83.0
Hydrogen (%)	5.7	3.0	6.1	4.4
Nitrogen	1.9	2.0	1.7	1.7

Parameter	UCR	CR	UCRB	CRB
(%)				

UCR= Uncarbonized Rice Husk, CR= Carbonized Rice Husk, UCRB= Uncarbonized Rice Husk Briquette, CRB= Carbonized Rice Husk Briquette

3.2. FTIR Analysis

Figures 3 to 5 show the FTIR analysis of the uncarbonized rice husk, carbonized rice husk, and carbonized rice husk briquette. Many peaks present on the uncarbonized rice husk spectrum disappeared on the carbonized spectrum while the remaining ones were weak to a great extent. This is consistent with the breaking of many bonds on the carbonized rice husk leading to the liberation and elimination of volatile species during carbonization. Many bands decreased dramatically indicating the decrease in functionality from the main matrix.

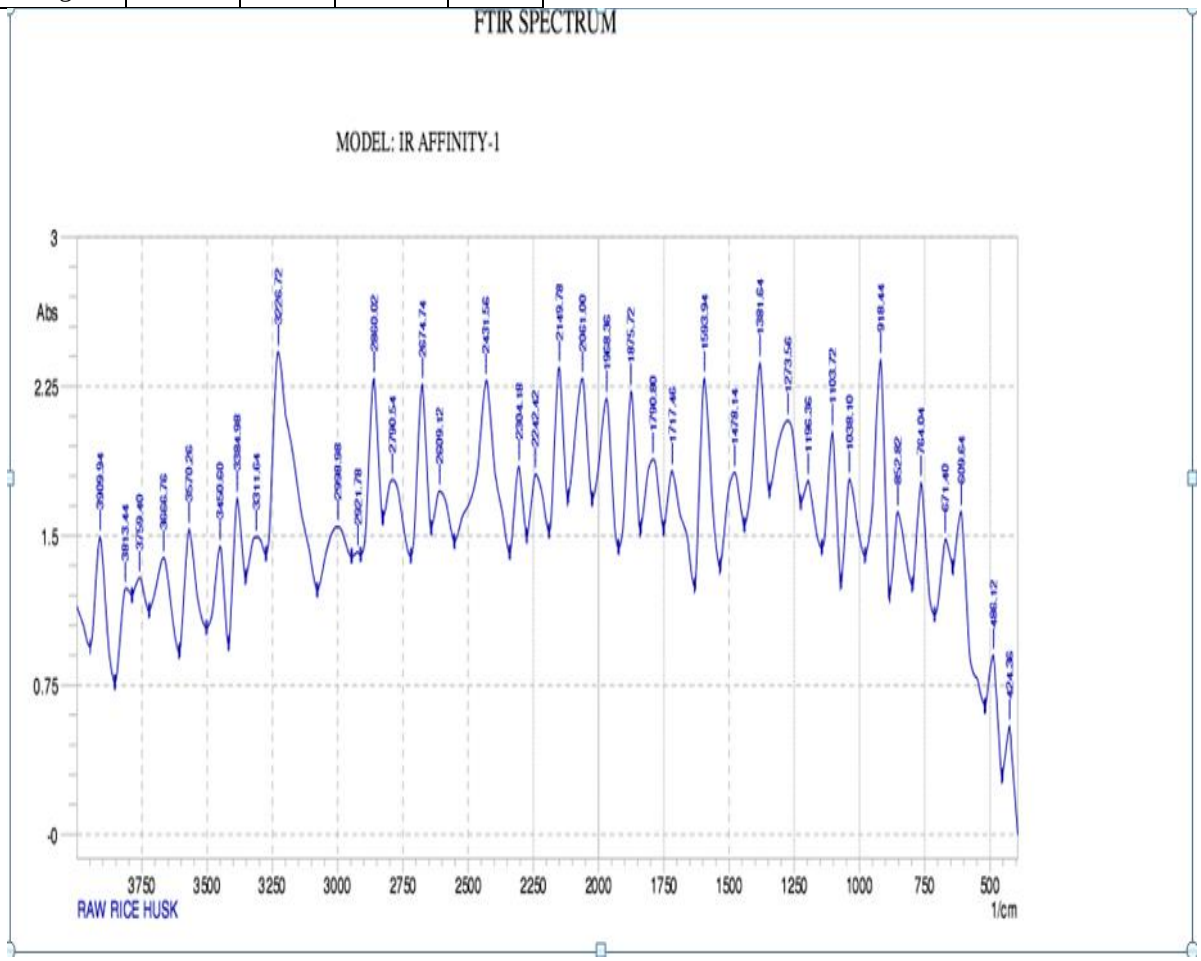

Figure. 3 FTIR of Uncarbonized Rice Husk

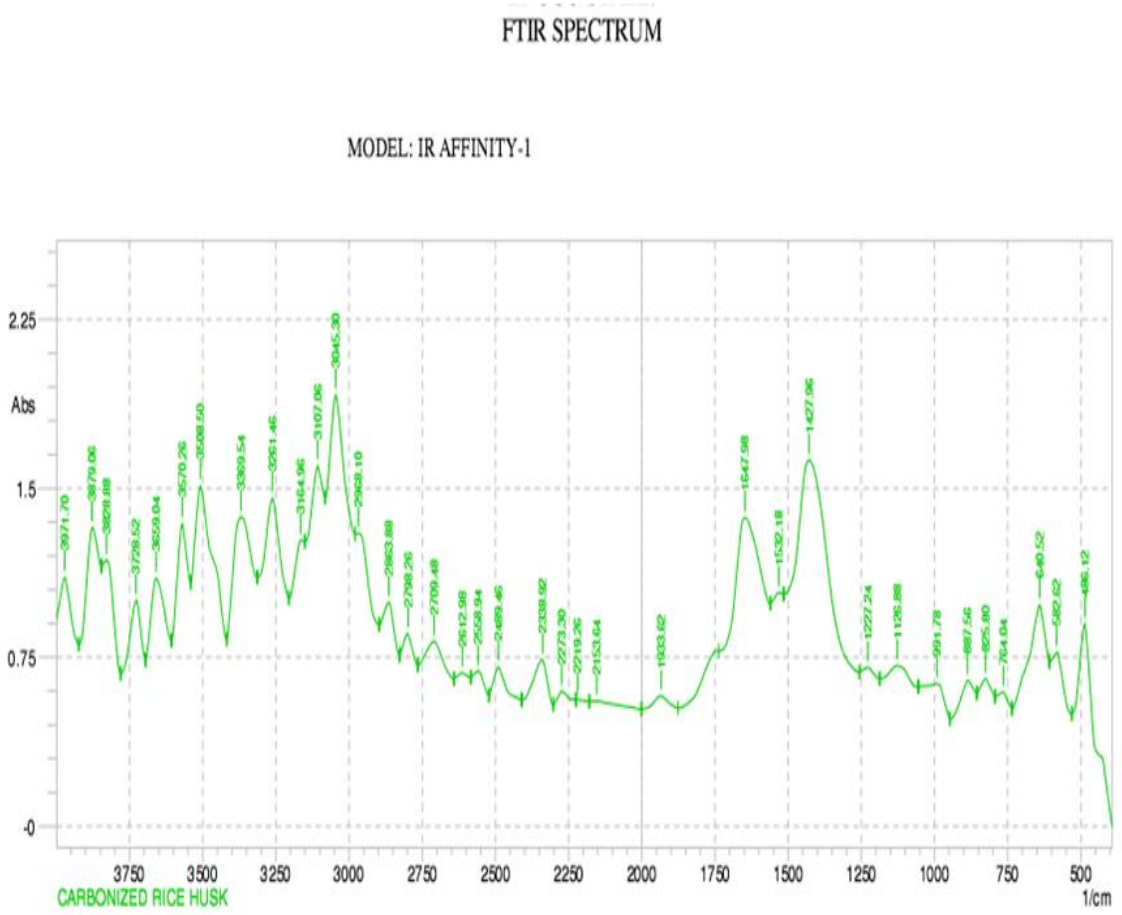

Figure 4. FTIR of Carbonized Rice Husk

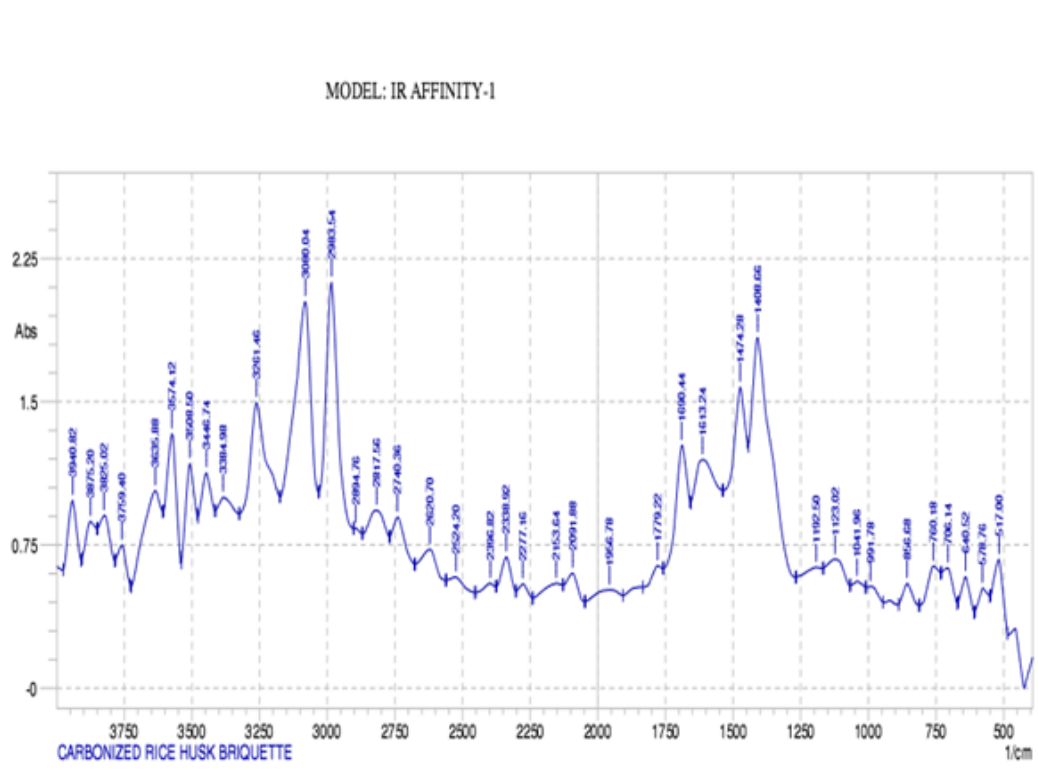

Figure 5. FTIR of Carbonized Rice Husk Briquette

3.3.Briquettes Thermal And Emission Characteristics

Thermal performances and emission characteristics of the briquette produced from carbonized and uncarbonized rice husks were presented in Table 2, while Table 3 shows the IWA ISO standard specification for stove testing(IWA 2012).

Uncarbonized rice husk briquette contains high particulate matter ($PM_{2.5}$) of 13.2039mg/MJ and high carbon monoxide (CO) of 0.4433mg/MJ. The carbonized rice husk briquette showed a significant reduction with particulate matter ($PM_{2.5}$) of 0.5102mg/MJ and carbon monoxide (CO) of -0.00964mg/MJ. This reduction can be attributed to the breaking of many bonds on the carbonized sample leading to the liberation and elimination of volatile species.

It was observed that the thermal efficiency of the briquette produced from the carbonized rice husk increased to 0.46 compared to 0.203 recorded for the uncarbonized rice husk briquette. The Energy consumption rate of the carbonized rice husk briquette was lower than the uncarbonized one. The low carbon monoxide content of the briquette produced from the carbonized rice husk made the briquette to be classified as smokeless one and a substitute for coal briquette concerning environmental pollution. The specific fuel consumption of uncarbonized briquette was 96.5502g/liter compared to 80.12107g/liter for the carbonized one.

Table 2 shows the IWA specification standard for briquette. IWA standard provides a framework for rating cooking stoves against tiers of performance for a series of performance indicators including fuel use (efficiency), total emission, indoor emission, and safety. The higher the tier number, the higher the quality of the briquette produced. From the result, briquette produced from both carbonized and uncarbonized rice husk lied on tier 4. This confirmed that the produced briquettes were of high quality.

The burning rate of the uncarbonized one was 14.35541g/min compared to 6.478456g/min recorded for the carbonized one. The burning rate suggests the quantity of fuel consumed during combustion. It shows that uncarbonized one consumes more fuel than the carbonized sample. It took 12minutes for the uncarbonized rice husk briquette to boil one liter of water compared to 6minutes taken for the carbonized one.

Table2 Thermal Performance of The Briquettes

	Units	**Uncarbonized rice husk briquette**	**Carbonized rice husk briquette**
IWA Performance Metrics			
High Power Thermal Efficiency	%	0.203931	0.462201
High Power CO	g/MJ	0.443276	-0.00964
High Power PM	mg/MJ	13.20391	0.510256
Basic Operation			
Time to boil Pot # 1	Min	12	6
Burning rate	g/min	14.35541	6.478456
Thermal efficiency	%	0.203931	0.462201
Specific fuel consumption	g/liter	96.5502	80.12107
Temp-corrected specific consumption	g/liter	94.65706	78.96294
Firepower	Watts	2626.679	3390.077
Equivalent Dry Fuel Consumed	G	86.13243	77.74147
Energy Consumption			
Temp-Corrected Time to Boil	Min	11.82654	5.882353
Energy Consumption Rate	kJ/min	203.4046	157.6007
Temp-Corr Specific Energy Consumption	kJ/liter	1920.924	1341.215

	Units	Uncarbonized rice husk briquette	Carbonized rice husk briquette
Specific Energy Consumption Rate	MJ/min/L	0.228007	0.162425
Dry Fuel Consumed		87.2355	77.91
Total Energy Consumed	KJ	1895.309	1236.057
Energy Delivered to the Cooking Pot	MJ	0.564083	0.385677
Average Cooking Power	kW	1.598235	0.543518

Figures 6 to 9 show the carbon dioxide, carbon monoxide, and particulate matter emissions at pot temperature and relative humidity during the test for the briquette. Carbon dioxide emission was highest immediately the briquettes were introduced and gradually decreased as the burning time increased. The reduction in carbon dioxide emissions was because the combustion was slowing down. As the combustion was coming to an end, the carbon dioxide increased. Much of the particulate matters were released initially as the burning test started and decreased as time increased.

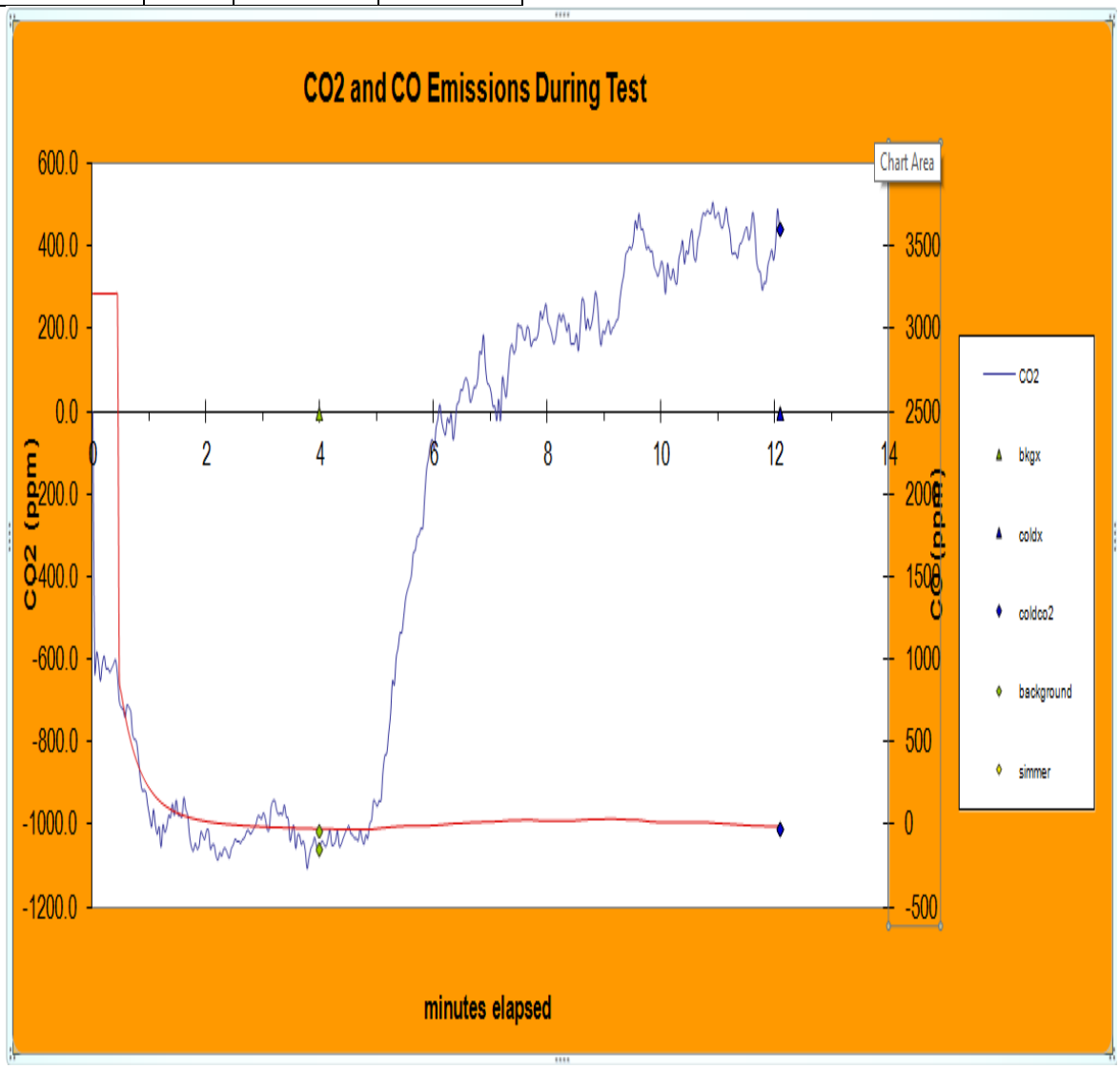

Figure 6 CO_2 and CO Emissions During the Test For Briquettes Produced from Uncarbonized Rice Husk

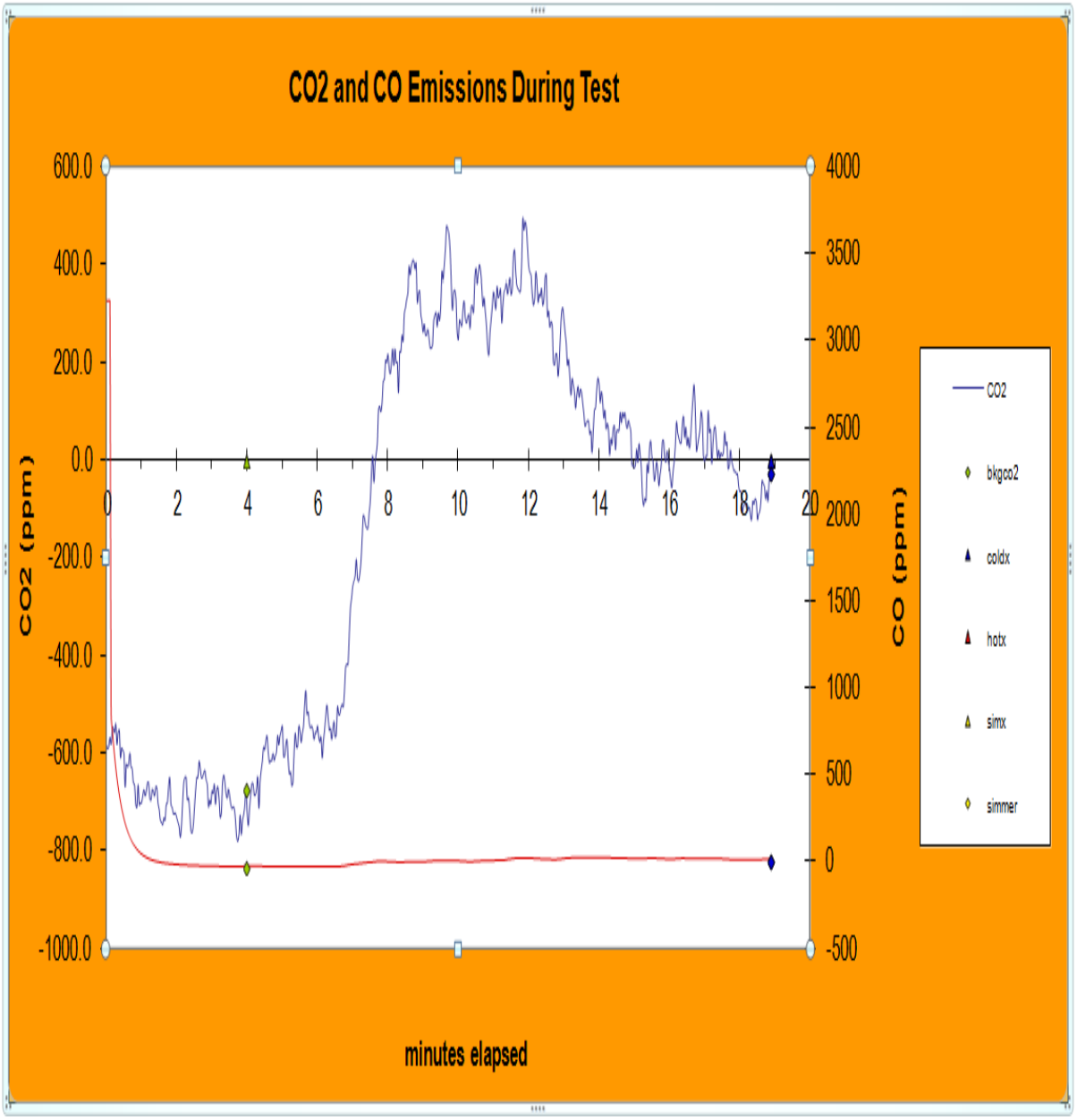

Figure 7 CO_2 and CO Emissions During The Test For Briquettes Produced From Carbonized Rice Husk

DOI: 10.51975/21360202.som
Journal of the Nigerian Society of Chemical Engineers, 36(2), 2021

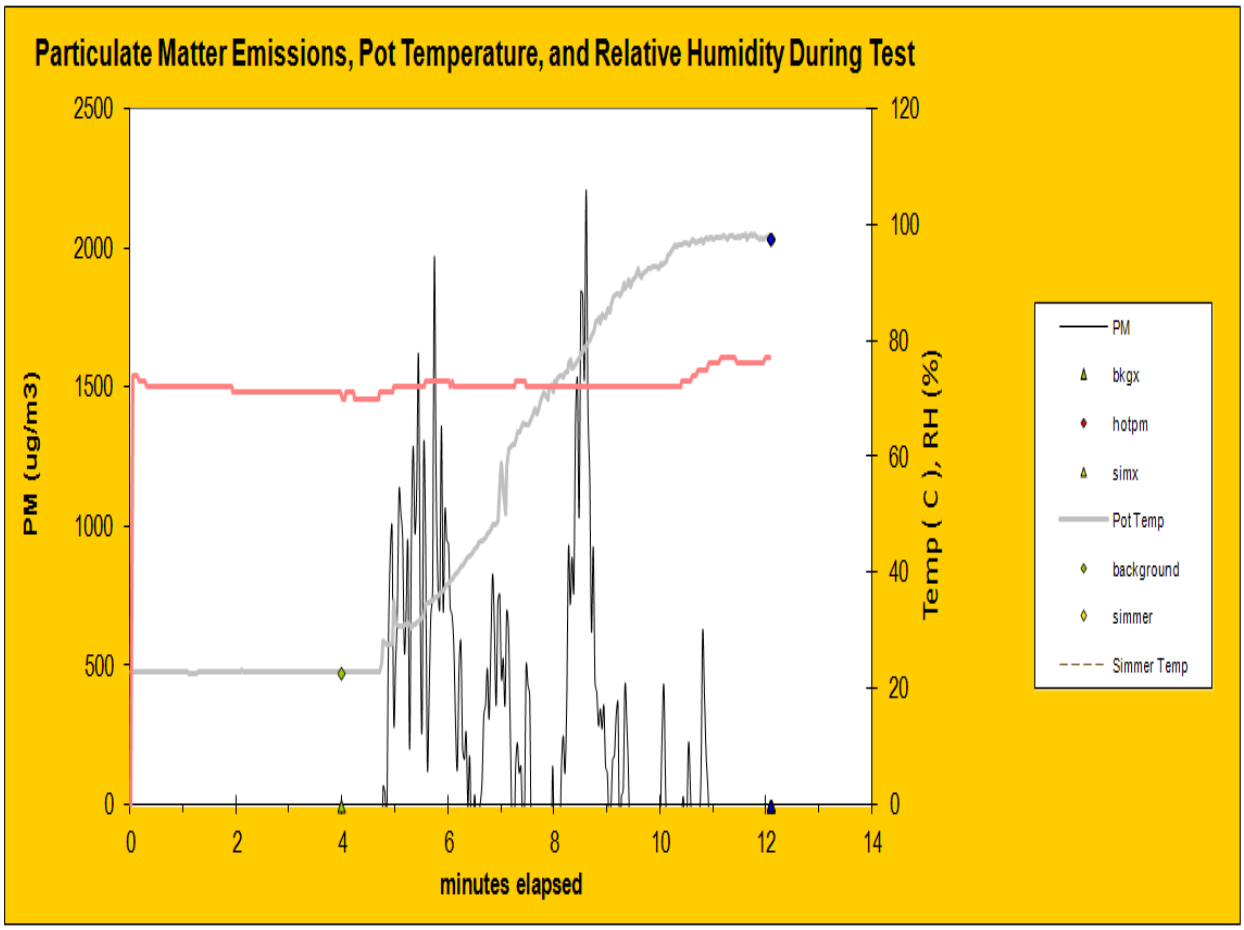

Figure 8 Particulate Matter Emissions, Pot Temperature, and Relative Humidity During the Test for Briquettes Produced from Uncarbonized Rice Husk

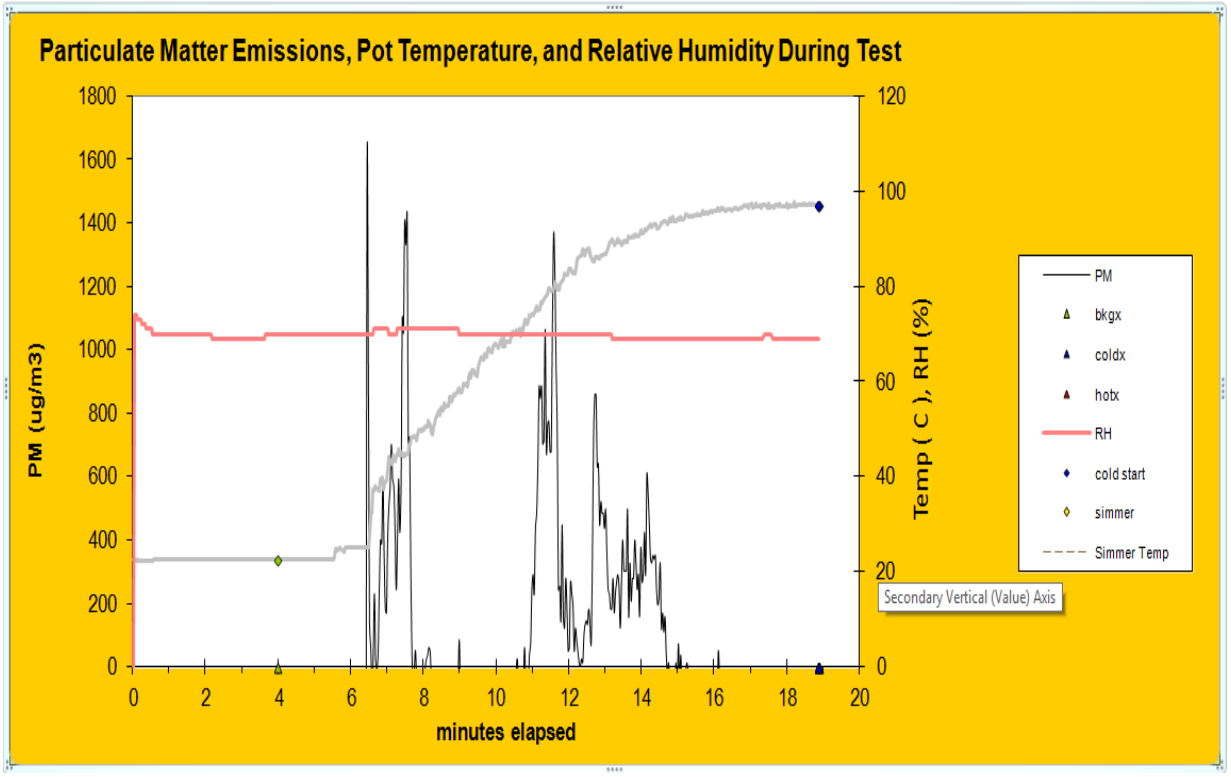

Figure 9 Particulate Matter Emissions, Pot Temperature, and Relative Humidity during the Test for Briquettes Produced from Carbonized Rice Husk

TABLE 3: IWA VITA WBT Ties_2012 Specification for stove testing

IWA VITA WBT Tiers	Units	Tier0	Tier 1	Tier 2	Tier 3	Tier 4
High Power Thermal Efficiency	%	<0.15	≥0.15	≥0.25	≥0.35	≥0.45
Low Power Specific Consumption	MJ/min/L	>0.05	≤0.05	≤0.039	≤0.028	≤0.017
High Power CO	g/MJ	>16	≤16	≤11	≤9	≤8
Low Power CO	g/min/L	>0.2	≤0.2	≤0.13	≤0.1	≤0.09
High Power PM	mg/MJd	>979	≤979	≤386	≤168	≤41
Low Power PM	mg/min/L	>8	≤8	≤4	≤2	≤1
Indoor Emissions CO	g/min	>0.97	≤0.97	≤0.62	≤0.49	≤0.42
Indoor Emissions PM	mg/min	>40	≤40	≤17	≤8	≤2
Safety	Index	<45	≥45	≥75	≥88	≥95

4.0 CONCLUSION

Briquettes were produced from carbonized and uncarbonized rice husk using a locally fabricated hydraulic press. The carbonized briquettes showed better proximate properties than the uncarbonized ones. The thermal properties of the briquettes improved due to the carbonization of rice husk before briquette production. Carbon monoxide emissions of the briquette equally reduced as a result of carbonization. The briquette was found smokeless due to the low carbon monoxide content and a great substitute for coal briquette concerning environmental pollution. Both briquettes were classified under tier four according to the IWA specification standard for briquette. This confirmed the produced briquettes of high quality.

REFERENCES

AjitKaur, M. R., and Krishnendu, K (2017) Densification of Biomass by Briquetting: A Review. *International Journal of Recent Scientific Research* . 2017; Vol8,10 : 20561-20568

Aina, O.M.,Adetognu, A.C., and Iyiola, K A (2009).Heat energy from value-added sawdust briquettes of Albiziazygia.*Ethiopian Journal of Environmental Studies and Management*; 2009; Vol 2,1pp.42-49.

Akowuah, J.O., Kamaushuir, F.,and Miotchual, S.J.(2012).Physico-chemical characteristics and market potential of sawdust charcoal briquette. *International Journal of Energy and Environmental Engineering;* 2012; Vol 3, 20 pp1-6

A.O.A.C. (1975).Official Methods of Analysis, 12th edition, Association of Officials Analytical Chemist, Washington DC; 1975.

Bhattacharya, S.C., and Salam, P.A. (2002). Low greenhouse gas biomass option for cooking in the developing countries, *Biomass and Bio-Energy*, 2002: Vol 22, pp305-317.

Chukwueyem, S.R., Adeniyi, O.A., Williams, J.K., Magnus, O.A., Peter, D.G., Margaret, J.H., Ibrahim, A.U., and Emeka, R.O., (2015). Analysis of energy market conditions in Nigeria. Central Bank of Nigeria (Occasional Paper No. 55), 2015.

Deepak, K.B., Jnanesh, N.A.(2015).Biomass Briquettes- A renewable source of clean energy. *The International reviewer* 2015; Vol 2,2 pp 27-30

Husain, Z.,Zainac, Z., Abdullah, Z. (2002). Briquetting of palm fiber and shell from the processing of palm nuts to palm oil. *Biomass and Bioenergy*, 2002; Vol22: pp505-509

International Workshop Agreement (IWA) (2012). ISO Standard Specification for stove testing 2012

Oladeji, J.T. (2011). Comparative fuel characterization of Briquettes produced from two species of corncob, *Researcher*; 2011,Vol3,4.

Siti-Farhana,B. (2011).To study the production viability of Bio-Briquette from oil palm decanter cake, Faculty of Chemical and Natural Resources University Malaysia Pahang, 2011.

UNEP. (2007). Converting Waste Agricultural Biomass into a Resource.Compendium of Technologies.United Nations Environmental Programme.Division of Technology, Industry, and Economics International Environmental Technology Center Osaka/Shiga, Japan, 2007.

World Health Organisation.(2006) .Fuel for life, household Energy and Health. 20 Avenue Appia, 1211 Geneva 27 Switzerland, 2006

DOI.10.51975/21360203.som
Journal of the Nigerian Society of Chemical Engineers, 36(2), 2021

INVESTIGATION OF QUALITATIVE PARAMETERS IN SOAP PRODUCED FROM BLEND OF NEEM AND CASTOR OIL

[*]Usman, A.H. and Mukhtar, B.
Department of Chemical Engineering, Ahmadu Bello University, Zaria.
[*]Corresponding author, e-mail: ahusman@abu.edu.ng and ahusman2016@gmail.com

ABSTRACT

Soap is a chemical compound formed by interaction of fatty acids and metal radicals. Different types of vegetable oils have been found to be good candidates for soap production due to their saponifiable nature. However, edible oils are often expensive to use for soap production due to competing demand between commercial and domestic buyers. So, in this work, blend of nonedible neem and castor oils were used at different proportions to produce various soap samples. The foregoing was achieved via the two well-known processes of soap production, that is; the hot and cold processes. The work investigated the parameters that influence the quality of soap and determined their optimum values using various blends of the oils. Six samples were produced, and their properties analyzed and compared with two commercial samples to determine a blend with the most desirable qualities. The yield, foamability, pH, hardness and cleansing power of the produced soap samples were determined. It was found that the blend of 60 ml neem oil and 40 ml castor oil was the best with a yield of 70.4%, foamability of 11.8 cm, pH of 10.42 and a high cleansing power. The results were found to be consistent with those of the two commercial samples used as controls.

Keywords: *Castor, cleansing power, foamability, hardness, neem, oil, soap samples*

1.0 INTRODUCTION

There are several ways of describing what a soap is; it can be regarded as any cleansing agent that is produced in different forms such as bars, granules, and liquid (Warra, 2013). However, in simple chemistry terms, soap is a chemical compound formed from saponification reaction of fatty acid components of vegetable oils and/or animal fats with alkalis. The reaction involves splitting of esters into alcohol and sodium or potassium salts of fatty acids (Hassan *et al.*, 2015). Although the sodium and/or potassium-based soaps are the commonly used cleaning agents and formed the basis of this work, it is worth mentioning that there are other forms which are exclusively used for other purposes. These include aluminum, calcium, chromium and magnesium-based soaps. They are insoluble soaps that are utilizable as lubricants, thickeners of oils and paper sizing (Warra, 2013).

Mak-Mensah and Firempong (2011) studied the chemical properties of neem oil-based toilet soap. They found that the produced soap showed good medicinal characteristics that makes neem oil an ideal substitute to the edible palm oil for soap production. Ameh *et al*. (2013) produced and characterized antiseptic soap using the blend of neem and shea butter oils at various proportions. They analyzed such properties as foamability, hardness, pH as well as the antibacterial properties of the produced soaps and reported that the properties agree closely with commercial samples from other sources. The consistency of their results indicates that the neem oil can act as a raw material for soap manufacturing. Similarly, Hassan *et al.* (2015) utilized a blend of neem and *Acacia nilotica* seed oils to produce soap. The researchers extracted the oils from the seeds by Soxhlet extraction method before producing their samples. Based on the oil yields and chemical analysis reported, they contended that the neem and *Acacia nilotica* seed oils are good sources of fatty acids for commercial purposes especially in soaps production. Moreover, other studies revealed medicinal benefits of employing neem oil for antiseptic soap production. It has been reported that neem oil-based soaps are capable of healing diseases like eczema (Schimutterer and Ascher, 1986). The neem extracts also find applications in other areas such as insect antifeedants, growth disruption, (Alfred and Patrick, 1985; Warra, 2009), anti-inflammatory uses (Schimutterer and Ascher, 1986, Ameh *et al*., 2013), and highly bactericidal in nature (Upadhyay *et al.*, 2010).

Castor oil on the other hand is a naturally occurring and environmentally friendly oil obtained from a plant seed

called *Ricinus communis*. It is usually extracted by mechanical pressing or solvent extraction techniques. Although the castor seed oil is believed to have a wide range of applications which includes biodiesel production (Ndana, *et al.,* 2011), its main use is in soap production, lubricants and coatings manufacturing (Patel *et al.,* 2016). Despite being found to be a promising raw material for production of soap, castor oil may not necessarily give requisite physicochemical properties when singly used. The foregoing could be because castor oil contains various carboxylic acid groups (Mishra, 2009) which may in turn give varying physicochemical characteristics. Some researchers have demonstrated the applicability of the castor oil as a raw material in soap and detergents synthesis. One of such studies was conducted by Mishra (2009). The researcher carried out a study that involves the use of the castor oil as a blending stock with other types of oils to produce different soap samples. The work focused on the analysis of the properties of soap produced by both single and blends of various oils at varying ratios. The results showed that castor oil is a good source of fatty acid for saponification reaction, and it produced a soap with a high cleansing power and lathering ability. However, because of its varying chemical composition, castor oil-based soaps are usually soft in nature. Therefore, to achieve desirable physicochemical properties, it should be used as a blend with other oils.

Even though the study by Mishra (2009) and a host of other works available in published literature have been able to utilize different blends of other oils to produce soaps and detergents, there has been little attention on the use of the blend of castor and neem oil. Most of the published literature focused on other uses of these oils such as biodiesel production. Hence, this work was aimed at using the blends of the castor and neem oils to produce and determine a soap sample with best quality parameters. The choice of the aforementioned oils was informed by the fact that they are nonedible, available, less expensive, and have favorable medicinal properties for soap synthesis.

2.0 MATERIALS AND METHODOLOGY

The materials and equipment used in this work are shown in Table 1.

Table 1: Materials and equipment

Materials	Equipment
Neem oil	Liquid-in-glass thermometer
Castor oil	pH meter (Kent EIL 7055)
Sodium hydroxide	Round bottom flask
Distilled water	Weighing balance (MT-501)
Perfume	Stirring rod
Phenolphthalein	Beaker

2.1 Preparation of the soap samples

To prepare the soap samples, a blend of oil containing 60 ml of neem oil and 40 ml of castor oil was measured and transferred into a container. The content was then heated to 50 ^{o}C to increase the saponification rate between the alkali and the oil (hot process). A calculated amount of NaOH was weighed and added to a fixed amount of distilled water to form a solution (Mak-Mensah and Firempong, 2011). The prepared solution was then poured gently to the heated oil blend and stirred gently in one direction to ensure thorough mixing of the solution. The soap was then poured into a soap mold and allowed to cool for 24 hours. The produced soap was then weighed. The procedure was used to prepare different soap samples with varying blending ratios. Also, for the cold process, a similar procedure was adopted except that the process was allowed to take place at room temperature.

Amount of sodium hydroxide pellets required was determined as follows (Mishra, (2009)):

Amount of NaOH = Amount of oil x saponification value of oil.

Amount of distilled water = Amount of oil x 0.3

Calculation of Yield:

For all the soap samples prepared using different blends of the oils, the weight was measured for the dried samples. Yield was calculated by dividing the weight of

the soap by the weight of the raw materials used. The soap samples produced were analyzed and compared with the commercial samples by determining their properties.

2.2 Determination of foamability and pH

One (1) g of the soap sample was dissolved into a 50 ml of water in a 250 ml measuring cylinder and was shaken vigorously for 2 minutes. Then the height of the foam was monitored and recorded after 4 minutes. This procedure was repeated for the various soap samples. It was also done for the two commercial samples obtained from the market (Hassan *et al. 2015*).

In order to measure the pH, one 1 g of the produced soap was dissolved in 10 ml distilled water and the pH of the solution was determined using a pH meter. This procedure was repeated for the soap samples produced at various blends and also for the commercial samples (Ameh *et al*. 2013).

2.3 Determination of cleansing power and hardness

To determine the cleaning property of the prepared soaps, a drop of oil was placed on four separate strips of filter paper. The filter papers with the oil spot were immersed in separate test tubes containing soap solutions. Each was shaken vigorously for 1 minute after which the filter papers were removed and rinsed with distilled water and the degree of cleanliness in each filter paper was visually observed. The procedure was repeated for commercial samples to compare the cleanliness of the prepared soap and that of the commercial sample.

For the hardness test, a method reported by (Ameh *et al*. 2013) was adopted. In the method, a soap sample was placed on top of a flat table and a hardness needle with a load attached to the top was placed gently on top of the soap vertically (with the pointed end on top of the soap). The depth by which the needle goes into the soap was marked and measured with a transparent ruler. It was then recorded. The procedure was repeated for all the samples produced and the commercial samples.

3.0 RESULTS AND DISCUSSION

Table 2 gives the properties of the commercial soap samples (Control 1 and Control 2) used as standards for comparison with the results obtained in this work.

Table 2: Properties of the commercial samples

Samples	pH	Foamability(cm)	Cleansing power	Hardness
Control 1	9.48	12.3	Very good	Very Hard
Control 2	10.7	12.0	Good	Very Hard

3.1 Foamability test results of the produced soap samples

Table 3 presents the result of the foamability test carried out on the produced soap samples using both the cold and hot process methods.

Table 3: Foamabilities of the produced soap samples

	Hot process	Cold process
Samples	Foamability(cm)	Foamability(cm)
50ml Neem+50ml Castor	10.7	10.8
60ml Neem+40ml Castor	11.8	11.6
70ml Neem+30ml Castor	11.0	11.9

From Table 3, it can be seen for the hot process the soap sample containing 60 ml neem oil and 40 ml castor oil had the highest foamability followed by a sample containing 70 ml neem and 30 ml castor oil, with the sample containing equal proportion of neem and castor having lowest foamability. However, for the samples produced via cold process, a proportion of 70 ml neem and 30 ml castor oil gave soap with the highest foamability followed by sample containing 60 ml neem and 40 ml castor oil with the sample of equal proportions having the lowest value.

The foamabilities of the soaps can considerably be compared with those of the two commercial samples: control 1 and control 2. It can be observed that though the foamability of the blend containing 70 ml neem and 30 ml castor oil produced via cold process exceeded that of control 2, however, its foam stability (time duration of the foam) was observed to be lesser than that of the commercial sample. Usually, the efficiency of a soap is assessed through the amount and stability of its foam. Thus: the soap obtained from a blend of 70 ml neem and 30 ml castor produced via cold process can ideally be considered to have a higher efficiency. However, the foam produced by this sample was seen to persist for a shorter period compared to that of 60 ml neem and 40 ml castor produced via the hot process, thereby making it less desirable. Also, even though the foamabilities of the soaps produced via the different methods appeared to be similar, the foams from the samples produced via the hot process showed higher stability.

The observed variability in the foamabilities of the soaps could also be ascribed to the difference in the fatty acids content of the utilized oils in the formulation. Phanseil, 1998 reported that, saturated fatty acids such as lauric and myristic acids produce soaps with fluffy lather and high cleansing power. Therefore, the difference in fatty acid composition in the castor and neem oils could be the factor that contributed to the observed contrast in the lathering ability.

3.2 pH value

Table 4 shows the pH values of the various soap samples produced from both the hot and cold processes.

Table 4: pH values of the produced soap samples

	Hot process	Cold process
Samples	**pH**	**pH**
50ml Neem+50ml Castor	10.20	10.58
60ml Neem+40ml Castor	10.42	11.00
70ml Neem+30ml Castor	10.62	11.54

Based on the results in Table 4, it can be noted that the sample containing 70 ml neem and 30 ml castor oil produced via cold process have the highest pH value of 11.54 while that with equal proportions of the oils showed a lowest pH of 10.58. The blend of 60 ml neem and 40 ml castor oil showed an intermediate value of 11.0. For the hot process, the sample with 50 ml neem and 50 ml castor oils had the lowest pH and that of 70 ml neem and 30 ml castor had the highest value. The variation in the pH values was likely due to the improper or incomplete saponification process which could possibly be overcome either by super fatting or using less amount of caustic soda solution. It is however, necessary to control the pH since a high pH value can be detrimental to the skin especially for toilet soap. A pH value within the range of 9-11 is usually acceptable for laundry soap (Mak-Mensah and Firempong, 2011; Onyango *et al*, 2014). Thus, except for the sample with 70 ml neem and 30 ml castor oils produced via cold process, the pH values of the other samples analyzed fall within the permissible range.

3.3 Yield

Table 5 gives the yield of the produced soap samples.

Table 5: Yield of the produced soap samples

	Hot process	Cold process
Samples	Yield (%)	Yield (%)
50ml Neem+50ml Castor	66.0	63.8
60ml Neem+40ml Castor	70.4	69.5
70ml Neem+30ml Castor	67.5	70.9

From Table 5 it can be seen that for the hot process, the soap sample containing 60 ml neem and 40 ml castor had the highest yield while the sample with equal proportion of the oils had the lowest yield. The cold process on the other hand, gave near-equal yields for both the samples with 60 ml neem, 40 ml castor and that of 70 ml neem and 30 ml castor oil. The difference in the yields among the various samples may be attributed to the type of oil used. This is perhaps because the yield of soap depends on the type of oil used and on the

carboxylic acid and base that make up the soap. Evaluating the yield is pertinent because the higher the yield the more economical is the process (Mishra, 2009).

3.4 Hardness and cleansing power

Table 6 gives the hardness and cleansing power of the various soap samples produced from the different blends of the neem and castor oils.

Table 6: Hardness and cleansing power of the soap samples produced

	Hot process	
Samples	Hardness	Cleansing power
50ml Neem+50ml Castor	Relatively hard	Good
60ml Neem+40ml Castor	Hard	Very good
70ml Neem+30ml Castor	Very hard	Good
	Cold process	
50ml Neem+50ml Castor	Soft	Good
60ml Neem+40ml Castor	Hard	Good
70ml Neem+30ml Castor	Hard	Good

Castor oil when used alone to produce soap usually gives a soft soap. However, when blended with a neem oil which is usually hard gives a soap with good hardness feel. It can be observed from Table 6 that for both hot and cold processes, the hardness of the soap samples increased with increase in the amount of the neem oil and became softer with increase in the fraction of castor oil. This shows the benefit of blending different oils in soap production which bring in the properties of both oils together to enhance the quality of the soap. It can also be seen that the soap with 60 ml neem and 40 ml castor oil produced via hot process has higher cleansing power and that of 70 ml neem and 30 ml castor in the cold process had demonstrated a poor cleansing ability.

4.0 CONCLUSION

Blends of neem and castor oils were used to produce various soap samples at varying proportions using the two well-known processes of soap production, that is; the hot and cold processes. The produced soaps were analyzed using several properties such as foamability, yield, cleansing power, hardness and pH and compared with two commercial samples. The sample containing 60 ml neem and 40 ml castor oil produced via hot process was found to be the best as its properties agreed closely with the two commercial samples. It had a pH of 10.42, yield of 70.4% and foamability of 11.8 cm. The sample was also hard and showed a higher cleansing ability than the other samples. Therefore, it can be concluded that within the limit of this work, the best blend that gave good quality soap was that of 60 ml neem and 40 ml castor oil.

REFERENCES

Alfred, I. I., Patrick, O. N., (1985). Integrated Food Sciences and Technology for the Tropics, *International Cole Edition*, pp78. Macmillan publishers.

Ameh, A. O., Muhammad, J. A., Audu, H. G., (2013). Synthesis and characterization of antiseptic soap from neem oil and shea butter oil. *African Journal of Biotechnology,* 12*(29),* pp4656-4662. Doi: 10.5897/ajb2013.12246.

Hassan, K.J., Zubairu, M.S., Oyewole, R.O., (2015). Production of Soap from Neem Seed Oil and *Acacia nilotica* Seed Oil. *International Journal of Modern Organic Chemistry*, 4*(1)*, pp70-84.

Mak-Mensah, E.E., Firempong, C.K., (2011). Chemical characteristics of toilet soap prepared from neem (*Azadirachta indica*). *Asian Journal Plant Science and Research,* 1*(4)*, pp1-7.

Mishra, D., (2009). Preparation of Soap Using Different Types of Oils and Exploring its Properties, Thesis, National Institute of Technology, Rourkela, Malaysia.

Ndana, M., Garba, B., Hassan, L. G., & Faruk, U. Z. (2011). Evaluation of Physicochemical Properties of Biodiesel Produced From Some Vegetable Oils of Nigeria Origin. *Bayero journal of pure and applied sciences*, *4*(1), 67-71.

Onyango P. V., Oyaro N., Aloys O., (2014). Assessment of the Physicochemical Properties of Selected Commercial Soaps Manufactured and Sold in Kenya, Department of Chemistry, Maasai Mara University, Narok, Kenya.

Patel, V. R., Dumancas, G. G., Viswanath, L. C. K., Maples, R., & Subong, B. J. J. (2016). Castor oil: properties, uses, and optimization of processing parameters in commercial production. *Lipid insights*, *9*, LPI-S40233.

Phansteil, O.N., Dueno, E., Xianghong, Q., (1998). Synthesis of Exotic Soaps in the Chemistry

Laboratory. *Journal of Chemical Education*, pp612-614.

Schumutterer, H., Ascher, K. R. S., (1986). Natural pesticides from the neem tree and other tropical plants. *Proceeding. 3rd International Neem Conference*, Nairobi, Kenya, 1986, pp2-4.

Upadhyay, R.K., Dwivedi, P., Ahmad, S., (2010). Screening of antibacterial activity of six plant essential oils against pathogenic bacterial strains. *Asian Journal of Medical Science, 2(3),* pp152-158.

Warra, A. A., Gunu, S. A., Aisha, J. A., (2009). Soap production from shea nut butter. *International Journal of Applied Science, 5*, pp410-412.

Warra, A.A., (2013). A report on soap making in Nigeria using indigenous technology and raw materials. *African Journal of Pure and Applied Chemistry*, 7*(4)*, pp139-145.

DOI: 10.51975/21360204.som
Journal of the Nigerian Society of Chemical Engineers, 36(2), 2021

STATISTICAL MODELLING AND OPTIMIZATION OF THE CONCENTRATION OF BIO-ETHANOL FROM WASTE PEELS OF *MANIHOTESCULENTA CRANTZ* USING RESPONSE SURFACE METHODOLOGY

Akhabue C.E[1] and *Otoikhian S.K.[2]

[1]Department of Chemical Engineering, University of Benin, Benin City, Nigeria.
[2,*] Department of Chemical Engineering, Edo State University Uzairue, Edo State, Nigeria
*Corresponding author e-mail: otoikhian.kevin@edouniversity.edu.ng

ABSTRACT

In this study, the optimization of the concentration of bio-ethanol from waste peels of Manihotesculenta Crantz (cassava) was carried out. The acid hydrolysis process was optimized using Response Surface Methodology (RSM). Central Composite Design (CCD) was employed to study the effect of hydrolysis temperature, pH, and acid concentration and also, for optimization of the bio-ethanol concentration from the peels of Manihotesculenta C. The anaerobic fermentation process was carried at room temperature (≈30^{0}C) for four days. Prior to this, the fermentation media was prepared by culturing yeast to ferment the sugar rich liquid. A quadratic statistical model was developed for the acid hydrolysis process and then validated. The model gave a significant p-value < 0.05 and also showed an insignificant lack of fit. The model predicted that at optimum acid concentration of 1.2 % v/v, temperature of 131.8 ^{0}C and pH of 5.3, a maximum bio-ethanol concentration of 24.48 g/L should be obtained. The prediction of the model was validated by a triplicate set of experiments carried out at the predicted optimum parameters which yielded an average value of 24.41 g/L for the bio-ethanol concentration. The results obtained indicate the viability of Manihotesculenta Crantz peels as a bio-fuel feedstock and corroborates the efficiency of CCD in determining the optimum values of the process parameters for the acid hydrolysis step of the bio-ethanol production process.

***Keywords**: Hydrolysis, bio-ethanol, optimization, Response Surface Methodology, model*

1.0. INTRODUCTION

Bio-ethanol is the most widely used bio-fuel worldwide, partially able to replace fossil fuels, reducing the environmental impact of greenhouse gas emissions Balat (2011); Cunha *et al*. (2018). There has been growing research on viable feedstocks for use in bio-ethanol production. First generation bio-ethanol is produced mainly from C_6 sugars such as sugar beets, cereals, and sugarcane while second-generation bio-ethanol is produced from renewable lignocellulosic biomass and industrial by-products or residues Ho *et al.* (2014); Naik *et al.* (2010). The second generation production of ethanol derived from lignocellulosic materials is being tested in pilot plants Taherzadeh & Karimi, (2007a); Taherzadeh & Karimi, (2007b); Taherzadeh & Karimi, (2008). The steps involved in the production of bio-ethanol include; pre-treatment, hydrolysis, fermentation and finally distillation process. Each of this process is specific that is, it has its own functionality and rationale. The hydrolysis process is important as it involves the breaking down of polysaccharide compounds such as lignin, hemicelluloses, cellulose to simple fermentable sugars which are further fermented using yeast (*Saccharomyces cerevisae*) to produce ethanol and carbon dioxide which is further distilled to separate the alcohol water mixture. The choice of feedstock for production of ethanol is important because it's not merely a matter of which one has the greatest yield, but also a question of economics. A model is simply a representation usually in terms of mathematical equations of a process so as to predict the behaviour and interactions of the process variables under varying conditions. Modelling involves generating a representation defined by a set of mathematical equations that conforms closely in reality to what actually takes place Levenspiel (1998); Otoikhian *et al.* (2017). As an important subject in the statistical design of experiments, the Response Surface Methodology (RSM) is a collection of mathematical and statistical techniques useful for the modeling and analysis of problems in which a response of interest is influenced by several variables and the objective is to optimize this response (Montgomery, 2013).In this work, bio-ethanol from waste peels of *Manihot esculenta Crantz* is produced and the Response Surface Methodology feature of the Design Expert version 7.0 (Statease inc.,

Minneapolis) is used to perform statistical modelling and optimization of the process parameters viz; temperature, pH and acid concentration for the hydrolysis step of the process. This work will serve to contribute to the knowledge on production of bio-ethanol from Lignocellulosic biomass in general and waste peels of *Manihot esculenta Crantz* in particular.

2.0. MATERIALS AND METHODS

2.1. Experimental Procedures

2.1.1. Feedstock Preparation and Pre-treatment

Waste cassava peels were collected from a local famer in Ekosodin, Benin City, Nigeria. The brownish part was removed and the whitish layer with starch content was carefully washed to remove all sand and dirt present. The cassava peel was then sun dried for approximately three days to remove extra moisture. The sample was ground to powder form of about 0.5-1mm using a grinding machine so as to increase the sample surface area. It was sieved to get a homogenous powder. The ground sample was subjected to pre-treatment, hydrolysis, fermentation and distillation processes to obtain bio-ethanol. The prepared feedstock was stored in an air tight container before usage. Cassava peels pre-treatment was carried out using an autoclave. 100 mL of 0.5 % sulfuric acid was added to 30 g of the sample to remove the lignin, reduce cellulose crystallinity and increase porosity of the material. The mixture was heated to 120 ^{o}C under a pressure of 25 psi for 1 hour (Mishra *et al.* 2011)

2.1.2. Acid Hydrolysis Process

The Acid hydrolysis process for optimization of bio-ethanol concentration was conducted using Design Expert 7 software. 50 g 0f grounded cassava peel was used for the experiment and variables for hydrolysis includes: dilute hydrochloric acid concentration in the range 0.5-2.5 % v/v, temperature (100-140 ^{o}C), and at time duration of 15 minutes. The pH of the hydrozylate was neutralized to 6.7. The solid residue was separated using filter paper to obtain the sugar- rich liquid after the hydrolysis process to separate the non – fermentable cellulose and lignin. The resulting precipitate was poured into an air tight container where the pH range of 4 – 7 for optimization studies was adjusted for each experimental run according to the design of experiment.

2.1.3. Fermentation Process

The fermentation process was carried out in an anaerobic condition (air tight container) at a temperature of 30 ^{o}C which is approximately room temperature. The fermentation process was carried out for period of four days. Prior to this, the fermentation media was prepared by culturing of the yeast which was used in this case to ferment the sugar rich liquid. The nutrient media was prepared by adding 5 g of NH_4SO_4, 1.5 g of KOH and 0.2 g $CaCl.2H_2O$ to 500 mL of distilled water and dissolving completely. The media was autoclaved for 3 minutes at a temperature of 120 ^{o}C and pressure of 10 pounds per square inch.

2.2. Experimental Design

Response Surface Methodology (RSM) was used to optimize bio-ethanol production process from cassava peels and investigate the influence of different process variables on the bio-ethanol production. The central composite design was applied to study process variables. A total of twenty (20) experimental runs for the three identified design independent variables, namely: hydrolysis, acid concentration (A), pH (*B*), hydrolysis temperature (*C*), with low (−Alpha) and high (+Alpha) level were selected. Factorial points were augmented with five (5) replicates at the center point to assess the pure error. Response selected was bio-ethanol concentration. The levels were selected based on preliminary study results. The design factors (variables) with low (−1) and high (+1) levels and the central values (zero levels) chosen for experimental design are presented in Table 1 for *A*, *B*, *C*, respectively.

Table 1: Variables in the experimental design

Factors	Symbol	Coded and Actual levels				
		-α	**-1**	**0**	**+1**	**+α**
Acid hydrolysis concentration	*A*	0.5	0.9	1.5	2.1	2.5
Hydrolysis Temperature	*B*	100	108.1	120	131.9	140
pH	*C*	4	4.6	5.5	6.4	7

2.2.1. Statistical Analysis

Once the experiments were preformed, the next step was to perform a response surface experiment to produce a prediction model to determine curvature, detect interactions among the design factors (independent variables), and optimize the process, that is, determine the local optimum independent variables with maximum concentration of bio-ethanol. The model used in this study to estimate the response surface is the quadratic polynomial represented by the following equation:

$$Y = \beta_o + \sum \beta_i x_j + \sum \beta_{ij} x_i x_j + \sum \beta_{ii} {x_i}^2 + e_i \quad (1)$$

Where Y is the bio-ethanol concentration (g/L), β_o is the value of the fixed response at the centre point of the design, and β_i, β_{ij}, and β_{ii} are the linear, interactive, and quadratic coefficients, respectively, e_i is the error term, $x_i$and x_j are the independent variables (factors) under study.

The statistical software Design Expert 7.0 was used for design of experiments, regression, graphical, statistical analysis, Analysis of Variance (ANOVA) and optimization of the hydrolysis process.

2.3. Bio-ethanol Concentration Determination:

Colour Reaction and Colorimetry

The concentration of bio-ethanol in the fermentation sample was determined using a spectrophotometric method. To an aliquot of standard stock solution containing 1.6 mg/mL, 5 mL of sodium dichromate solution, 5 mL of acetate buffer pH 4.3 and 25 mL of 1N sulphuric acid was added in 50 mL of volumetric flask. The mixture was shaken gently for 1 minute and allowed to stand for 120 minutes as incubation period at room temperature resulted in formation of green coloured reaction product. Following incubation period the absorbance at 600 nm was read on 562 UV-Vis spectrophotometer model 752.

This procedure was followed for each of the samples prepared. Software supplied with the instrument was used to read the concentration of the samples from the plot concentration curve for standard and concentration of sample was calculated using equation (2) (Sumbhate *et al*. 2002).

$$Percentage\ of\ ethanol\ in\ sample\ (\%) = C_s \times \frac{A_u}{A_s} \times 100 \quad (2)$$

Where; $C_s\ is$ Concentration of standard, $A_u\ is$ Absorbance of standard and $A_s\ is$ Absorbance of sample.

3.0. RESULTS AND DISCUSSION

3.1. Central Composite Design of Experiment for the Optimization Studies.

In the experimental procedure carried out, three input variables; acid concentration, hydrolysis temperature, and pH were studied to determine the optimum of bio-ethanol concentration produced from cassava peels using the central composite design.

3.1.1.Model Fitting and Analysis of Variance

The central composite design was used to analyse the different effect of variables; acid concentration, temperature and pH, this resulted in 20 experimental runs with the various range of values, as shown in Table 2 with the response or dependent variable chosen as bio-ethanol concentration. Equations (3) and (4) are the quadratic statistical models in terms of actual and coded variables that were obtained after applying multiple regression analysis to the experimental data; this was used to calculate the predicted bio-ethanol concentration from experimental runs.

$$Y = 351.01911 + 74.58564A + 2.86552B + 46.96746C - 0.33358AB - 0.99702AC - 0.025102BC - 10.87848A^2 - 7.82119 \times 10^{-3}B^2 - 3.99932C^2 \quad (3)$$

$$Y = 20.13 - 2.12A + 4.16B - 1.37C - 2.36AB - 0.53AC - 0.27BC - 3.85A^2 - 1.11B^2 - 3.18C^2 \quad (4)$$

Where A, B and C are the acid concentration, temperature, pH respectively, in order to check the analysis of variance (ANOVA) and to check the adequacy of the model obtained the statistical analysis was performed. The ANOVA results and the statistical information for the for the second order response surface model are shown in Tables 3 and 4 respectively.

The model F-value of 264.50 and very low value of (<0.0001) showed that the model was significant. Each term in the model was also checked for significance.

Value of prob<0.05 is an indication that the model term is significant. Values greater than 0.1000 are insignificant model terms. The adequacy of the model was further checked. There was an insufficient lack of fit. According to Montgomery & Runger (2010) the lack of fit is an indication of the failure of the model represnting the experiment data at which some points

not included in the regression or variance in the model cannot be acounted for by random errors. This therefore implies that if there is a significant lack of fit, the model is discarded. From the ANOVA, the lack of fit F-value of 0.89 implies that it not significant relative to pure error. There is a 54.73 % chance that the lack of fit F-value this large could be due to noise.

Table 2 Central composite design for the optimization of variables and the response values.

Std	Run	Factor 1 A: Acid conc. $(v/v\,\%)$	Factor 2 B: temp. ℃	Factor3 B: pH	Response Ethanol conc. (g/L)	predicted Ethanol conc. (g/L)
1	13	0.9	108.1	4.6	8.21	8.15
2	6	2.1	108.1	4.6	9.36	9.69
3	14	0.9	131.9	4.6	22.08	21.72
4	9	2.1	131.9	4.6	13.81	13.83
5	3	0.9	108.1	6.4	7.21	7.00
6	16	2.1	108.1	6.4	6.26	6.43
7	10	0.9	131.9	6.4	20.03	19.51
8	20	2.1	131.9	6.4	9.63	9.50
9	4	0.5	120.0	5.5	12.24	12.80
10	2	2.5	120.0	5.5	6.02	5.67
11	19	1.5	100.0	5.5	10.24	9.98
12	5	1.5	140.0	5.5	23.52	23.98
13	17	1.5	120.0	4.0	13.49	13.42
14	8	1.5	120.0	7.0	8.53	8.81
15	18	1.5	120.0	5.5	19.85	20.11
16	11	1.5	120.0	5.5	20.04	20.11
17	1	1.5	120.0	5.5	19.92	20.11
18	15	1.5	120.0	5.5	21.23	20.11
19	7	1.5	120.0	5.5	19.67	20.11
20	12	1.5	120.0	5.5	20.08	20.11

Table 3: Analysis of Variance (ANOVA) for response surface quadratic model

Source	Sum of squares	Degree of freedom	Mean Square	F value	p-value prob ≥F
Model	701.25	9	77.92	264.58	<0.0001 significant
X_1	61.29	1	61.29	208.11	< 0.0001
X_2	236.60	1	236.60	803.44	< 0.0001
X_3	25.53	1	25.53	86.69	< 0.0001
X_1X_2	44.51	1	44.51	151.14	< 0.0001
X_1X_3	2.24	1	2.24	7.59	0.0203
X_2X_3	0.57	1	0.57	1.93	0.1954
X_1^2	213.18	1	213.18	723.90	< 0.0001
X_2^2	17.63	1	17.63	59.87	< 0.0001

DOI: 10.51975/21360204.som
Journal of the Nigerian Society of Chemical Engineers, 36(2), 2021

Source	Sum of squares	Degree of freedom	Mean Square	F value	p-value prob ≥F
X_3^2	145.86	1	145.86	495.31	< 0.0001
Residual	2.94	10	0.29		
Lack of Fit	1.39	5	0.28	0.89	0.5473 Not significant

Table 4: Statistical information for ANOVA

Std. Dev.	**0.54**	R^2	**0.9958**
Mean	14.57	Adj R^2	0.9921
C.V. %	3.72	Pred R^2	0.9818
PRESS	12.79	Adeq Precision	47.7240

The quality of the model developed was evaluated based on the correlation coefficient, R^2 value. A model developed should be best at low standard deviation and high R^2 statistics which is closer to unity as it will give predicted value closer to the actual value for the response (Ahmad, Hameed, & Ahmad 2009; Lenihan et al. 2010; Rahman et al. 2007).

In this work, R^2 value was 0.9958. This indicated that 99.58 % of the total variation in the final concentration was attributed to the experimental variables studied. The high R^2 equally showed that the predicted value would be more accurate and closer to its actual value (Mohd & Rasyidah 2010). The standard deviation for the model was 0.54 which indicated that the predicted values for this model are still considered as suitable to correlate the experimental data. The adequate precision which measured the signal to noise ratio was 47.7240 which indicated an adequate signal. Also the "pred R^2 of 0.9818 was in reasonable agreement with the "Adj R^2 of 0.9921.

3.2. Diagnostic Plots

The quality of the model developed was further assessed using residual plots. Residual is the difference between the experimental value and value predicted by the model. Some of the residual plots used were: normal plot of residuals which indicates whether the residuals follow a normal distribution, and plot of predicted vs.

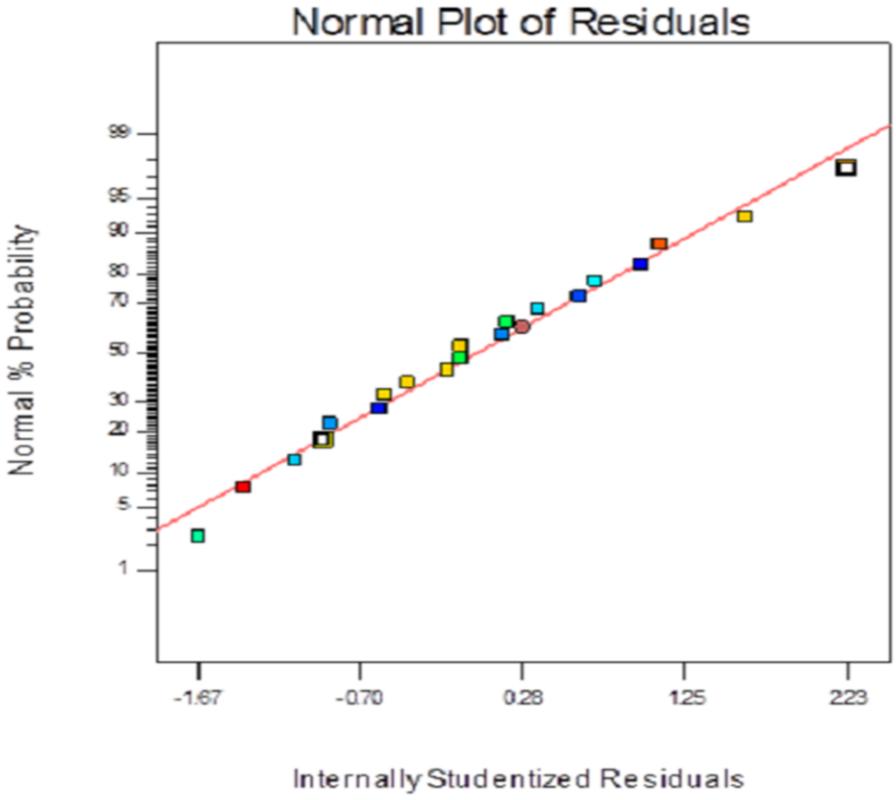

Figure 1: Residual Plots Normal Plot of Residuals

Actual response values which helps to detect a value, group of values that are not easily predicted by the model (Onuigbo, 2017). The residual plots are shown in Figures 1 and 2.

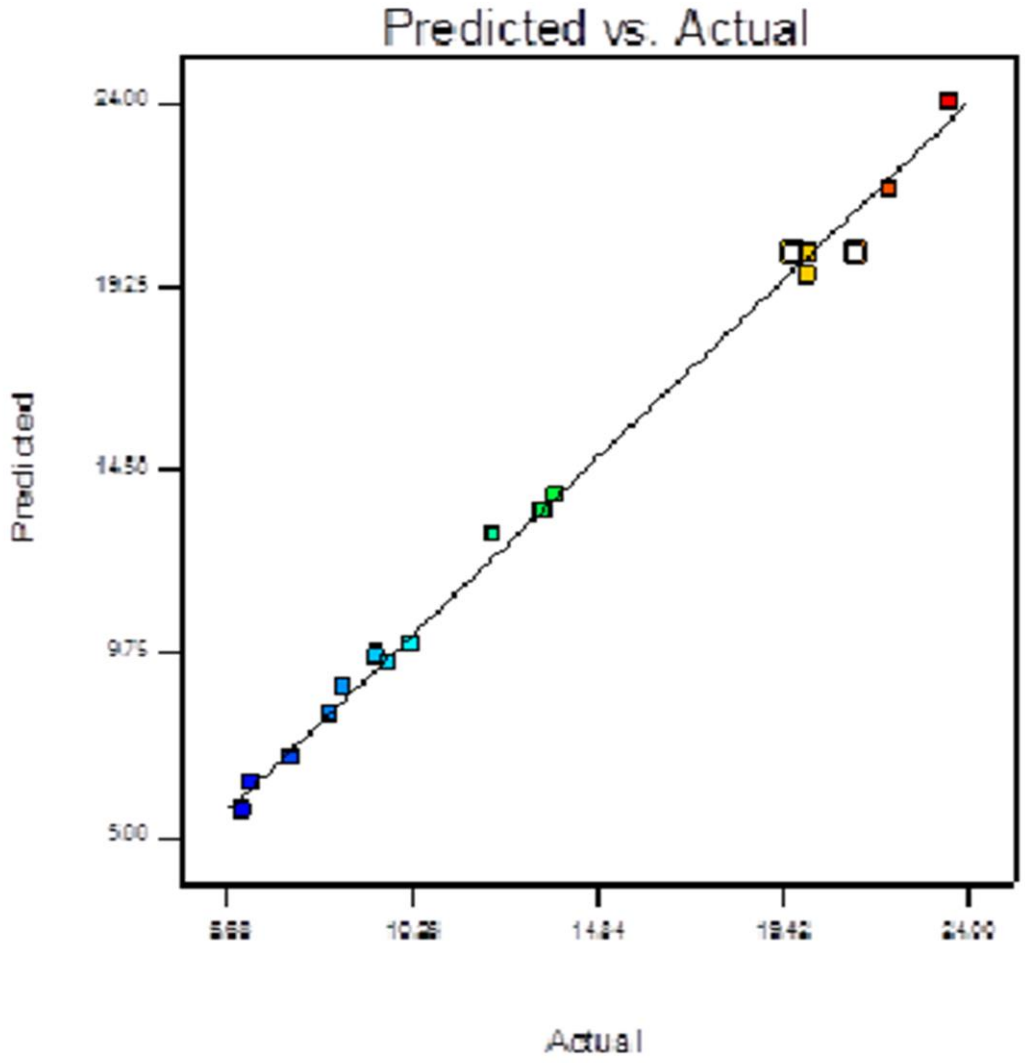

Figure 2: Residual Plot of Predicted vs. Actual Response Values.

3.3. Combined Effects of Different Variables on Bio-ethanol Concentration Produced

Response surface curves were plotted to examine the effect of the interaction between the independent variables and to determine the optimum levels of the variables.

3.3.1. Combined Effect of pH And Acid Concentration on Bio-ethanol Concentration

Figure 3 below shows the interaction between independent variables, pH and acid concentration keeping temperature constant at a value of 120 ^{0}C. From the plot it is observed that at a constant acid concentration of (0.9 % v/v), decreasing pH from 6.4-4.6 causes an increase in ethanol concentration, this effect being as a result of increase in the acidic medium as pH decreases. Increasing acid concentration from 0.9-2.1, at a high pH of 6.4 and at a low pH of 4.6,

shows similar effect as bio-ethanol concentration increases to an optimum before a gradual decrease. This trend observed may be attributed to the catalytic activity of the acid. Increasing the rate of the fermentation medium, results in the release of more hydrogen ion that eventually acts as catalytic agent during hydrolysis.

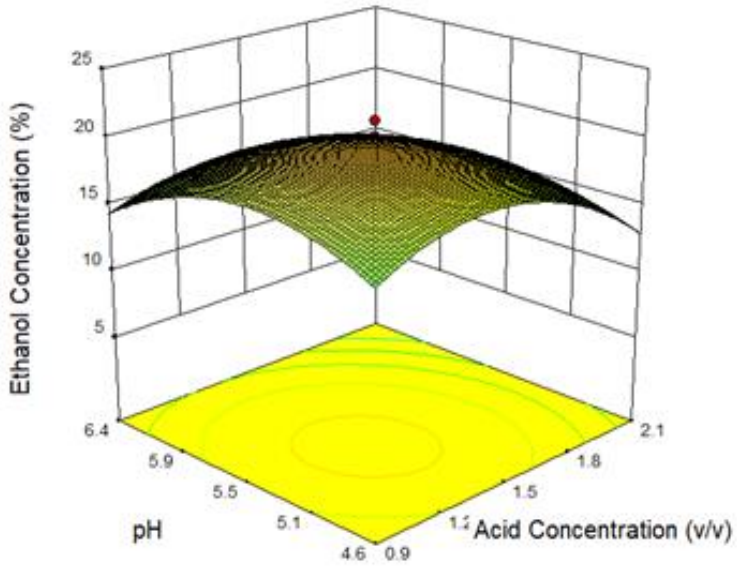

Figure 3: Response surface model plot of simultaneous effect of pH and hydrolysis acid concentration on bio-ethanol concentration produced.

3.3.2. Combined Effect of Hydrolysis pH and Temperature on Bio-ethanol Concentration

Figure 4 shows the combine effect of temperature and pH keeping acid concentration constant at a value of 1.5, from the plot it is observed that at low and high values of pH 4.6 and 6.4 respectively, the same effect is observed, which is a progressive increase in rate of ethanol produced with respect to increase in temperature from 108 ^{0}C to 131.9 ^{0}C. This effect could be associated with acidic medium of pH since acidic medium favours Fermentation process.

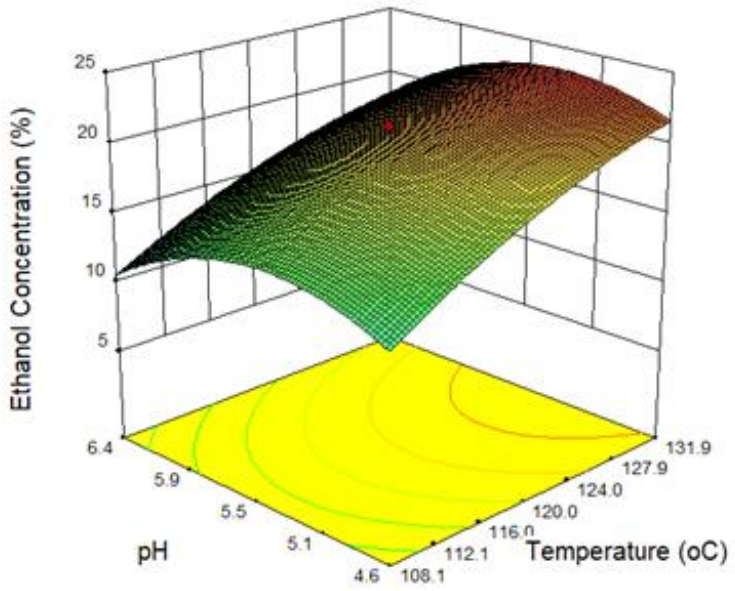

Figure 4: Response surface model plot of simultaneous effect of pH and temperature on bio-ethanol concentration produced.

At low temperature of 108.1, increase in pH causes an initial increase in ethanol concentration to an optimum before a gradual decrease; also at high temperature of 131.9 ^{0}C the same effect is also noticed. This decrease in concentration could be as a result of low activity of the yeast as pH increases.

3.3.3. Combine Effect of Acid Hydrolysis Concentration and Hydrolysis Temperature on Bio-ethanol Concentration

Figure 5 below shows the effect of acid concentration and hydrolysis temperature on ethanol concentration when pH is maintained constant at a value of 5.5, from the plot it is observed that increasing the temperature of the medium led to significant increase in ethanol production at low value of acid concentration (0.9 % v/v), this could be attributed to increase in the rate of collision of the molecules of the reacting species.

At a high value of acid concentration (2.1 % v/v) increase in temperature from 108 ^{0}C - 131.9 ^{0}C led to an initial increase in ethanol concentration up to an optimum after which further increase led to a decrease. This could be as a result of unfavorable temperature of the reacting medium.

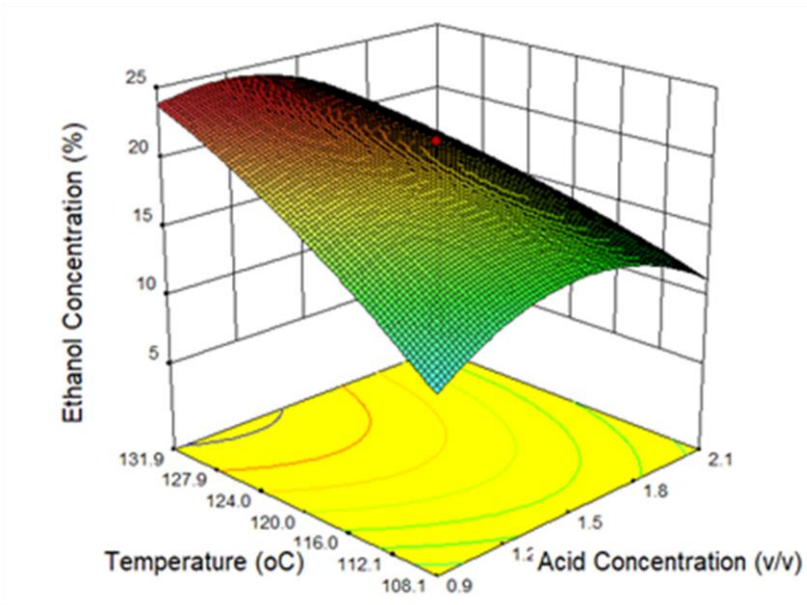

Figure 5: Response surface model plot of simultaneous effect of temperature and hydrolysis acid concentration on the concentration of the ethanol produced.

At low temperature of 108.9 ^{0}C increase in acid concentration from 0.9 - 1.5 % v/v resulted to an increase in ethanol concentration produced this could be attributed to the catalytic activity of the acid during hydrolysis process resulting in high yield of simple sugar and thus increase in the fermentation of simple sugar to bio-ethanol. At high temperature of 131.9 ^{0}C, increase in acid concentration led to a decrease in ethanol concentration. This effect could be as a result of elevated temperature which is not favourable.

3.4. Validation of Statistical Model

To confirm the validity of the statistical model, three confirmation experimental runs were performed at the chosen optimum hydrolysis conditions indicated in Table 6. The result shows that maximum experimental ethanol concentration of 24.48 g/L obtained was close to the predicted value of 24.41 g/L. The excellent correlation between the predicted and measured values of these experiments shows the validity of statistical model.

Table 6: Solution for optimum conditions

Acid Conc. $(v/v\,\%)$	Temperature ℃	pH	Ethanol Conc. (g/L)
1.2	131.8	5.3	24.48

4.0. CONCLUSION

Drawing from the results obtained in this work, it is seen that the model developed using the Central Composite Design (CCD) in Response Surface Methodology

(RSM) to represent the acid hydrolysis step for the production of ethanol from cassava peels is valid as it gave a significant p-value < 0.05 and also showed an insignificant lack of fit. A triplicate set of experiments carried out at the optimum values predicted by the model yielded an average value of 24.41 g/L for the ethanol concentration which was very close to the predicted value of 24.48 g/L running at optimum acid concentration of (1.2 % v/v), temperature of 131.8 ^{0}C and pH of 5.3.

5.0. ACKNOWLEDGEMENT

All authors whose work where used in this present work are specially acknowledged and appreciated. This work received no funding from external sources.

6.0. REFERENCES

Ahmad, A. A., B. H. Hameed & A. L. Ahmad. (2009). Removal of Disperse Dye from Aqueous Solution Using Waste-Derived Activated Carbon: Optimization Study. *Journal of Hazardous Materials* 170(2):612–19. doi: 10.1016/j.jhazmat.2009.05.021.

Balat, Mustafa. (2011). "Production of Bio-ethanol from Lignocellulosic Materials via the Biochemical Pathway: A Review.*Energy Conversion and Management* 52(2):858–75. doi: 10.1016/j.enconman.2010.08.013.

Cunha, Manuel, Aloia Romaní, Margarida Carvalho, & Lucília Domingues. (2018). "Boosting Bio-ethanol Production from Eucalyptus Wood by Whey Incorporation." *Bioresource Technology* 250 (256–64). doi: 10.1016/j.biortech.2017.11.023.

Ho, Dang P., Huu Hao Ngo, & Wenshan Guo. (2014). A Mini Review on Renewable Sources for Bio-fuel. *Bioresource Technology* 169 (write issue number) (742–49). doi: 10.1016/j.biortech.2014.07.022.

Lenihan, P., Orozco, A., O'Neill, E., Ahmad, M. N. M., Rooney, D. W. & Walker, G. M.. (2010). Dilute Acid Hydrolysis of Lignocellulosic Biomass: *Chemical Engineering Journal* 156(2):395–403. doi: 10.1016/j.cej.2009.10.061.

Levenspiel, Octave. 1998. *Chemical Reaction Engineering*. Third edition, Singapore: John Wiley & Sons.

Mishra, M., Chandrashekhar B., Tanushree C., & Kanwal S. (2011). Production Of Bio-Ethanol From Jatropha Oilseed Cakes Via Dilute Acid Hydrolysis And Fermentation in Saccharomyces C. (editor). *International Journal of Biotechnology Applications* 3:41–47. doi: 10.9735/0975-2943.3(1.41-47).

Mohd, A. A., & Rasyidah A. (2010).Optimization of Malachite Green by KOH – Modified Grape Fruit Peel Activated Carbon: Application of Response Surface Methodology." *The Chemical Engineering Journal* 751-988.

Montgomery, D. C. (2013). *Design and Analysis of Experiments*. Eighth edition. Hoboken, NJ: John Wiley & Sons, Inc.

Montgomery, D. C., and George C. R. (2010). *Applied Statistics and Probability for Engineers*. John Wiley & Sons.

Naik, S. N., Vaibhav V., Goud, P. K. R., & Ajay, K. D. (2010). Production of First and Second Generation Bio-fuels: A Comprehensive Review. *Renewable and Sustainable Energy Reviews* 14(2):578–97. doi: 10.1016/j.rser.2009.10.003.

Onuigbo, O. G. (2017). "Statistical Approach to Optimizing Bio-ethanol Concentration from Cassava Peels Using Response Surface Methodology. University of Benin, Nigeria.

Otoikhian, S. K., B. P. Agbodekhe, E. O. Aluyor, & T. O. K. Audu. (2018). Mass-Transfer Modeling of the Active Step in the Synthesis of a Novel Catalyst for Bio-diesel Production, *Petroleum Technology Development Journal* 8(2).

Otoikhian, S. K., Agbodekhe, B. P., Anakhu, E.A., Diamond, B. & Aluyor, E. O. (2017). Modelling the Mass Transfer Kinetics of the Grafting of 4-Chloromethylstyrene onto Polyethylene Substrate. *Journal of Bio-fuels* 8(1):33. doi: 10.5958/0976-4763.2017.00006.X.

Rahman, S. H. A., Choudhury, J. P. Ahmad, A. L. & Kamaruddin, A. H.(2007).. Optimization Studies on Acid Hydrolysis of Oil Palm Empty Fruit Bunch Fiber for Production of Xylose. *Bioresource Technology* 98(3):554–59. doi: 10.1016/j.biortech.2006.02.016.

Sumbhate, S., Satish N., Damodar G., Ajay T., & Rajesh J. (2002). Colorimetric Method for the Estimation of Ethanol in Alcoholic-Drinks. *Journal of Analytical Techniques* 1.

Taherzadeh, M. J., & Keikhosro, K. (2007). Acid-Based Hydrolysis Processes for Ethanol from Lignocellulosic Materials: A Review. *BioResources* 2.

Taherzadeh, Mohammad J, & Keikhosro K. (2007). Enzyme-Based Hydrolysis Processes for Ethanol from Lignocellulosic Materials: A Review. *BioResources* 2(3)

Taherzadeh, Mohammad J. & Keikhosro, Karimi. (2008). Pretreatment of Lignocellulosic Wastes to Improve Ethanol and Biogas Production: A Review. *International Journal of Molecular Sciences* 9(9):1621–51. doi: 10.3390/ijms9091621.

DOI: 10.51975/21360205.som
Journal of the Nigerian Society of Chemical Engineers, 36(2), 2021

COMPUTATIONAL FLUID DYNAMICS SIMULATIONS OF TAYLOR BUBBLE RISE IN FLOWING LIQUIDS

Abubakar, H. A.
Department of Chemical Engineering, Ahmadu Bello University, Zaria.
(abuabib2006@gmail.com; haabubakar@abu.edu.ng)

ABSTRACT

Systematic analysis of the effect of gravitational, interfacial, viscous and inertia forces acting on a Taylor bubble rising in flowing liquids characterised by the dimensionless Froude (U_c), inverse viscosity (Nf) and Eötvös numbers (Eo) is carried out using computational fluid dynamic finite element method. Particular attention is paid to cocurrent (i.e upward) liquid flow and the influence of the characterising dimensionless parameters on the bubble rise velocity and morphology analysed for Nf, Eo and U_c ranging between [40, 100], [20, 300] and [−0.20, 0.20], respectively. Analysis of the results of the numerical simulations showed that the existing theoretical model for the prediction of Taylor bubble rise velocity in upward flowing liquids could be modified to accurately predict the rise velocity in liquids with high viscous and surface tension effects. Furthermore, the mechanism governing the change in morphology of the bubble in flowing liquids was shown to be the interplay between the viscous stress and total curvature stress at the interface.

Keywords: *Taylor bubble, finite element, slug flow, CFD, rise velocity*

1.0 INTRODUCTION

Taylor bubbles are elongated bullet-shaped gas bubbles constrained within the wall of a vertical pipe containing a stagnant or flowing liquid in a slug flow. Slug flow is one of the flow regimes in two-phase gas-liquid flows in vertical pipes and is prevalent in large and small-scale two-phase gas-liquid flows, ranging from applications such as the production and transportation of hydrocarbons to microfluidic cooling of electronics and flow of red blood cells. The understanding of the behaviour of a single Taylor bubble in stagnant and flowing liquids is considered as paradigm for the slug flow in vertical pipes because of the near-periodicity of the gas-liquid flows in the regime.

The behaviour of a Taylor bubble is governed by the interaction of different forces that act on it. These forces include gravitational, interfacial, viscous and inertia forces, corresponding to the influence of the acceleration due to gravity (g), surface tension (γ), viscosity (μ) and liquid velocity (u), respectively. The relative magnitudes of these forces, defined in terms of a number of dimensionless groups, are used in describing the behaviour of a rising Taylor bubble in liquids.

A Taylor bubble rising through liquids can be parametrised by the dimensionless inverse viscosity number, Nf, Eötvös number, Eo and Froude number, Fr define as follow,

$$Nf = \rho(gD^3)^{½}/\mu,\ Eo = \rho gD^2/\gamma,\ Fr = u/\sqrt{gD} \quad (1)$$

Depending on the choice of velocity used in defining Fr, three Froude number types can be distinguished; Froude number that is based on the tube center liquid velocity, tube mean liquid velocity and the bubble rise velocity denoted as U_c, U_m and U_b, respectively.

Taylor bubble is generally conferred with topological symmetry and can be sectioned into three distinct regions, namely *nose*, film and *bottom* with each region having specific features used for its characterisation. The bubble rise velocity is one of the features that characterised the nose region of a rising Taylor bubble and its determination has been extensively studied. Neglecting surface tension effect and assuming an inviscid flow around the bubble nose, Dumitrescu (1943) and Davies & Taylor (1950) theoretically and independently show that the rise velocity of the bubble in stagnant is

$$u_b = C_s\sqrt{gD} \quad (2)$$

where u_b denotes dimensional bubble rise velocity and C_s is a dimensionless proportionality that is physically equivalent to Froude number with values in the range 0.33-0.36 (Nicklin et al., 1962; Polonsky et al., 1999).

For a Taylor bubble rising in a flowing liquid with negligible viscous and surface tension effect, Nicklin et al. (1962) proposed a correlation that relates the bubble rise velocity to the mean liquid velocity, which in dimensionless form is given as

$$U_b = C_m U_m + C_s \quad (3)$$

where C_m is dimensionless constant whose value is taken to be approximately 1.2 and 2 in turbulent and

laminar flows (Bendiksen, 1985; Collins et al., 1978; Nicklin et al., 1962), respectively.

White & Beardmore (1962) used a large pool of experimental data generated using different liquids to demarcate limits in which surface tension, inertia, viscous or a combination of these forces have negligible influence on a bubble rising in stagnant liquid. It was established that beyond Eo > 70 and $Eo^3Nf^{-4} > 3 \times 10^5$, a region known as inertia regime, surface tension and viscosity have insignificant effect on the rise velocity of the bubble. Later experimental, theoretical and numerical studies in liquids (Brown, 1965; Kang et al., 2010; Lu & Prosperetti, 2009; Zukoski, 1966) have provided further insights on the role of surface tension and viscosity on the rise velocity in both inertia and non-inertia regimes The effect of both viscosity and surface tension is to reduce the bubble rise velocity.

The correlation of Viana et al. (2003), recently modified by Lizarraga-Garcia et al. (2017) to account for the effect of pipe inclinations, for the prediction of the effect of surface tension (Eo) and viscosity (Nf) relative to gravity on bubble rise velocity in stagnant liquid is given in (4).

$$U_b = 0.34[1 + (14.793/Eo)^{3.06}]^{-0.58} \Big/ \left[1 + \beta^{\Theta^{-1:0295\theta^{-1}}}\right] \quad (4)$$

where

$$\beta = Nf[31.08(1 + (29.868/Eo)^{1.96})^{0.49}]^{-1}$$
$$\Theta = -1.45[1 + (24.867Eo)^{9.93}]^{0.094}$$

For flowing liquid, analytical solution for determining the effect of liquid velocity profile on the rise velocity and shape of Taylor bubble was presented by Collins et al. (1978) and later extended by Bendiksen (1985) to account for the effect of surface tension. Both studies focused on upward flowing liquid in which the liquid motion due to the bubble was taken to be inviscid and irrotational. The analytical solution of Bendiksen (1985) is of the form

$$U_b = C_c U_c + C_s \quad (5)$$

Generally, numerical simulations are used to complement experimental and theoretical studies. It is clear that studies carried out in both stagnant and flowing liquids are largely limited to inertia regime. For stagnant liquid, the correlation of Viana et al. (2003) have been shown to reasonably predict the rise velocity of Taylor bubble in both inertia and non inertia regime because of incorporation of Nf and Eo dependency. However, for flowing liquid, it is unlikely that the existing models, equations (3) and (5) can adequately predict the rise velocity in non inertia regime. In addition, there is much more to be done in understand the underlying mechanisms governing the dynamics of Taylor bubble rise in flowing liquids.

To this end, a preliminary systematic study is carried out to simulate a rising Taylor bubble in flowing liquid for regime in which the influence of viscosity and surface tension are not negligible. In section 2, computational fluid dynamic model is developed for the problem. Description of the problem to be studied is given in section 2.1, governing equations together with the boundary conditions for the problems provided in sections 2.2 and the numerical strategy for solving the model is described in section 2.3. Systematic analysis of the influence of the dimensionless parameters that characterised the model developed in section 2 are discussed in section 3. Validity of the existing theoretical and empirical models are investigated in section 3.1 and the underlying physics of the solution to the problem discussed in section 3.2.

2.0 COMPUTATIONAL FLUID DYNAMIC MODELLING OF A RISING TAYLOR BUBBLE

2.1 Problem Description

An axisymmetric Taylor bubble of constant volume V_b in which the dynamics within it is represented by a constant pressure P_b is imagined. The bubble is assumed to be rising in a flowing liquid of constant density ρ, viscosity μ, interfacial tension γ and tube center velocity of magnitude u_c in a vertical pipe of diameter D in a frame of reference that moves with velocity $\mathbf{u}_b$ of the bubble nose. Cylindrical co-ordinates system is adopted, so that the coordinates along and perpendicular to the axis of symmetry are z and r, respectively, with the origin of z chosen as the nose of the bubble. The problem therefore is to find the bubble rise velocity, U_b, pressure, P_b and shape of a Taylor bubble as it rises through the flowing liquid so that its volume, V_b, remains constant.

2.2 Governing Equations and Boundary Conditions

The steady motion of an isothermal, incompressible Newtonian liquid in a domain Ω with boundary Γ is governed by the time independent Navier-Stokes and continuity equations, supplemented with appropriate boundary conditions. Non-dimensionalised governing equations and boundary conditions using the

characteristic length, velocity and pressure scales, taken to be D, $\sqrt{gD}$ and ρgD, respectively, in a frame translated with velocity $\mathbf{u}_b$ of the bubble nose are given as

Momentum Equation

$$(\mathbf{u}.\boldsymbol{\nabla})\mathbf{u} - \boldsymbol{\nabla}.\mathbf{T} = \mathbf{0} \text{ in } \quad \Omega \tag{6}$$

Continuity Equation

$$\boldsymbol{\nabla}.\mathbf{u} = 0 \text{ in } \quad \Omega \tag{7}$$

where Ω denotes the domain of interest, **u** is vector of the fluid velocity in the moving frame of reference, **T** is the stress tensor and is related to the dependent variables of the problem as

$$\mathbf{T}(\mathbf{u}, \mathrm{p}) = -\mathrm{p}\mathbf{I} + \mathrm{Nf}^{-1}[\boldsymbol{\nabla}(\mathbf{u}) + \boldsymbol{\nabla}(\mathbf{u})^{\mathrm{T}}] \tag{8}$$

where p represents the dynamic pressure, **I** is the unit tensor and $(.)^{\mathrm{T}}$ is the transpose operator.

Appropriate boundary conditions are prescribed at the boundary of the domain to make the problem well posed and the solution unique. The boundary denoted by Γ can be divided into Γ_{in} , Γ_{out} , Γ_{wall} , Γ_{sym} and Γ_b as shown in Figure 1 with the subscripts *in*, *out*, *wall*, *sym* and *b* representing the inlet, outlet, wall, symmetry and bubble boundaries, respectively.

Boundary conditions

Wall: $\mathbf{u} = -\mathbf{u}_b$ on Γ_{wall} (9)

Inlet: $\mathbf{u} = \mathbf{u}_{in} - \mathbf{u}_b$ on Γ_{in} (10)

Outlet: $\mathbf{n}.\mathbf{T} = \mathbf{0}$ on Γ_{out} (11)

Symmetry axis: $\mathbf{u}.\mathbf{n} = 0$ and $\mathbf{n}.\mathbf{T} \times \mathbf{n} = \mathbf{0}$ on Γ_{sym} (12)

Gas-Liquid Interface:

$$\mathbf{n}.\mathbf{T}.\mathbf{n} + \mathrm{P_b} - \mathrm{z} - \mathrm{Eo}^{-1}\mathrm{k} = 0, \ \mathbf{n}.\mathbf{T} \times \mathbf{n} = \mathbf{0} \ \&$$
$$\frac{\mathrm{dr_b}}{\mathrm{dt}}.\mathbf{n} - \mathbf{u}.\mathbf{n} = 0 \text{ on } \Gamma_b \tag{13}$$

where $\mathbf{r}_b$ represents the position vector of the interface between the liquid and the gas phases with component r and z; κ is the curvature of the interface and **n** is the unit normal vector to the interface. It should be noted that gravity is absent in (6) but appears in (13) as z because the hydrostatic component of pressure has been subtracted from the total pressure, leaving only the hydrodynamic part.

For consistent system, additional equation is needed to determine the unknown dimensionless bubble pressure and is given as

$$V_b + \frac{2\pi}{3}\oint_{\Gamma_b}[r_b.n]d\Gamma_b = 0 \tag{14}$$

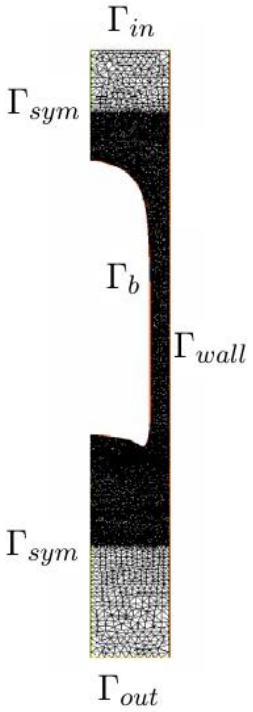

Figure 1: Schematic representation of axisymmetric Taylor bubble mesh structure.

2.3 Finite Element Simulations

The governing equations (6) and (7) under the boundary conditions (9)-(14) are solved, for a given Nf, Eo and U_c to be simulated, using consistent penalty Galerkin finite element method. Essentially, the equations are transformed into their weak forms, the dependent variables in the equations approximated using suitable basis functions, the domain divided into subdomains around which the approximated variables are defined and the discrete non-linear system of equations solved using Newton method. The implementation was done in FreeFem++ (Hecht, 2012), an easy-to-use open-source high-level multiphysics finite element package with advanced mesh generation and adaptation capabilities. Figure 1 shows a typical mesh structure used for the numerical simulation. Regions around the bubble, where the dynamics is intense, are finely resolved compared to regions far from the bubble. Further details on the meshing and the implementation method carried out in FreeFem++ for Taylor bubble rising in stagnant liquid including the validations carried out can be found in Abubakar & Matar (2021b).

3.0 RESULTS AND DISCUSSIONS

3.1 Bubble Rise Velocity in Flowing Liquids

The morphology of a rising Taylor bubble in upward flowing liquids is bullet-shaped and axisymmetric as observed in stagnant liquids and its rise velocity is a combination of its rise velocity in stagnant liquid and a contribution due to the flowing liquid ahead of the bubble. Figure 2 shows the steady state bubble shape for a Taylor bubble rising in a flowing liquid for U_c = 0.20, Nf = 60 and Eo = 220.

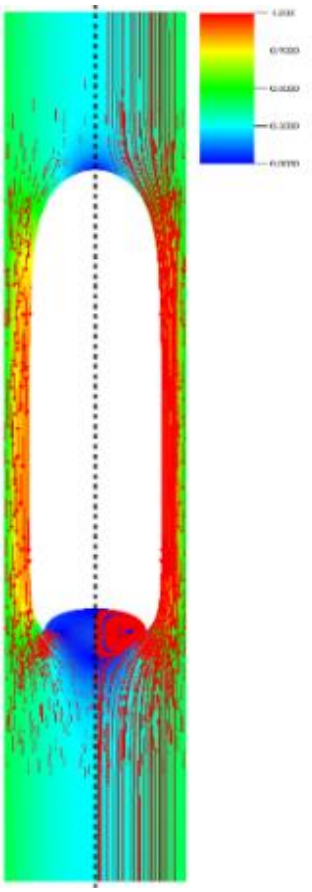

Figure 2: Steady state solution for U_c = 0.20, Nf = 60 and Eo = 220 showing combined pseudo-colour, vector and streamline plots in rising bubble frame of reference.

The rise velocity is determined to be 0.4770 and the flow field solution is captured by the pseudo-colour, vector and streamline plots merged into a single plot, shown in Figure 2, as inspired by Kang et al. (2010). The vector field and streamline plots, superimposed on the pseudo-colour plot, are shown on the left and right of the symmetry axis, represented by the dashed black lines, respectively. From the colour map in Figure 2, it is clear that the nose of the bubble is a stagnation point in frame of reference that moves with bubble rise velocity because the magnitude of velocity at this point is zero. This is confirmed by the vector and streamline fields around the bubble as the flow approaching the nose get diverted into the film region.

Comparison is made in Figure 3 between the bubble rise velocity prediction from the numerical simulations, and existing empirical and theoretical models. The correlation of Bendiksen (1985), shown to correctly predict the rise velocity in upward flowing liquids, is recalled and the parameters defined.

$$U_b = C_c U_c + C_s$$

$$C_s = 1.145\left[1 - \frac{20}{Eo}\left(1 - e^{-0.0125Eo}\right)\right] \qquad (15)$$

$$C_c = \frac{0.486}{\sqrt{2}}\sqrt{21 - \frac{136}{Eo}}\left[\frac{1.-0.96e^{-0.0165Eo}}{1.-0.52e^{-0.0165Eo}}\right] \qquad (16)$$

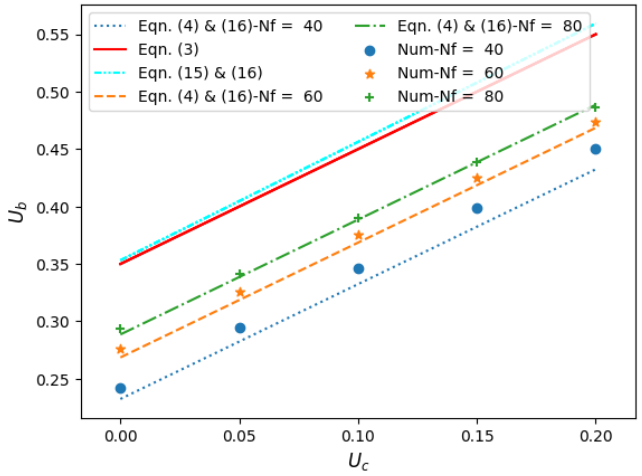

Figure 3: Effect of U_c on bubble rise velocity for Eo = 180 and varying Nf. Comparison between numerical result (markers), empirical prediction (solid line) and theoretical predictions (dashed line).

In Figure 3, the empirical prediction using (3) of Nicklin et al. (1962), theoretical prediction using (15) and (16) of Bendiksen (1985), modified theoretical prediction using (16) of Bendiksen (1985) complemented by (4) of Viana et al. (2003) in place C_s, and the numerical prediction from this study are shown.

It is evident that both the empirical and theoretical correlations over-predict the bubble rise velocity. This is not unexpected because the correlations were derived for cases in which flow due to the bubble motion was considered as inviscid, which only holds in regimes where both the effect of surface tension and viscous forces on the bubble rise velocity are negligible. When

DOI: 10.51975/21360205.som
Journal of the Nigerian Society of Chemical Engineers, 36(2), 2021

the correlation of Bendiksen (1985) is modified using the correlation of Viana et al. (2003), which accounts for the effect of viscosity and surface tension, for the computation of C_s, reasonable agreement, which improves as Nf is increased, is seen between the theoretical prediction and numerical results. Therefore,

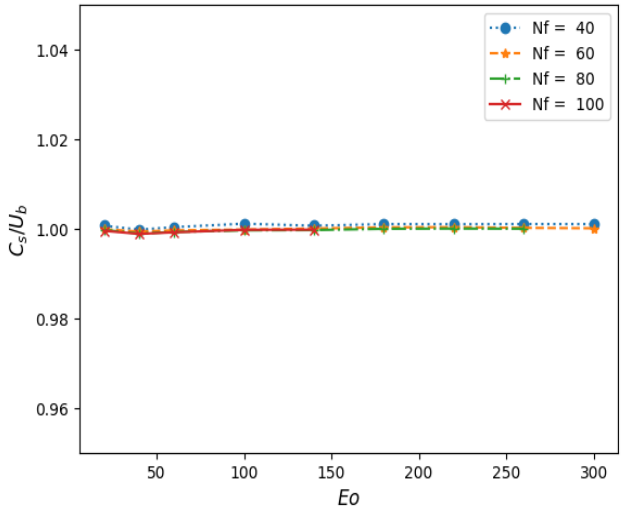

Figure 4: Effect of inverse viscosity and Eötvös numbers on parameter Cs in (Eqn 5).

equation (5) can be used for the computation of bubble rise velocity in regime where surface tension and viscous forces are significant if its parameters are modified to account for the effect of both Nf and Eo.

The estimated values of C_s and C_c for the numerical simulations carried out for upward liquid flow accounting for the effect of Nf and Eo, are shown in Figures 4 and 5, respectively. The values were obtained from the intercept and slope of the plot of U_b versus U_c for upward liquid flow, respectively. It is discernible from Figure 4 that the numerical results agree well with previous experimental and numerical observations. C_s is physically the bubble rise velocity in a stagnant liquid, so that the scaling of the C_s obtained from the intercept of U_b versus U_c plot with numerical value of the rise velocity for the stagnant liquid for the same condition of Nf and Eo should give a constant value of 1.0. Similarly, Figure 5 shows that though C_c depends on Nf and Eo, there exist limits beyond which C_c becomes independent of surface tension and viscous forces, as seen for Taylor bubble in inertia regime. This is because for constant Nf the figure shows that C_c is going to plateau to a constant value at higher values of Eo and for constant Eo, the consecutive distance between the plots for different Nf will decrease as Nf is increased before eventually merging.

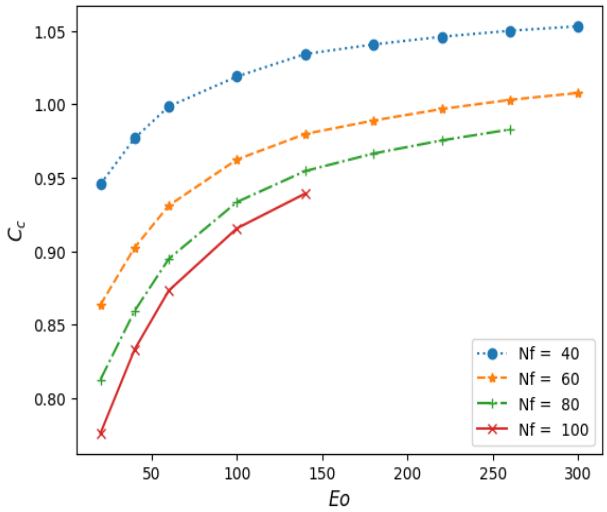

Figure 5: Effect of inverse viscosity and Eötvös numbers on parameter Cc in (Eqn 5).

3.2 Steady State Bubble Shape and Flow Fields Analysis

The characterising dimensionless numbers for Taylor bubble dynamics in flowing liquids are Nf, Eo and Fr. Effects of Nf and Eo on bubble shape, rise velocity and surrounding flow fields for stagnant liquids have been analysed in Abubakar & Matar (2021b). It is observed that for a fixed value of flowing liquid velocity, the effects of inverse viscosity and Eötvös numbers are as observed in stagnant liquids (see Figures 6 and 7).

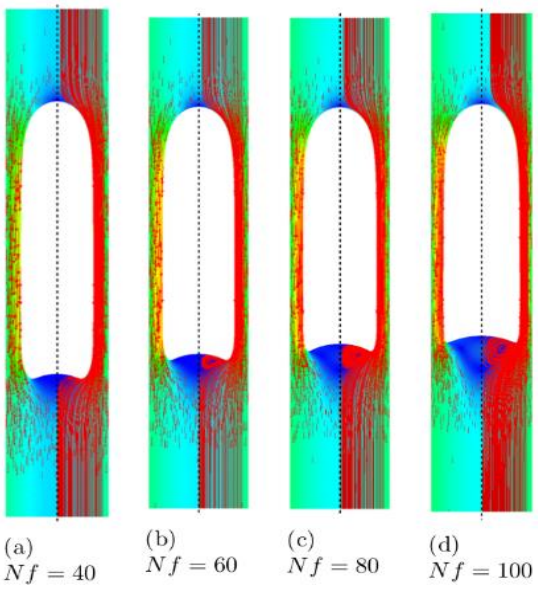

Figure 6: Effect of Nf on steady state shape and the surrounding flow field for Eo = 100 and U_c = 0.15; showing streamlines and vector field superimposed on velocity magnitude pseudo-colour plot.

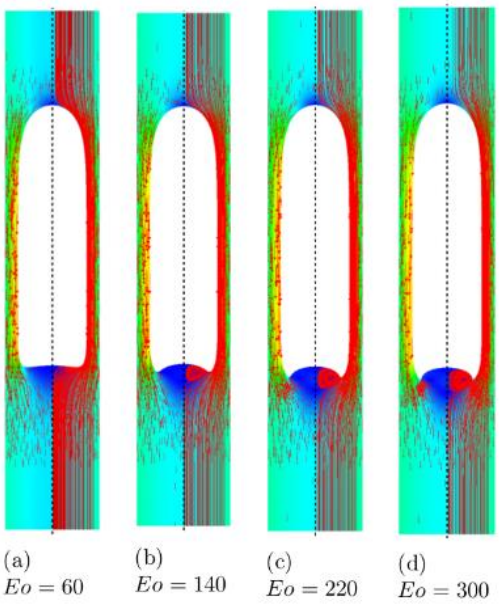

Figure 7: Effect of Eo on steady state shape and the surrounding flow field for Nf = 60 and U_c = 0.10; showing streamlines and vector field superimposed on velocity magnitude pseudo-colour plot.

Froude number based on tube center liquid velocity is a measure of the relative importance of inertia force due to the flowing liquid to buoyancy force due to gravity. For co-current liquid flow, the direction of flow of liquid is the same as that of buoyancy force due to gravity, thereby enhancing the rise velocity of the bubble. On the contrast, in counter-current or downward liquid flow, the liquid flow opposes the force of buoyancy thereby decreasing the bubble rise velocity.

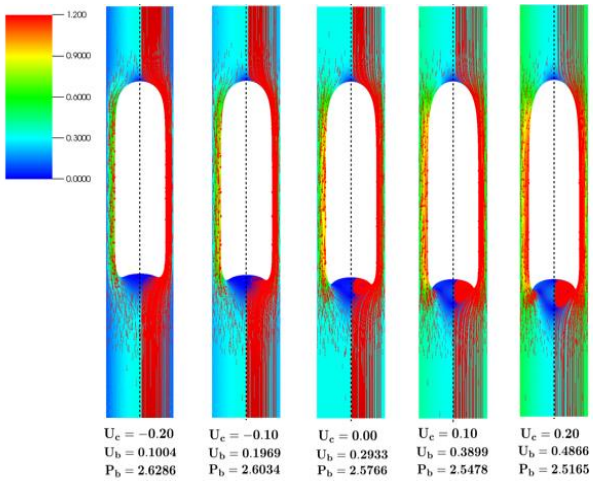

Figure 8: Effect of U_c on steady state bubble shape and the surrounding flow field at Nf = 80 and Eo = 180; showing streamlines and vector field superimposed on velocity magnitude pseudocolour plot on the right and left side of the symmetry axis.

For completeness and clearer perspective to the influence of inertia on bubble rise velocity and morphology, cases of upward and downward liquid flow are included in Figure 8 for a constant Nf = 80 and Eo = 180. The most apparent effect of inertia on the morphology and flow field around the Taylor bubble is the emergence and subsequent increase in the intensity of vortices in the bubble wake, accompanied by increased concavity of the bubble bottom, as the magnitude of liquid flow velocity decreases and increases in counter-current and co-current flows, respectively. This, as noted when discussing stagnant liquid case (Abubakar & Matar, 2021b), is linked to the increased magnitude of the liquid emerging from the film into the liquid slug, which is a manifestation of the increase in bubble rise velocity, as liquid changes from downward to upward flow and subsequent increase in the upward liquid velocity. Quantitatively, the effect of liquid flow imposition on the bubble rise velocity and jetting velocity are shown in Figure 9 and 10, respectively.

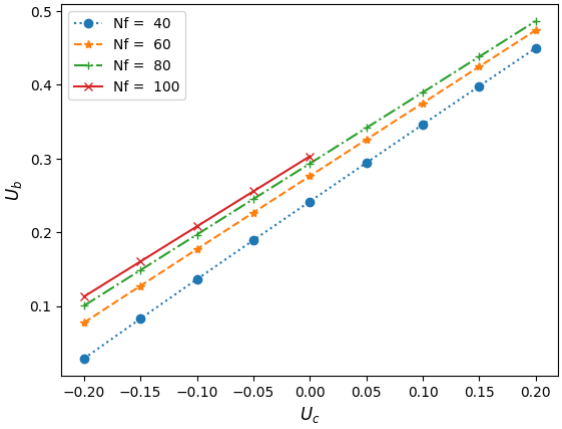

Figure 9: Effect of U_c on steady state bubble rise velocity at Eo = 180 and different Nf.

Noticeably also is the decrease in the curvature radius of the bubble nose with increase (resp. decrease) in the magnitude of the upward (resp. downward) liquid velocity. This pointing of the bubble nose can be attributed to the decrease in the normal stress, given by equation (17), exerted on the bubble nose relative to that in stagnant liquid as a result of the increased (resp. decreased) supportive (resp. opposing) inertia force in upward (resp. downward) liquid flow as the velocity magnitude is increased (resp. decreased).

$$\sigma_n = -\left[-p_T + 2Nf^{-1}\mathbf{n}.\frac{d\mathbf{u}}{d\mathbf{n}}\right] = P_b - Eo^{-1}\kappa \quad (17)$$

where σ_n denotes the normal stress in the direction of unit normal vector and p_T is the total pressure which is related to the hydrodynamic pressure by

$$p_T = p + z$$

DOI: 10.51975/21360205.som
Journal of the Nigerian Society of Chemical Engineers, 36(2), 2021

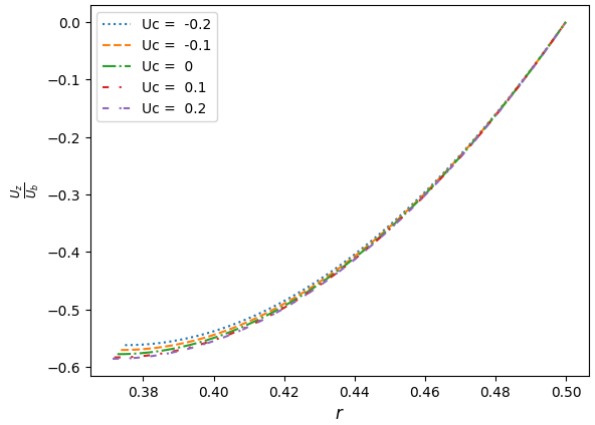

Figure 10: Effect of Froude number on axial velocity profile in the fully developed film region for Nf = 80 and Eo = 180 in a fixed frame of reference.

It is clear from Figure 11 that interface normal stress is a (resp. an) decreasing (resp. increasing) function of increased liquid velocity magnitude in upward (resp. downward) liquid flow.

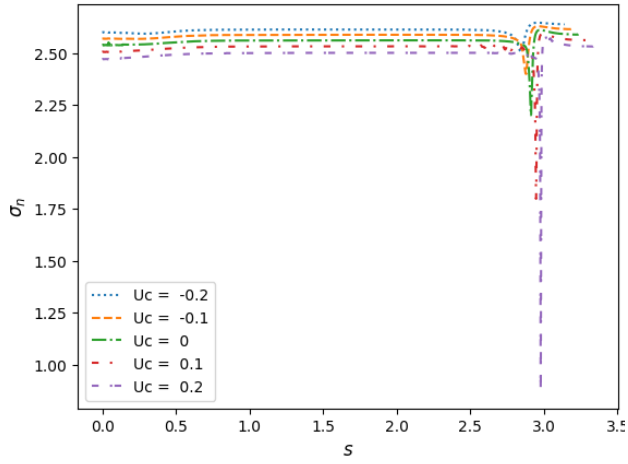

Figure 11: Effect of U_c on steady state interface normal stress (17) at Nf = 80 and Eo = 180.

Within the equilibrium film, as is the case for stagnant liquid, the normal stress, the total pressure and the bubble pressure less the curvature stress in the r − θ plane are equal, which is responsible for the observed decreased (resp. increased) in bubble pressure with increasing (resp. decreasing) upward (resp. downward) liquid flow velocity magnitude (see Figure 8). Outside the equilibrium film region, i.e the nose, developing film and bottom regions, it is the interplay between the viscous stress and total curvature stress that determines the shape of the regions. To clarify further (see Figure 12), the normal stress is modified by choosing the reference pressure to be the bubble pressure, so that (17) becomes

$$\sigma_n^* = -\left[-p_T^* + 2Nf^{-1}\mathbf{n}.\frac{d\mathbf{u}}{dn}\right] = -Eo^{-1}\kappa_b \qquad (18)$$

where κ_b is the curvature in the r−θ plane and

$$p_T{}^* = p_T - P_b$$

Thus, the equilibrium film region normal stress is equal to the curvature stress in the r−θ plane. As the nose region is approached, the net effect of viscous stress on the normal stress in upward (resp. downward) liquid flow is to decrease (resp. increase) the normal stress relative to that in a stagnant liquid, which in order to satisfy the normal stress balance at the interface, the total curvature stress has to increase (resp. decrease), leading to the observed decrease (resp. increase) in the radius of curvature of the nose for upward (resp. downward) liquid flow.

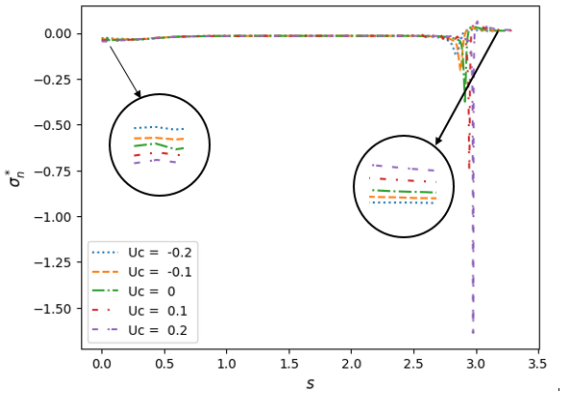

Figure 12: Effect of U_c on steady state modified interface normal stress (18) at Nf = 80 and Eo = 180.

4.0 CONCLUSIONS

The steady state solution of a Taylor bubble rising in flowing liquids characterised by the dimensionless Froude, inverse viscosity and Eötvös numbers is computed. The computation was carried out using previously validated Galerkin finite element method. The underlying physics governing the influence of the Froude number on the bubble shape elucidated, and the modification needed for the existing analytical solution to correctly predict Taylor bubble rise velocity in non-inertia regime suggested. Analysis of the results showed that it is the interplay between the viscous and curvature stresses that determines the shape of the nose, developing film and bottom regions. For upward (resp. downward) liquid flow, the bubble nose and bottom become pointed (resp. flattend) and concave (resp. convex) as the liquid velocity magnitude is increased.

REFERENCES

Abubakar, H. A. (2019). Taylor bubble rise in circular tubes: steady-states and linear stability analysis. PhD thesis, Imperial College London.

Abubakar, H. A. & Matar, O. K. (2021a). Taylor bubble rise in circular tubes: linear stability analysis. Submitted to J. Fluid Mech.

Abubakar, H. A. & Matar, O. K. (2021b). Taylor bubble rise in circular tubes: steady states numerical simulations. Submitted to J. Fluid Mech..

Bendiksen, K. (1985). On the motion of long bubbles in vertical tubes. Int. J. Multiphase Flow 11, 797–812.

Brown, R.A.S. (1965). The mechanics of large gas bubbles in tubes I. Bubble velocities in stagnant liquids. Can. J. Chem. Eng 43, 217–223.

Collins, R., De Moraes, F., Davidson, J. & Harrison, D. (1978). The motion of a large gas bubble rising through liquid flowing in a tube. J. Fluid Mech. 89, 497–514.

Davies, R.M. & Taylor, G. (1950). The mechanics of large bubbles rising through extended liquids and through liquids in tubes. Proc. R. Soc. Lond. A 200, 375–390.

Dumitrescu, D.T. (1943). Strömung an einer Luftblase im senkrechten Rohr. Z. Angew. Math. Mech 23 (3), 139–149.

Griffith, P. & Wallis, G. B. (1961). Two phase slug flow. ASME: J. Heat Transfer 83, 07–320.

Hecht, F. 2012 New development in FreeFem++. J. Numer. Math. 20 (3-4), 251–265.

Kang, C.W., Quan, S.P. & Lou, J. (2010). Numerical study of a Taylor bubble rising in stagnant liquids. Phys. Rev. E. 81, 1539–3755.

Lizarraga-Garcia, E., Buongiorno, J., Al-Safran, E. & Lakehal, D. (2017). A broadly applicable unified closure relation for Taylor bubble rise velocity in pipes with stagnant liquid. Int. J. Multiph. Flow 89, 345–358.

Lu, X & Prosperetti, A. (2009). A numerical study of Taylor bubbles. Ind. Eng. Chem. Res. 48, 242–252.

Nicklin, D., Wilkes, J. & Davidson, J. (1962). Two phase flow in vertical tubes. Trans. Inst. Chem. Engrs 40, 61–68.

Polonsky, S., Shemer, L. & Barnea, D. (1999). The relation between the Taylor bubble motion and the velocity field ahead of it. Int. J. Multiphase Flow 25, 957–975.

Viana, F., Pardo, R., Yánez, R., Trallero, J.L. & Joseph, D.D. (2003). Universal correlation for the rise velocity of long gas bubbles in round pipes. J. Fluid Mech. 494, 379–398.

White, E.T. & Beardmore, R.H. (1962). The velocity of rise of single cylindrical air bubbles through liquids contained in vertical tubes. Chem. Eng. Sci. 17, 351 361.

Zukoski, E.E. (1966). Influence of viscosity, surface tension, and inclination angle on motion of long bubbles in closed tubes. J. Fluid Mech. 25, 821–837.

DOI: 10.51975/21360206.som
Journal of the Nigerian Society of Chemical Engineers, 36(2), 2021

TECHNOECONOMIC ANALYSIS OF REFINING NIGERIAN LIQUEFIED NATURAL GAS CONDENSATE

***Oseni I. O.[1] Agbonghae E. O.[1] Nwaozuzu C. N.[2]**
[1]NNPC R&D Division, EPCL LifeCamp Complex, Eleme, Rivers State, Nigeria.
[2]Emerald Energy Institute (EEI), University of Port Harcourt, Choba, Rivers State, Nigeria
Corresponding Author: *Oseni I. O. (chemical_idrees@yahoo.co.uk)

ABSTRACT

Condensate refining is among the strategies proposed to solve the light oil glut around the globe. The Nigerian Liquefied Natural Gas (NLNG), which is the Nigerian government's best performing investment in the natural gas value chain, produces plant condensate as a by-product. In this paper, the economics of a refinery designed to use NLNG plant condensate is evaluated under an optimistic oil price forecast and a pessimistic oil price trend. A gasoline producing refinery configuration was chosen for this study, and it comprises of a naphtha splitter, a Penex isomerisation unit and a Continuous Catalytic Reforming (CCR) unit. The product yields and plant costs were determined by established correlations and industry estimates. The proposed refinery will convert 40,000 bpd plant condensate into 96% gasoline, 3% LPG and 1% hydrogen, and economic indicators such as Net Present Value (NPV), Internal Rate of Return (IRR) and Profitability Index (PI) were used to assess the economic viability of the refinery. The optimistic scenario of oil price forecast resulted in an NPV of $ 531.90 million, an IRR of 20.09% and a PI of 3.16, while the pessimistic scenario gave an NPV of $16.26 million, an IRR of 11.16% and a PI of 1.07. These results prove that a condensate refinery with the proposed configuration is economically feasible and interested investors in Nigeria's refining space should explore this possibility.

1. INTRODUCTION

Oil and gas contribute the most to the world energy mix (IEA, 2017), and a significant part of these are petroleum products like transportation fuels and petrochemicals. Therefore, nations must understand the dynamics of petroleum products demand and supply to guarantee energy security (Sovacool, 2012). Though renewable sources of energy are forecasted to grow in developing nations, the growth in petroleum energy demand is predicted to dwarf it up to 2040 (OPEC, 2017a). Nigeria's demand for gasoline increased by 50,000 bpd between 2012 and 2016 while its demand for diesel increased by 22,000 bpd (OPEC, 2017b). Nigeria has four refineries with a total capacity of 446,000 bpd, and they comprise the 210,000 bpd Port-Harcourt Refinery (old and new); the 125,000 bpd Warri Refinery; the 110,000 bpd Kaduna Refinery; and the 1,000 bpd Niger Delta Petroleum Resources Refinery. Nigeria has about 37.5 billion barrels of oil in proven reserves (OPEC, 2017b) but the bottleneck has been its failure in petroleum refining for domestic consumption, which has necessitated its heavy reliance on the importation of gasoline. Figure 1 shows the demand of petroleum products and Nigeria's local production in 2016 (OPEC, 2017b), and the difference was imported.

The Department of Petroleum Resources (DPR) has issued more than 30 licences for the establishment of new refineries in Nigeria to make up for the shortfall in domestic refining (DPR, 2018). The Dangote and OPAC Refineries are among the companies granted licensees that have made concrete moves towards establishment of their refineries. Other licensees are either sourcing for funding or at the design stage.

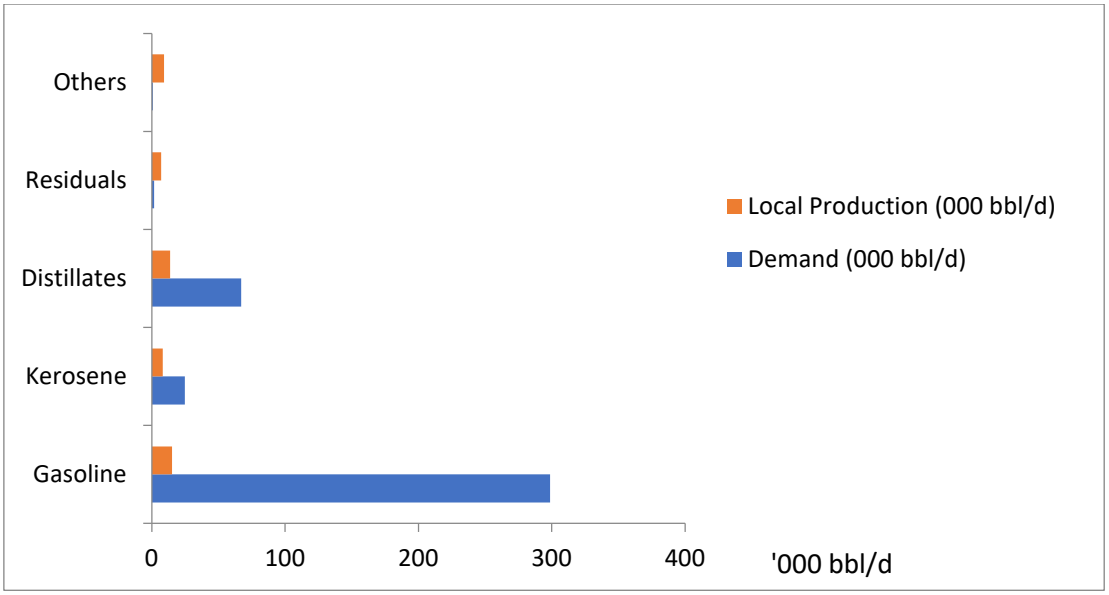

Figure 1: Nigeria's petroleum product demand versus local production 2016 (OPEC, 2017b)

There are different strategies that are used to improve transportation fuel pool in addition to traditional crude oil refining, and they include: whole naphtha blending with high octane gasoline (Lois *et al.*, 2003), use of Compressed Natural Gas (CNG) in place of transportation fuels (Tabar *et al.*, 2017), blending of biofuels with fossils fuels (Al-Mashadani & Fernando, 2017), and refining of Natural Gas Liquids (NGL) usually called gas condensates (Okorokov & Vilenskii, 1995).

Pyziur (2015) notes that condensates are used as diluents for heavy crudes, refinery blending feedstock, petrochemical feedstock, and boiler fuels but their increased production has necessitated its direct refining into gasoline.

Condensates are either lease condensates which are produced at the wellhead or plant condensates (also called natural gasoline) which are produced during natural gas processing activities (EIA, 2013) and more than 80% of condensates are of the lease type (Pyziur, 2015). Condensates can be refined like crude oil in a refinery. A condensate splitter or Condensate Fractionation Unit (CFU) is used to perform atmospheric distillation (Begum *et al.*, 2010). The main product of its distillation is naphtha, with kerosene, diesel, and some Liquefied Petroleum Gas (LPG) as co-products. The naphtha can be reformed to high octane gasoline or sold as petrochemical feedstock.

Condensate refining could be added to the mix of Nigeria's effort to close the demand and supply gap locally for petroleum products like gasoline and diesel.

Nigeria's plant condensate is from its numerous natural gas processing installations and Nigeria Liquefied Natural Gas (NLNG) plant. NLNG has the capacity to produce a minimum of 5 million tonnes per annum (mtpa) of plant condensate and LPG from its six trains which currently produce 22 mtpa of Liquefied Natural Gas (LNG), and the produced condensate is currently shared among the shareholders and exported by them. LNG plant condensate is usually very light and sweet, having been treated by the LNG process and hence, LNG plant condensate can easily be refined to petroleum products. Since NLNG has sixteen LNG long-term contracts with its clients (NLNG, 2018a), which guarantees its operations and availability of condensate feedstock for a refinery. This paper evaluates the techno-economics of locating a condensate refinery close to the NLNG plant in Bonny, Rivers State, Nigeria. The evaluation presented in this paper is pertinent because if a condensate refinery is successfully located close to NLNG plant, it would increase Nigeria's local refining capacity by adding value to the condensate produced by NLNG and save Nigeria some of the foreign exchange currently being spent in the importation of petroleum products.

There are several papers on condensate fractionation/refining modelling in the open literature and, to the best of our knowledge, none of them focused on the technoeconomics of condensate refining in Nigeria. Begum *et al.* (2010) used Aspen HYSYS V7.1 to model an actual condensate fractionation process in Bangladesh using different designs for the column and natural gas as feedstock, and their work only addressed condensate fractionation and excluded product upgrade

processes. Bentahar *et al.* (2013) studied the use of local materials to formulate catalysts that can convert condensate fractions into high quality gasoline through isomerization. Mohamed *et al.* (2016) determined the optimum configuration of an isomerization unit in the Mideast Oil Refinery (MIDOR) located in Egypt and their work resulted in better products specification and reduced costs. In the work of Mohamed *et al.* (2016), eight different configurations for the same feed conditions were investigated and they concluded that adding a de-isopentanizer to the existing plant was the most economic modification with a return on investment (ROI) of 26.6% for a product with a RON of 87. Adjimah and Luki (2017) assessed the economics of refining condensate against condensate sales for Atuabo Gas Processing plant in Ghana, and their study was based on estimating the potential products from refining condensate through comparison with an existing plant owned by Sinopec in China. The findings of Adjimah and Luki (2017) indicated positive higher NPV for the case of refining plant condensate but their economic analysis did not consider escalation of costs and depreciation of assets. Gary *et al.* (2007) presented some detailed installation cost estimates for refining units such as desalter, atmospheric distillation column, vacuum distillation, continuous catalytic reformer (CCR), isomerization unit, etc. in the US Gulf Coast. The estimates of Gary *et al.* (2007) did not include costs of utilities, storage, and product purification but they provided utility costs per barrel of raw material processed in the units.

2. METHODOLOGY

The methodology adopted for this work includes: (1) LNG plant condensate characterization, (2) process modelling and simulation and (3) Cost Estimation and Economic Analysis. Figure 2 shows the sequence of steps adopted for the techno-economic evaluation presented in this paper.

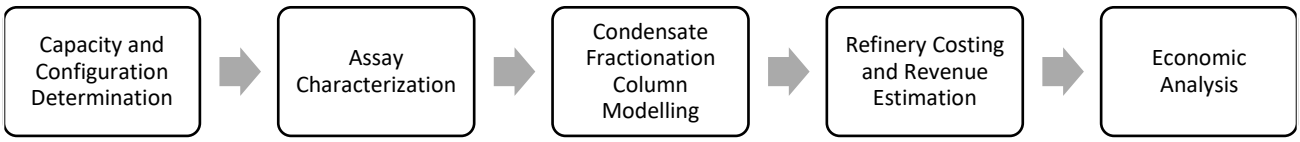

Figure 2: Research Steps.

2.1 LNG Plant Condensate Characterization

A commercial LNG plant condensate assay was used in this study. Table 1 shows some of its relevant properties, which include its density and ASTM D86 temperature profile (QatarPetroleum, 2018). Aspen HYSYS V8.0 was used for the characterization of the plant condensate, as well as the modelling of the CFU.

Table 1: Properties of Commercial LNG plant condensate

Parameters	Units	Method	Average	Low	High
Relative Density		ASTM D 40520	0.6665	0.6678	0.6696
API Gravity		ASTM D 129-80	79.88	80.4	99
SayboltColor		ASTM D 156+30	+30	+30	00
Free Water and Particulates		ASTM D 4176-94	Nil	Nil	Nil
B S & W	%vol	ASTM D 400795	Nil	Nil	Nil
RVP @ 100 ^{o}F	Psia	ASTM D 323-99/a	11.4	11.2	11.5
Distillation		ASTM D86			
Initial Boiling Point (IBP)	°C		36	35	37
10% Vol.	°C		46.5	46	47
50% Vol.	°C		58.5	57	60
90% Vol.	°C		100.5	99	102
Final Boiling Point (FBP)	°C		136	134	138
Recovery	%Vol.		99	99	99
Residue	%Vol.		0.5	0.5	0.5

2.2 Process Modelling and Simulation

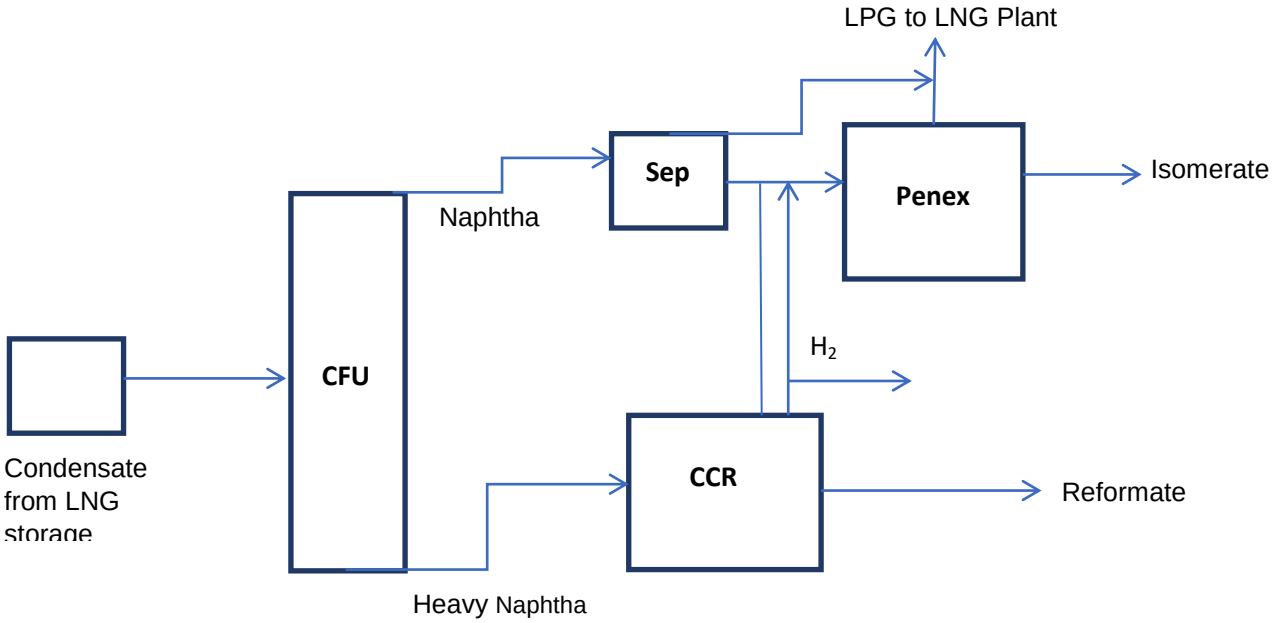

Figure 3: Block flow diagram (BFD) of adopted condensate refinery configuration

The suggested refinery configuration is shown in Figure 3. The condensate, which comprises mainly C_5 and C_6, is fractionated into light naphtha (LN) and heavy naphtha (HN). The light naphtha is converted into isomerate using the UOP Penex process while the heavy naphtha is converted to reformate using the UOP CCR process. A mixture of both products form the final gasoline output of the refinery. The capacity of the refinery is estimated as 40,000 bpd considering NLNG's 1.5 mtpa of condensate production and the condensate's density of 0.665g/cm^3.

Table 2: Some of the process parameters of the converged CFU model

Parameter	Value
Reflux Ratio	1.5
No of Trays	24
Feed Tray	10
Condenser Pressure	135.6 kpa
Reboiler Pressure	178.8
Tray Efficiency	80%
Feed Temperature	127 C

The Peng Robinson equation of state was used in the model as it has been proven to be accurate in predicting hydrocarbon behaviour. The CFU was modelled using a distillation column with a partial condenser and a reboiler. The process parameters used were based on an industrial naphtha splitter. Table 2 shows some of the process parameters of the converged CFU model.

The flowrates of the LN and HN were used to size the CCR and Isomerization units. The individual fixed capital cost components for the units were summed up to arrive at the total fixed cost or inside battery limit (ISBL) cost. The outside boundary limit (OSBL) cost was estimated as 10% of ISBL cost (i.e. 10% of the total capital cost). OSBL accounts for tankage, boilers,

cooling towers, power generation, etc. and the 10% estimate was utilized because NLNG has some of these facilities existing already. A working capital of 5% of total capital cost was also assumed in this study. The assumptions for OSBL cost and working capital were based on the recommendations of Towler and Sinnot (2008).

2.3 Cost Estimation and Economic Analysis

The Aspen Plus Economic Analyser, V8.0 (APEA®, V8.0), which is based on 20212 US Dollar, was used to estimate the capital cost (CAPEX) and operating cost (OPEX) of the CFU. The CFU CAPEX and OPEX include the costs of maintenance and operations, consumables, piping, electrical, overheads, tankage, utilities, etc. The costing of the isomerisation process unit was based on the work of Cusher (2003), who provided cost estimates and yields for a 10,000 bpd UOP Penex isomerization process on a 2001 US Dollar basis. The costing of the CCR process unit was estimated from the work of Lapinski et al (2003), who provided cost estimates for a 20,000 bpd UOP CCR process on a 1995 US dollar basis. The various cost estimates were translated to a capacity basis of 40,000 bpd and 2017 US Dollar basis in this study using the "sixth tenth" rule and the Nelson-Farrar indices. The reason for choosing 2017 as the base year of the economic analysis is because yearly data was available up to 2017 and this study was conducted in 2018.

The 2018 CPI forecasts of United States Energy Information Agency (US EIA) were used to estimate the operating costs and shipping costs over the economic life of the refinery. The price of condensate was estimated using naphtha prices as a proxy. The price of naphtha was taken as a discounted price of gasoline. Gasoline and LPG prices were forecasted using linearly regressed models between their prices and crude oil price. The regression models used monthly data between 2010 and 2017 from S&P Platts. The price of hydrogen was estimated as the cost of producing hydrogen based on the work of James et al (2016).

The following assumptions were used for the economic analysis in this paper:

i. The estimations in this work are based on NLNG's stated plant condensate production of 1.5 mtpa (NLNG, 2018a).
ii. Base year of analysis is 2017. This is because yearly data was available up to 2017 as at the time this study was undertaken, which is 2018.
iii. The economic life of the refinery is 16 years as mentioned by Mian (2011) in his analysis of US tangible property classification.
iv. Naphtha is considered a proxy for plant condensate. Naphtha (condensate proxy) is assumed to be 85% of gasoline price.
v. Considering S&P Platts data, a $15 difference is assumed as the 2017 cost of shipping (CIF plus trader margin) between West Africa (WA) and North West Europe (NWE).
vi. A discount rate of 10% is assumed.
vii. Condensate is priced at export parity (i.e. NWE free on board (FOB) price less shipping); gasoline is priced at import parity (i.e. NWE FOB price plus shipping), while LPG is priced at NWE Cost plus Insurance and Frieght (CIF) price less shipping.
viii. Hydrogen price is de-escalated by 1% each year, assuming technology causes a drop in its production cost. The price was assumed as the projected lowest cost of hydrogen production by James et al. (2016), which is $2,580 per ton of hydrogen
ix. The refinery is estimated to take one and half years for construction and six months for commissioning and start-up.
x. The plant is assumed to run for 8000 hours in a year or 333 days. This is to allow for plant maintenance and unanticipated shutdown.

The CPI indices were used to escalate future shipping costs. Initial capital allowance of 50% and annual capital allowance of 25% was used to compute depreciation allowance as stated in the Companies Income Tax Act (CITA). Revenue was determined by the yearly volumes of products. A tax rate of 30% was used as stated in CITA while Education tax (ET) was computed based on 2% of operating margin. The NPV, IRR, PI, and Government take were estimated to show the economic feasibility of the proposed condesate refinery. A sensitivity analysis was performed to show the response of the NPV to changes in discount rate, project capital cost, operating costs, naphtha/gasoline spread and shipping costs. Finally, the analysis compared the economic indices for EIA's optimistic oil price forecast to its low oil price forecasts.

3. RESULTS AND DISCUSSION

3.1 Process Modelling and Simulation Results

The Aspen HYSYS model converged with light naphtha from the top of the CFU and heavy naphtha from the bottom of the CFU. Table 3 shows the predicted flowrates of light naphtha and heavy naphtha products

with their ASTM D86 temperature profiles, while Table 4 shows the refinery products and the predicted gasoline research octane number (RON). The predicted light and heavy naphtha cuts temperature ranges are close to their standard specifications. The standard specification of light naphtha has a cut range of 25°C to 90°C while that of heavy naphtha is in the range of 85°C to 190°C. Figure 4 shows the converged Aspen HYSYS process model of the CFU.

Table 3 Model predicted product flowrates and D86 profile

Percentage	Light Naphtha	Heavy Naphtha
Flowrate (m^3/hr)	79.49	185.5
Flowrate (bpd)	28,000	12,000
D86 Profile (%)	Temperature (C)	
5	41.54	97.20
20	43.70	98.74
50	50.02	103.80
70	55.00	109.30
90	66.84	118.60
100	90.24	151.00

Table 4: Condensate refinery product summary

Product	Daily Prod. (ton/day)	RON
Gasoline Blend	4,071.80	92.76
LPG	138.06	
Hydrogen	24.55	

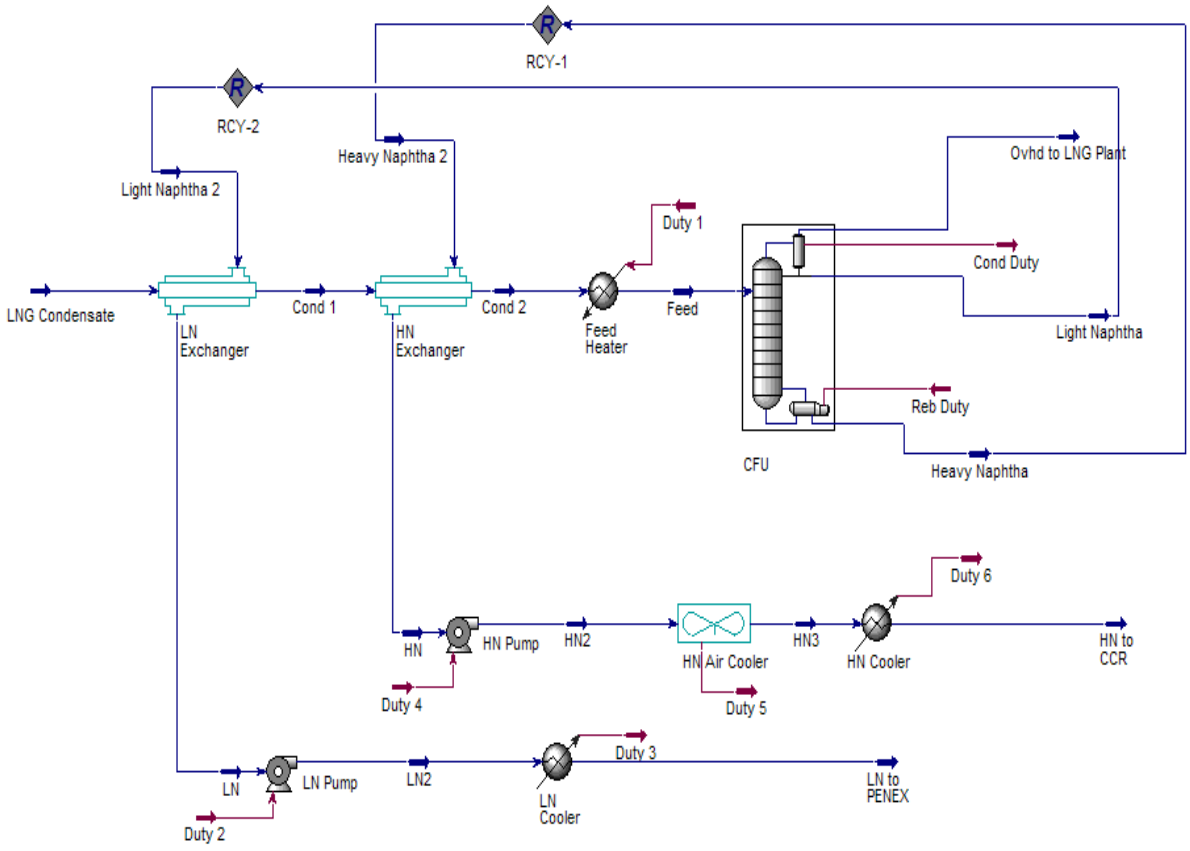

Figure 4: The converged CFU model on HYSYS

3.2 Estimated Costs and Economic Analysis Results

Table 5 shows the total costs of the condensate refinery in 2017 US dollar basis.

Table 5: Total condensate refinery capital and operating costs

Cost	$
Total Unit Capital Cost	213,526,277.18
OSBL cost	21,352,627.72
Working Capital	11,743,945.24
Total Capital Cost	246,622,850.14
Total Operating Cost	70,265,232.37

The regressed relationships between oil price with gasoline and LPG are as follows:

$$Gasoline_p = 8.1306Oil_p + 103.08$$

$$LPG_p = 8.2658Oil_p - 44.035$$

where Oil price is in $/bbl of Brent Crude and Gasoline price is in US$/ton of Gasoline 95RON 10ppm FOB ARA Spot Barges. LPG price is in $/ton of Average Propane/Butane CIF North West Europe (NWE)

Table 6: Profitability Indices

Index	Optimistic Case (Base Case)	Low Price Case
NPV Refinery (MM$)	531.90	16.26
Govt. Take (MM$)	548.32	89.30
Partners' Take (MM$)	271.27	8.30
Discounted PO (years)	5.30	17.23
ROI (%)	37.00	9.00
PI	3.16	1.07
IRR (%)	20.09	11.16

Table 6 shows the economic indices of the refinery for two different forecasts of oil price, and Appendix A contains the EIA oil price forecasts and CPI data. The Nigerian Government's take represents its 49% equity (which translates to dividends) and the taxes received. The refinery NPV for the optimistic case is positive and has a value of $531.90 million; the IRR is 20.09%, which is higher than discount rate of 10%. These two factors make the refinery economically feasible. The refinery will return an estimated $531.90 million (present value) on a CAPEX of $246.62 million and this return is equivalent to investing in a venture with a rate of return of 20.09%. This is higher than the assumed interest rate of 10% if the money is kept in a bank. The after-tax ROI is 37% and the PI of 3.16 is greater than one, which implies positive returns on the dollar. The investment would break even in about 6 years as implied by the discounted PO of 5.3 years.

The NPV for the low oil price case is positive at $16.26 million and the IRR is 11.16% which is marginally higher than discount rate of 10%. These two factors

make the refinery economically feasible; however, the low returns might encourage diversion of capital to other ventures. The refinery will return an estimated $16.26 million (present value) on a CAPEX of $246.62 million and this return is equivalent to investing in a venture with a rate of returns of 11.16%. The after-tax ROI is 9% and the PI is slightly greater than one at 1.07. This implies very little positive returns on the dollar. The investment would break even after 17 years as implied by the discounted PO of 17.23 years.

Oil prices strongly affect the profitability of the refinery eventhough the raw material is an LNG by-product. The comparison of the two cases shows that the higher the oil price the more profitable the refinery. This is because the price of gasoline, which mainly determines profitability, is positively correlated to the price of oil.
The government take is higher than its partners' take in both cases due to tax receipts. This makes the proposed condensate refinery beneficial to the government. The optimistic oil price case suggests the government could rake in about $100 Million yearly which is about 5% of the reported 2018 government subsidy of about $2 billion on gasoline (Vanguard, 2018).

The spider chart in figure 5 shows the sensitivities of the NPV of the investment to the data estimated for this study, which include: discount rate, OPEX (less raw material costs), CAPEX, Naphtha-Gasoline price ratio and shipping (CIF plus trader margin). The Naphtha-Gasoline price ratio affects the NPV the most and their relationship is inversely related. Every 5% increase in the Naphtha-Gasoline price ratio, which implied a decrease in price difference between gasoline and naphtha, results in about $300 million reduction of the NPV. Discount rate is also inversely related to NPV; however, its effect was far less than that of Naphtha-Gasoline price ratio. Every 10% change in discount rate results to about $50 million inverse change in NPV. OPEX and CAPEX affect the NPV of the investment slightly and they are inversely related to NPV. Every 10% change in these two factors result in about $10 million and $20 million changes in NPV. Shipping is the only factor that was directly related to NPV. Every 10% change in shipping results in about $30 million dollar change in NPV. This trend between NPV and Shipping is because of the import parity pricing of gasoline; an increase or decrease in shipping costs implies a huge increase or decrease in gasoline revenues and by implication NPV.

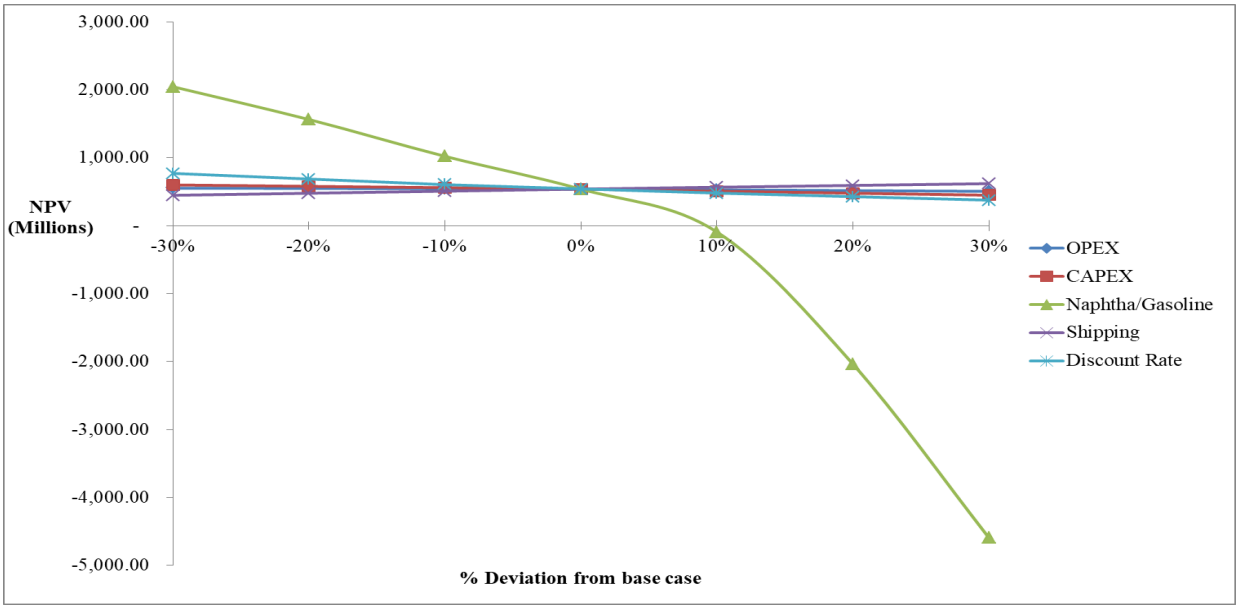

Figure 5: Sensitivity analysis of estimated factors

The difference between the gasoline price and plant condensate price which is represented by Naphtha-Gasoline price ratio is a major determinant of the profitability of the project. An increase in this ratio results in lower profitability or infeasibility of the project and vice-versa. The break-even ratio (i.e. when NPV is zero) for the optimistic case is 0.928 while that of the low oil price case is 0.855. Above these ratios, the proposed condensate refinery will be economically infeasible.

The effect of costs estimation has a less significant effect on the economics of the plant. The CAPEX and

OPEX were based on costs estimate which may have errors of up to 50% from actual costs. The sensitivity analysis showed that a 30% deviation from actual costs does not change the NPV significantly or result to economic infeasibility.

The CIF and trader margin represented by shipping estimate is significant to the economics of the refinery. This is because the gasoline revenue is based on import parity pricing. It trends proportionately to the NPV. The higher the shipping rates, the higher the import parity price of gasoline sold by the refinery.

The tax allowances for the parent NLNG plant as stated in the NLNG Act Schedule (2) (if any still exist) was not applied to the proposed condensate refinery since the condensate refinery will not be producing a pioneer product; however, an argument can be made for the pioneer nature of the process.

4. BENEFITS OF THE PROPOSED NLNG CONDENSATE REFINERY WORK

The techno-economic analysis of the condensate refinery proposed in this paper throws up the following benefits:

- The refinery has a gasoline capacity of about 5 million litres daily. This is about 10% of Nigeria's current consumption. Producing gasoline and selling at CIF Nigeria prices saves a part of subsidy paid for mother vessels demurrage as they are offloading into smaller vessels. This cost is pegged at $280,000 maximum for a period of 10 days by the Petroleum Products Pricing Regulation Agency (PPPRA). NLNG produced gasoline can be transported by smaller vessels.
- This investment can result to an increase in the tertiary education tax fund (TET Fund) which would translate to benefit for the educational sector of Nigeria.
- The refinery would pay investors what they currently earn from selling condensate since it would buy its raw material (condensate). This represents the current model of NLNG where it sells plant condensate. Therefore, the suggestion of a condensate refinery does not change its current earnings; it only presents an opportunity to increase its earnings through investment.
- The analysis is denominated in dollars due to the nature of oil and gas business and Nigeria's reliance on importation of plants machinery and parts. However, the refinery products are meant for the local market and would be bought by Nigerian petroleum marketers. Government could ensure all transactions are done in naira so that foreign exchange expenses on petroleum products could be reduced.

5. CONCLUSION

This paper shows that NLNG plant condensate could be used as feedstock for the production of gasoline by using a condensate refinery with isomerization and catalytic reforming process units. The unit capital cost of the refinery was estimated as $6000 per barrel. NLNG's current production of a minimum of 1.5 mtpa of condensate guarantees the raw material supply for a 40,000bpd condensate refinery. The suggested configuration will convert 40,000 bpd plant condensate into 96% gasoline, 3% LPG and 1% hydrogen.

The optimistic scenario of oil price forecast resulted in an NPV of $ 531.90 million, an IRR of 20.09% and a PI of 3.16, while the pessimistic scenario gave an NPV of $16.26 million, an IRR of 11.16% and a PI of 1.07. The government take for the optimistic case is $548.30 million while that of the low oil price case is $89.30 million. This proves the proposed condensate refinery is economically feasible provided that the Naphtha-Gasoline price ratios are low enough, which is very likely.

The benefits to the Nigerian government would include improved product supply by cutting lead time of some gasoline delivery, improved NLNG dividends that could upset about 5% of Nigeria's current subsidy, increased employment, reduced foreign exchange expense and increased technology transfer.

In summary, this work can serve as a primer to a more detailed analysis of the possibilities that lie in the NLNG condensate refinery investment proposed in this paper. Policy makers could also use this work as a basis for discussion on a quick way to satisfy petroleum products demand.

NOMENCLATURE

APEA	Aspen Plus Economic Analyser
ARA	Amsterdam-Rotterdam-Antwerp
ASTM	American Society for Testing and Materials
CAPEX	Capital Expenditure
CCR	Continuous Catalytic Reforming
CIF	Cost plus Insurance and Freight
CITA	Companies Income Tax Act

CNG	Compressed Natural Gas
CFU	Condensate Fractionation Unit
CPI	Consumer Price Index
DPR	Department of Petroleum Resources
EIA	Energy Information Administration
ET	Education tax
FOB	Free on Board
HN	Heavy Naphtha
IEA	International Energy Agency
IRR	Internal Rate of Return
ISBL	Inside Battery Limit
LN	Light Naphtha
LNG	Liquefied Natural Gas
LPG	Liquefied Petroleum Gas
MIDOR	Mideast Oil Refinery
NGL	Natural Gas Liquids
NPV	Net Present Value
NLNG	Nigerian Liquefied Natural Gas
NEW	North West Europe
OPEC	Organization of the Petroleum Exporting Countries
OPEX	Operating Expenditure
OSBL	Outside Boundary Limit
PI	Profitability Index
PO	Pay Out
PPPRA Regulation	Petroleum Products Pricing Agency
ROI	Return on Investment
RON	Research Octane Number
TET	Tertiary Education Tax Fund
US	United States

REFERENCES

Adepetun, S., & Kemi, S. (1996). The Liquefied Natural Gas Project. *Energy Policy, 24*(6), 593-596.

Adjimah, J. O., & Luki, B. N. (2017). Assessing The Economic Cost Benefit Analysis of Fractionating Raw Condensate Into Specific Products by the Atuabo Gas Processing Plant Ghana. *Journal of Economics and Sustainable Development, 8*(10), 64-94.

Al-Mashadani, H., & Fernando, S. (2017). Properties, performance, and applications of biofuel blends: a review. *AIMS Energy*, 735-767.

Alsahhaf, T. A., Fahim, M. A., & Elkilani, A. (2010). *Fundamentals of Petroleum Refining.* Amsterdam: Elsevier.

Begum, D. A., Rahman, A., & Kirtania, K. (2010). Condensate Fractionation Column: Design Variation study by Simulation. *Journal of Chemical ENgineering, 25*(1), 65-70.

Bentahar, N., Khelassi, S., & Abdelrazek, F. (2013). Production of Clean Gasoline from Condensate. *Egyptian Journal of Petroleum, 22*, 345 - 350.

Chang, A.-F., Pashikanti, K., & Liu, Y. A. (2012). *Refinery Engineering: Integrated Process Modeling and Optimization.* Weinheim: Wiley-VCH.

Cusher, N. A. (2003). UOP Penex Process. In R. A. Meyers, *Handbook of Petroleum Refining Processes.* McGraw-Hill.

DPR. (2018). *Licensed refineries in Nigeria granted as at April 2018* . Retrieved September 22, 2018, from Department of Petroleum Resources Website: https://www.dpr.gov.ng/downstream/refinery/

EIA. (2013). *EIA's Proposed Definitions for Natural Gas Liquids.* Washington DC: US Energy Information Administration.

EIA. (2018). *Analysis and Projections: Annual Projections to 2050*. Retrieved November 11, 2018, from US EIA: https://www.eia.gov/analysis/projection-data.php#annualproj

Favennec, J. P., & Pegyre, A. (2001). Refining: A technical summary investments, margins, costs, probable future developments. In J. P. Favennec, *Refinery Operation and Management* (Vol. 5). Paris: Technip.

Gary, J. H., Handwerk, G. E., & Kaiser, M. J. (2007). *Petroleum Refining Technology and Economics* (5th ed.). Boca Raton: CRC.

IEA. (2017). *World Energy Report.* Paris: International Energy Agency.

James, B. D., DeSantis, D. A., & Saur, G. (2016). *Final Report: Hydrogen Production Pathways Cost Analysis (2013 - 2016).* Arlington: Strategic Analysis Inc.

Kaes, G. (2000). *A Practical Guide to Staedy State Modeling of Petroleum Processes* (1st ed.). Colbert: Kaes Enterprises Inc.

Lapinski, M., Baird, L., & James, R. (2003). UOP Platforming Process. In R. A. Meyers, *Handbook of Petroleum Refining Processes* (pp. 4.3-4.31). McGraw-Hill Education.

Lois, E., Gupta, A. K., & Keating, E. L. (2003). Fuels. In Third (Ed.), *Encyclopedia of Physical Science and Technology* (pp. 275 - 314).

Ludwig, E. E. (1999). *Applied Process Design for Chemical and Petrochemical Plants* (3rd ed., Vol. 1). Houston: Butterworth-Heinemann.

Meyers, R. (2003). *Handbook of Petroleum Refining Processes.* McGraw-Hill.

Mian, M. A. (2011). *Project Economics and Decision Analysis: Deterministic Models* (2nd ed., Vol. 1). Tulsa: PennWell Corporation.

Mohamed, M. F., Shehata, W. M., Abdel Halim, A. A., & Gad, F. K. (2016). Improving gasoline quality produced from MIDOR light naphtha isomerization unit. *Egyptian Journal of Petroleum*.

Nairametrics. (2017, June 9). *30% of Nigeria's forex was spent on fuel importation in 2016 fuel importation in 2016*. Retrieved September 22, 2018, from Nairametrics Website: https://nairametrics.com/30-of-nigerias-forex-was-spent-on-fuel-importation-in-2016/

NLNG. (2018a). *NLNG Facts and Figures*. Retrieved Spetember 23, 2018, from NLNG website: http://nlng.com/Media-Center/Pages/Fasts-and-Figures.aspx

NLNG. (2018b). *NLNG News.* Retrieved March 06, 2019, from NLNG Website: http://www.nlng.com/NIGNLNG/News.aspx?ID=31

NLNG. (2018c). *NLNG products*. Retrieved September 22, 2018, from NLNG website: http://www.nlng.com/Business-with-NLNG/Pages/Our-Products.aspx

NLNG. (2018d). *Profile*. Retrieved September 23, 2018, from NLNG Website: http://www.nlng.com/Our-Company/Pages/Profile.aspx

NNPC. (2018). *NNPC, NLNG committed to Train 7 Realization*. Retrieved September 23, 2018, from NNPC Group Website: http://nnpcgroup.com/PublicRelations/NNPCinthenews/tabid/92/articleType/ArticleView/articleId/91/NNPC-NLNG-committed-to-Train-7-Realization.aspx

Nwaoha, C., & Wood, D. A. (2014). A review of the utilization and monetization of Nigeria's natural gas resources: Current realities. *Journal of Natural Gas Science and Engineering, 18*, 412-432.

Okorokov, V. A., & Vilenskii, L. M. (1995). Modular units for the refining of oil and gas condensate into motor fuels. *Chemical and Petroleum Engineering, 31*, 718-721.

OPEC. (2017a). *Annual Statistical Bulletin.* Vienna: Organization of the Petroleum Exporting Countries.

OPEC. (2017b). *World Oil Outlook.* Vienna: Organization of the Petroleum Exporting Countries.

Parkash, S. (2003). *Refining Processes Handbook.* Burlington: Elsevier.

Punchng. (2018, August 30). *We've paid $15bn dividends, $6.5bn taxes to FG*. Retrieved September 23, 2018, from Punch Newspaper website: https://punchng.com/weve-paid-15bn-dividends-6-5bn-taxes-to-fg-nlng/

Pyziur, M. (2015). *Condensate: An EPRINC primer.* Washington: Energy Policy Research Foundation Inc.

QatarGas. (2018). *Laffan Refinery*. Retrieved September 22, 2018, from QatarGas Website: http://www.qatargas.com/english/operations/laffan-refinery

QatarPetroleum. (2018). *Condensates*. Retrieved September 23, 2018, from Qatar Petroleum Website: https://www.qp.com.qa/en/marketing/Documents/Plant_Condensate.pdf

Silla, H. (2003). *Chemical Process Enginnering: Design and Economics.* New York: Marcel Dekker Inc.

Sovacool, B. K. (2012). Energy Security: Challenges and Needs. *WIREs Energy Environ, 1*, 51-59.

Tabar, R. A., Hamidi, A. A., & Ghadamian, H. (2017). Experimental investigation of CNG and gasoline fuels combination on a 1.7 L bi-fuel turbocharged engine. *International Journal of Energy and Environmental Engineering, 8*, 37-45.

ThisDayLive. (2018, July 11). *nlng-pays-off-shareholders-5-45bn-borrowed-to-build-six-lng-trains*. Retrieved September 23, 2018, from ThisDayLive Website: https://www.thisdaylive.com/index.php/2018/07/11/nlng-pays-off-shareholders-5-45bn-borrowed-to-build-six-lng-trains/

Towler, G., & Sinnot, R. (2008). *Chemical Engineering Design: Principles, Practice and Economics of Plant and Process Design.* Burlington: Butterworth-Heinemann.

Towler, G., & Sinnot, R. (2008). *Chemical Engineering Design: Principles, Practice and Economics of Plant and Process Design* (3rd ed., Vol. 6). Burlington: Butterworth Heinemann.

Vanguard. (2018, June 19). *Fuel subsidy hits N2.4bn daily* . Retrieved September 22, 2018, from Vanguard News: https://www.vanguardngr.com/2018/06/fuel-subsidy-hits-n2-4bn-daily/

APPENDIX A

US EIA Forecasted Oil prices and CPI Data (EIA, 2018)

Year	CPI (Energy Commodities and Services)	EIA Optimistic Forecast for Brent Price ($)	EIA Low Oil Price Forecast for Brent Price ($)
2016	1.90	43.74	43.74
2017	1.99	52.43	52.43
2018	2.02	54.07	27.71
2019	2.13	58.85	30.68
2020	2.36	75.10	33.28
2021	2.50	85.10	36.99
2022	2.60	90.74	38.03
2023	2.71	95.75	39.32
2024	2.82	99.92	40.48
2025	2.90	103.74	41.55
2026	2.97	108.32	42.42
2027	3.06	112.26	44.49
2028	3.14	116.82	45.81
2029	3.24	121.29	47.25
2030	3.32	125.27	48.65
2031	3.42	130.82	50.81
2032	3.51	135.07	52.43
2033	3.60	139.99	54.37
2034	3.70	145.44	56.42
2035	3.79	150.43	58.53
2036	3.89	154.57	60.73
2037	4.01	161.98	63.59
2038	4.12	167.53	65.84
2039	4.24	172.93	68.53
2040	4.35	178.98	71.08

DOI: 10.51975/21360207.som
Journal of the Nigerian Society of Chemical Engineers, 36(2), 2021

REDUCING UNEMPLOYMENT IN NIGERIA – THE ROLE OF TERTIARY INSTITUTIONS IN THE ENTREPRENEURIAL DEVELOPMENT OF ENGINEERING GRADUATES

Aluyor, E.O. and *Otoikhian, S.K.
Department of Chemical Engineering, Edo State University Uzairue, Edo State, Nigeria.
*Corresponding author e-mail: otoikhian.kevin@edouniversity.edu.ng

ABSTRACT

In Nigeria, the number of unemployed persons in recent times increased to 23,187,000 in the fourth quarter of 2020 from 21,765,000 in the second quarter of 2020, hence this paper is an exposition on the role of tertiary institutions in the entrepreneurial development of engineering graduates most of whom are unemployed. A brief discuss on the need for engineering-based entrepreneurship is presented. The key challenges hindering engineering entrepreneurship in Nigeria are highlighted. Some of the roles and strategies which the tertiary institutions in Nigeria can deploy to foster entrepreneurship amongst engineering graduates are presented and include; highly functional and strategic entrepreneurship development centers with think tanks, funding support for the most promising business ideas of students, business and entrepreneurship-motivated research, engaging with government and policymakers to make entrepreneurship fostering policies and minimize bottlenecks to business amongst others. Edo State University Uzairue is presented as a case study of a tertiary institution in Nigeria that has taken some steps in the right direction as regards entrepreneurial development. It is concluded that all stakeholders such as the government, industry, NGOs, and the students/graduates must partner with the tertiary institutions to achieve commendable results on the uphill task under consideration.

Keywords: *Entrepreneurship, tertiary institutions, engineering, unemployment, development, Nigeria.*

1.0 INTRODUCTION

Engineers are expected to be innovative, problem solvers, and highly resourceful. Entrepreneurship on the other hand entails identifying a gap and/or a problem and establishing a business to bridge the identified gap or solve the problem in return for profit. It is glaring that Nigeria has a plethora of challenges and problems to be solved. Challenges such as insecurity, food shortage, water shortages, poor power supply, and over-reliance on import-based products amongst many others are some of the challenges to be tackled via engineering entrepreneurship. It is thus superfluous to mention that a well-trained engineer with adequate exposure and training in business and entrepreneurship skills will find Nigeria a goldmine, a place with ample business opportunities. Some of the many challenges bedeviling Nigeria are opportunities in disguise. However, the potentials of these opportunities will never be realized without entrepreneurial strides (Nnanna & Opara, 2012; Fulgence, 2015).

The Chemical Engineering curriculum, for example, covers the core areas of Chemical Engineering such as chemical reaction engineering, chemical engineering design, transport phenomena, biochemical engineering, environmental engineering, engineering economics, software application in chemical engineering, etc. as well as the required foundational courses (Aluyor et al., 2019). This is comparable to other engineering curriculums from a variety of engineering divisions, however, they have failed to address the country's severe unemployment problem.

The Malaysia Education Blueprint 2015 – 2025 (Higher Education) (MEB 2015-2025), for example, was launched by the Ministry of Education in recognition of the importance of entrepreneurship development in the country. It requires academic programs in institutions of higher learning (IHL) to include entrepreneurship education to produce graduates with entrepreneurial skills (Karim, 2016). The Ministry of Education wants all IHL graduates to be employment creators rather than job seekers. Even before they graduate, students should be encouraged to establish their businesses (Ministry of Education Malaysia, 2015). This new direction by the Malaysian Ministry of Education has paved the way for a review and modification of the Bachelor of Civil Engineering (Honours) program (BCE (Hons)) at Universiti Tenaga Nasional (UNITEN) to promote entrepreneurship education and foster entrepreneurial

capabilities among its alumni (Karim, 2016).

The Massachusetts Institute of Technology (MIT) was also studied for the economic impact of entrepreneurship and it was discovered that 50 to 100 percent more engineering than science alumni went on to establish companies. Researchers found that engineering students were just as likely to start their businesses than business majors were and that more than 20 percent of MIT's total founders were from the electrical engineering and computer science department amongst others (Roberts & Eesley, 2009). Thus, the number of courses, programs, and experiential learning opportunities that teach engineering students about entrepreneurship has increased significantly. This initiative has received support from influential publications and professional organizations such as the National Academy for Engineering (NAE) and the American Society for Engineering Education (ASEE) (Rover, 2005).

Not many engineering-based entrepreneurial initiatives and support, however, have been witnessed amongst the graduates of engineering programs in Nigeria. The most popular career path amongst these graduates is to seek white-collar or blue-collar employment in already established firms or companies. Most engineering graduates end up underemployed, working in non-engineering positions in these companies, receiving paltry salaries, and may never get to apply the many years of core engineering training received, yet many others remain unemployed (Dean & Rubrica, 2018). The number of unemployed persons in Nigeria increased to 23,187,000 in the fourth quarter of 2020 from 21,765,000 in the second quarter of 2020 (NBS, 2021).

What are the key challenges inhibiting engineering entrepreneurship in Nigeria? What are some of the things that the tertiary institutions in Nigeria can do to help to surmount these challenges? This paper attempts to presents some answers to these questions.

2.0 ENTREPRENEURSHIP IN ENGINEERING

Most engineering graduates who have ventured into businesses and entrepreneurial activities have not done so in areas that utilize their technical engineering training. It is not uncommon to see a trained/training engineer going to also train as a barber or tailor for some months either *pari passu* or post their engineering training in the tertiary institutions. These engineering graduates then begin a barber's shop or practice tailoring (sometimes packaged as fashion designing) as entrepreneurship. So when the average engineering graduate is asked about entrepreneurship, what readily comes to her/his mind is starting a trading business or learning a semi-skilled craft which they will then practice, usually as a backup plan to landing some white-collar job in a large multi-national corporation. This level of entrepreneurial engagement is not out of place as it also serves to mitigate the endemic unemployment challenge along with its attendant consequences in the country. The thrust of this paper, however, is to go beyond this surface-level scope and understanding of entrepreneurship to explore entrepreneurial possibilities and efforts based on the application of core engineering training, technical know-how, and business competence.

The major challenges to engineering-based entrepreneurship activities include; lack of awareness or deficiency in ideas for entrepreneurship in engineering, difficulty in accessing business capital, and a foreboding business environment in Nigeria. A 2019 World Bank Report ranked Nigeria 131st economies in the world for ease of doing business an improvement from the 146th that was recorded in 2018, policies that create bottlenecks for entrepreneurial-minded persons, an educational system that is not entrepreneurship-focused but rather overly employee production focused, high cost of capital for business amongst several other issues make fostering engineering entrepreneurship in Nigeria an uphill task (Metu and Nwokoye, 2014; Ofili, 2014; Okeke and I, 2014).

3.0 THE ROLE OF TERTIARY INSTITUTIONS

In tackling the challenges itemized in the previous section, the tertiary institutions should do the following;

i. Institute or revolutionize entrepreneurship development centers.

All world-class institutions of higher learning in developed countries have highly functional entrepreneurship development centers. These centers which come in different names for different institutions provide training to students on how to translate ideas to viable businesses. They provide consultancy services to both staff and students to translate their business ideas into actual businesses. These centers oversee annual entrepreneurship ideas competitions amongst university students, sourcing and providing funds to students with the best business ideas. These centers are in constant

dialogue with industry, government, and NGOs to generate funding as well as identify key areas for business development, they provide mentorship and guidance for business start-ups by students or recent graduates. They are at the heart of the entrepreneurial strides and engagements of the top universities. Many universities in Nigeria already have such centers instituted but these centers do not do more than administering a 2-credit unit course to 3rd or 4th-year students. Furthermore, the design and assessment of these courses are such that the students could earn credit without a practical understanding of entrepreneurship. The activities of these centers cannot be said to have translated to significant entrepreneurial breakthroughs especially with regards to entrepreneurship in engineering and technology with which this paper is concerned.

The operations of these centers should be expanded to accommodate more deliverables and services. The entrepreneurship courses should run through the curriculum from the first year to the final year with the first-year entrepreneurship courses providing general training in entrepreneurship and business and the higher-level courses between the third and fifth years providing robust and pragmatic training on entrepreneurship in engineering and technology. These courses may further be narrowed down to provide discipline-specific training on how the core technical knowledge from a given engineering discipline can be translated into entrepreneurial engagements. Engineering students should be trained to see entrepreneurial opportunities within their specific disciplines as well as in collaboration with other engineering and even non-engineering disciplines. In reality, no business can be established on the strength of a single discipline, a synergy amongst several disciplines is required to tackle the multi-faceted challenges in Nigeria and Africa at large and create businesses by so doing.

ii. A specially designed final-year entrepreneurship course project

Project-based learning is a key strategy for transferring and imbuing skills in students (Harmer, 2014). It is suggested that a good way to prod would be engineering graduates to begin to seriously consider and generate ideas for entrepreneurial exploits is to base the assessment of the final-year course on entrepreneurship on a detailed end-of-course business plan project. This business plan project should be undertaken by an interdisciplinary team of students with each member of the team contributing her/his technical know-how to the business idea and the plan for its execution. The business idea from engineering students should serve to tackle a local prevalent technological challenge like, as an example, developing and delivering affordable and scalable solar power solutions to homes to tackle the national energy crisis, not setting up a barber's shop, well maybe there is some engineering challenges in setting up a barber's shop but such should not be the type of engineering entrepreneurship breakthroughs and engagements that should be encouraged amongst engineering graduates who have undergone a 5-year rigorous training.

Furthermore, the plan should address pertinent issues such as sourcing for start-up funds, the techno-economic challenges to be faced, and how they will be surmounted amongst other issues. The best business plans amongst the pool of submissions could be supported with grants from the institutions of higher learning. This project should be carried out in partnership with industry and other businesses that may want to buy into or invest in some of the developed business ideas. Also, the higher-level courses in entrepreneurship should be delivered by not just academics (who have probably never established an engineering and/or technological based business or venture)

iii. Provide support on accessing capital for engineering and technological business solutions.

One of the biggest challenges to entrepreneurship in engineering is the huge start-up capital required. Institutions of higher learning could assist by serving as venture capitalists and also helping to engage and secure other investors for the most promising business ideas presented by engineering students. These businesses when successful will yield a good return on investment (ROI) to the institutions of higher learning and other investors while curbing the unemployment menace and solving a real-life problem based on applied engineering and technology. It becomes a win-win for all parties involved and for society at large.

Furthermore, the institutions of higher learning can leverage their strong rapport with banks and other financial institutions to secure healthy loans for these businesses with the institutions of higher learning serving as guarantors of the loan in exchange for some financial benefits from the businesses. The institutions of higher learning can engage in dialogue with funding organizations such as TETFund, NGOs, and private companies on funding for the best business proposals identified.

iv. Instill a possibility mentality in the engineering students

The average engineering student and recent graduate does not think much of the possibility for engineering and technology-based entrepreneurship exploits from a student or recent graduate. The mindset is that there are just too many challenges militating against the successful operation of an engineering and technology-based business in Nigeria. The poor state of infrastructural development, perceived inadequacy of government support, socio-economic instability, and the constant & complex interplay of political interests and powers in the country portends engineering entrepreneurship as a foreboding endeavor to undertake. The level of self-belief and motivation for engineering entrepreneurship is very low, hence the average engineering graduate will almost always run after paid employment positions rather than attempting to venture into the uncertain waters of entrepreneurship. The institutions of higher learning have a key role to play in creating a positive mindset concerning entrepreneurship and awakening the entrepreneurial spirit amongst students and recent graduates of engineering disciplines. Playing roles like normalizing struggles, simulating real-life challenges, and encouraging engagements with several methods of tackling them, mindset restructuring, and close mentorship as practical as the use of "possibility phrases words" like "not yet", "not entirely", demonstrating mistakes and embracing and celebrating corrections, etc. among numerous other proven steps can instill a "possiblilty mentality".

v. Core engineering courses should be delivered with a bias towards industrial practice, entrepreneurship, and soft skill development.

Students should be made to see and understand the practical applications of the core concepts that they learn in class. One cannot normally conceive a business idea from a potpourri of theoretical and mathematical abstractions without any link to real-life applications (Aluyor, Otoikhian, and Agbodekhe, 2019).

Furthermore, there is a need for the transfer of soft skills necessary for the successful management of people and resources as would be expected of any successful entrepreneur to be imbued in the delivery of the core engineering courses. There is a growing requirement for entrepreneurs and workers to exhibit a broad repertoire of soft skills such as excellent communication skills, strong leadership abilities, teamwork, adaptability, conflict resolution, problem-solving, etc. as the global business sector undergoes a rapid transformation. (Chikumba, 2011; Lowden *et al.*, 2011; Pitan and Adedeji, 2012; Choudary, 2014; Bakhshi *et al.*, 2017; Oloyede, Ajimotokan and Faruk, 2018).

vi. Creation of think tanks within the entrepreneurship development centers

The entrepreneurship centers should have as a core unit within it a think tank made up of the most forward and astute thinkers drawn from across the breadth and depth of the university community including academics, non-academics, and even specially selected students themselves. The functions of this think tank should include frequent brainstorming sessions/meetings on identifying, analyzing, and characterizing the myriads of challenges facing entrepreneurial developments amongst graduates coupled with well-thought-out potential and pragmatic solutions to these challenges. The reports and recommendations of such think tanks should be made available to the university community, relevant government organizations, NGOs, and industry with input welcome from all stakeholders. This think tank should also be responsible for research and studies on the state of entrepreneurial developments amongst graduates of the given institution of higher learning. A key factor in the success of any strategy is a firm establishment of robust feedback, monitoring, and evaluation (FME) system. The think tank should spearhead the FME of the entrepreneurial development initiatives of the institutions of higher learning.

vii. Engage with the government on engineering entrepreneurship friendly policies

The institutions of higher learning as citadels of knowledge should be at the forefront in engaging with government and policymakers to foster the creation and promotion of policies that enhance and incentivizes engineering entrepreneurship while putting away needless bottlenecks to smooth business operations in Nigeria.

viii. Research should be driven by their potential for commercialization

There is a need for more of the research activity by academia and students in the institutions of higher learning to be guided and motivated by the potential(s) of the results of these research (if successful) to be commercialized. This will result in researching business and entrepreneurship coupled with innovative solutions to real-life problems in mind.

ix. Outcome-Based Education as a driver for entrepreneurship

Outcome-Based Education (OBE) is a strategic approach to education that entails a clear definition of

the intended destination (outcomes) of the educational process before the journey is started. Outcome-Based Education (OBE) can be deployed by tertiary institutions to develop graduates that are poised to take up entrepreneurial initiatives. The OBE requires that students be given ample hands-on experience, projects, and tasks to develop core as well as soft skills. The OBE is well fitted to be tooled and used as a driver of entrepreneurial development in Nigerian tertiary institutions.

4.0 THE EDO STATE UNIVERSITY EXAMPLE.

At Edo State University, there is a highly functional entrepreneurship department. Entrepreneurship courses are imbued into the curriculum from the first year to the final year and are compulsory for all students. Furthermore, there is an annual business plan competition for final-year students and successful contestants are awarded business grants worth five million nairas (₦5 000 000) to support the execution of the best business plans.

Also, the students are exposed at the lower levels to various handcrafts to enhance the establishment of small and medium scale enterprises by students. For engineering students at the higher levels, the entrepreneurship course is taught by seasoned engineers with entrepreneurial exposure. Students are provided with the necessary guidance and mentoring to enable them to translate their business ideas into viable business solutions.

4.1 The Entrepreneurship Curriculum at Edo State University

The entrepreneurship curriculum at Edo State University is made up of three (3) courses spread over six semesters from the second year. One course per semester. The courses are; Introduction to entrepreneurial studies I & II, Entrepreneurial skills I & II, and Entrepreneurial development I & II.

4.1.1 Introduction to entrepreneurial studies I & II

The courses introduce students to the definitions, functions, types, and characteristics of entrepreneurship, entrepreneurship, and ethics, entrepreneurship theories, and practice. These courses further expose students to new venture creation; forms of business, business opportunities, starting a new business, innovation, legal issues in business, insurance, and environmental considerations, introduction to biographies of successful entrepreneurs, etc. (Edo State University, 2021).

4.1.2 Entrepreneurial skills I & II

These courses which are typically offered in the third year of studies at EDSU, train and equip students with practical skills and crafts for business creation. Students are required to select two categories/business areas in which they will be trained. The business areas on offer include; Agriculture/agro-allied businesses, Manufacturing, Information Communication Technology (ICT) amongst many others. The students are trained with abundant hands-on experience on how to make different products or render different services in their selected business areas. They are also further exposed to the business prospects and dynamics in their chosen business areas.

4.1.3 Entrepreneurial Development I & II

These courses are the final set of courses in the entrepreneurship training at EDSU. Students are exposed to the entrepreneurial process of writing feasibility studies and business plans. The students are required to form cooperative societies to collaboratively generate business ideas and funds. Course modules include; models of wealth creation, sustainability strategies, financial/ investment intelligence, and international business. The program involves Recognition, Rewards, and Awards (RRAs) and Mentorship. The training ends with the annual business plan competition in which the winners receive five million naira (₦5 000 000) worth of business grants.

5.0 CONCLUSION

The paper has examined the role of tertiary institutions in curbing unemployment through fostering entrepreneurship amongst engineering graduates. It is concluded that even though the task ahead of the tertiary institution is enormous, the tertiary institutions have what it takes to achieve much greater results in the successful undertaking of entrepreneurship amongst engineering graduates.

It is posited that the recommendations and ideas presented in this paper will serve to help tertiary institutions to achieve this uphill task. All stakeholders involved including government agencies, industry, NGOs, academia, and even the students themselves must all synergize in working to foster entrepreneurial exploits amongst engineering graduates

6.0 REFERENCES

Aluyor, E. O., Otoikhian, S. K. and Agbodekhe, B. P. (2019) 'A Chemical Engineering Curriculum-Meeting The Nigerian Need', Journal of the

Nigerian Society of Chemical Engineers, 34(1), pp. 77–92.

Bakhshi, H. et al. (2017) The future of skills: employment in 2030. United Kingdom: Pearson. https://scholar.google.com/scholar?q=Bakhshi,+H.+et+al.+(2017)+The+future+of+skills:+employment+in+2030.+United+Kingdom:+Pearson.&hl=en&as_sdt=0&as_vis=1&oi=scholart

Chikumba, S. (2011) 'Development Of Soft Engineering Skills For Industrial Engineering Technologists Through Effective Mentoring http://www.waceinc.org/philly2011/conference_proceedings/Refereed Papers/South Africa/STEADY

Choudary, D. V. (2014) 'The Importance Of Training Engineering Students In Soft-Skills': https://www.researchgate.net/publication/293313936. p. 5.

Dean, R. and Rubrica, B. (2018). An Action Research On Project-Based Learning And Understanding By Design And Their Effects On The Science Achievement And Attitude Of Science Students. [Online] Available At: Https://Files.Eric.Ed.Gov/Fulltext/Ed585254.Pdf.

Fulgence, K (2021). Employability Of Higher Education Institutions Graduates: Exploring The Influence Of Entrepreneurship Education And Employability Skills Development Program Activities In Tanzania. Afribary. Retrieved from https://afribary.com/works/employability-of-higher-education-institutions-graduates-exploring-the-influence-of-entrepreneurship-education-and-employability-skills-development-program-activities-in-tanzania

Harmer, N. (2014): Choice may not necessarily be a good thing": student attitudes to autonomy in interdisciplinary project-based learning in GEES disciplines https://www.tandfonline.com/doi/abs/10.1080/03098265.2016.1174817

Innocent, N. and Ignatius, O. (2012) 'The Relevance Of Engineering Entrepreneurship In The Growth Of The Nigerian Economy': https://www.researchgate.net/publication/330570307 p. 9.

Karim, M.S.A. (2016). Entrepreneurship Education in an Engineering Curriculum. Procedia Economics and Finance, [online] 35, pp.379–387. Available at: https://www.sciencedirect.com/science/article/pii/S2212567116000472.

Lowden, K. et al. (2011) Employers' perceptions of the employability skills of new graduates: research commissioned by the Edge Foundation. London: Edge Foundation.

Ministry of Education Malaysia, 2015. Malaysia Education Blueprint 2015-2025 (Higher Education). Putrajaya, Malaysia.

Metu, A. G. and Nwokoye, E. (2014) 'Entrepreneurship Development in Nigeria: Prospects and Challenges', SSRN Electronic Journal. DOI: 10.2139/ssrn.2622222.

Nnanna, I. and Opara, I. (2012). The Relevance Of Engineering Entrepreneurship In The Growth Of The Nigerian Economy. In: Nigerian Institiute of Industrial Engineers. [online] Nigerian Institiute of Industrial Engineers. Research gate. Available at: https://www.researchgate.net/publication/330570307 [Accessed 24 Jan. 2019].

Ofili, O. U. (2014) 'Challenges Facing Entrepreneurship in Nigeria', International Journal of Business and Management, 9(12), p. p258. DOI: 10.5539/ijbm.v9n12p258.

Okeke, M. I. and I, E. O. (2014) 'Challenges Facing Entrepreneurs in Nigeria', Singaporean Journal of Business, Economics and Management Studies, 3(5), pp. 18–34. DOI: 10.12816/0010956.

Oloyede, A. A., Ajimotokan, H. A. and Faruk, N. (2018) 'Embracing the future of engineering education in Nigeria: teaching and learning challenges', Nigerian Journal of Technology, 36(4), p. 991. DOI: 10.4314/njt.v36i4.1.

Pitan, O. and Adedeji, S. O. (2012) 'Skills Mismatch Among University Graduates in the Nigeria Labor Market', US-China Education Review A, 1, pp. 90–98.

Roberts, E.B. and Eesley, C.C. (2009). Entrepreneurial Impact: The Role of MIT. [online] Available at: http://entrepreneurship.mit.edu/article/entrepreneurial-impact-role-mit, [Accessed 14 Aug. 2011].

Rover, D.T. (2005). New Economy, New Engineer. Journal of Engineering Education, 94(4), pp.427–428.

JOURNAL OF THE NIGERIAN SOCIETY OF CHEMICAL ENGINEERS
INSTRUCTION TO AUTHORS

1. TYPES OF PUBLICATION

The Journal of the Nigerian Society of Chemical Engineers will publish articles on the original research on the science and technology of Chemical Engineering. Preference will be given to articles on new processes or innovative adaptation of existing processes. Critical reviews on current topics of Chemical Engineering are encouraged and may be solicited by the Editorial Board. The following types of articles will be considered for publication:

a. Full length **articles or review papers**.
b. **Communication** – a preliminary report on research findings.
c. **Note** – a short paper describing a research finding not sufficiently completed to warrant a full article.
d. **Letter to the Editor** – comments or remarks by readers and/or authors on previously published materials.

The authors are entirely responsible for the accuracy of data and statements. It is also the responsibility of authors to seek ethical clearance and written permission from persons or agencies concerned, whenever copyrighted material is used.

For now the journal is published twice in a year, March/April and September/October.

2. MANUSCRIPT REQUIREMENTS

a. The **Manuscript** should be written in clear and concise English and typed (single column) in Microsoft Word using double spacing on A4-size paper, Times New Romans font and 12 point. A full length article or review should not exceed 15 pages. Margin should be Normal (i.e. 2.54cm for Top, Bottom, Left & Right margins).
b. The **Manuscript** should be prepared in the following format: Abstract, Introduction, Materials and Methods, Results, Discussion, Conclusion, Acknowledgements, and References..
c. The **Manuscript** must contain the full names, address and emails of the authors. In the case of multiple authorship, the person to whom correspondence should be addressed must be indicated with functional email address. As an examples, authors' names should be in this format:
   Momoh, S. O., Adisa, A. A. and **Abubakar, A. S.**
   If the addresses of authors are different, use the following format:
   ***Momoh, S. O.[1], Adisa, A. A.[2]** and **Abubakar, A. S.[3]**
   Use star * to indicate the corresponding author.
d. **Symbols** should conform to America Standard Association. An abridged set of acceptable symbols is available in the fourth edition of Perry's Chemical Engineering Handbook. Greek letters, subscripts and superscripts should be carefully typed. A list of all symbols used in the paper should be included after the main text as **Nomenclature**.
e. All **Units** must be in the SI units (kg, m, s, N, etc).
f. The **Abstract** should be in English and should not be more than 200 words. The Abstract should state briefly the purpose of the research, methodology, results, major findings and major conclusions. Abstracts are not required for Communications, Notes or Letters.
g. **Citation** must be in the Harvard Format i.e. (Author, Date). Examples are (Smith, 1990) or (Jones et al, 2011). (Kemp, 2000) demonstrated that …..; (Mbuk, 1985; Boma, 1999; Sani, 2000) if more than two authors. (Telma, 2001a), (Telma, 2001b); etc if the citation have the same author and year of publication.
   For more information on Harvard Referencing: Guide visit **http://www.citethisforme.com/harvard-referencing**
h. **References** must also be in the Harvard Format i.e. (Author, Date, Title, Publication Information). References are listed in alphabetical order. Examples are shown below:
   Haghi, A. K. and Ghanadzadeh, H. (2005). A Study of Thermal Drying Process. *Indian Journal of Chemical Technology*, Vol. 12, November 2005, pp. 654-663
   Kemp, I.C., Fyhr, C. B., Laurent, S., Roques, M. A., Groenewold, C. E., Tsotsas, E., Sereno, A. A., Bonazzi, C. B., Bimbernet, J. J. and Kind M.(2001). Methods for Processing Experimental Drying Kinetic Data. *Drying Technology*, 19: 15-34.
i. **Tables** should contain a minimum of descriptive materials. Tables should be numbered serially throughout the manuscript in Arabic numerals (1, 2, 3, etc), and should be placed at the referenced point with captions (centralised) placed at the top of the table.
j. **Figures**, charts, graphs and all illustrations should be placed at the referenced point, numbered serially throughout the manuscript in Arabic numerals (1, 2, 3, etc) and incorporated in the text. Caption for Figures should be placed at the bottom of the Figure (centralised). Lettering set or symbols should be used for all labels on the figures, graphs, charts, photographs even when drawn in colours. (Note that figures drawn in colours may be unreadable if printed in black and white).
k. **Equations** should be typed using MS Word Equation Editor and should be centred and number serially

throughout the manuscript (in Arabic numeral) at the right margin.

l. Wherever possible, **Fractions** should be shown using the oblique slash. E.g. x/y
m. **Footnotes** should not be incorporated in the text.
n. **Acknowledgements** should appear at the end of the paper, before the list of references.

3. SUBMISSION OF MANUSCRIPTS

Manuscripts should be submitted by sending a Microsoft Word document (taking into account the Manuscript Requirements described in section 2 above) to the following email address: nschejournal@yahoo.com and copy stevmomoh@yahoo.com**.**
All correspondences are directed to the Editor-in-Chief using the submission emails addresses: nschejournal@yahoo.com and copy stevmomoh@yahoo.com. Meanwhile the online submission of articles on the journal website will soon be ready.

Authors should note that:

a. All authors listed in the manuscript have significantly contributed to the research.
b. All authors are obliged to provide retractions or corrections of mistakes.
c. All references cited are listed and financial support acknowledged.
d. It is forbidden to publish same research in more than one journal.

The fee charged for paper review and publication will be borne by the authors as follows:

a. Manuscript Review charges = N6,500 payable by both Members and Non-Member. Overseas is $30.00.
b. Publication Charges = N10,000 payable by Non-Members and Members who are not financially up-to-date. Overseas is $40.00.
c. Members would only get one (1) Journal free and buy the other if they so wish.
d. Corresponding Author whose paper is published on a particular edition would get one (1) free copy on behalf of all the co-authors. Other co-authors will buy if they so wish.

All fees are paid after the paper had been accepted for publication. These charges may be reviewed from time to time by the Governing Board of Directors of the Society.

4. ACCEPTED PAPERS

On acceptance, authors will be required to submit a copy of their manuscripts using Microsoft Word by emails to nschejournal@yahoo.com and copy stevmomoh@yahoo.com.

The following additional information should be observed for accepted papers: (i) Typed in Microsoft Word using 1.15 spacing on A4-size paper, Times New Romans font and 10 point; (ii) Margin should be 2.54cm for Top & Bottom; 2.20cm for Left & Right margins; (iii) The abstract should be one column document while the body of the manuscript should be double columns with 0.5cm gutter spacing except some tables and figures that may have to go in for one column document.

5. PUBLICATION

Full NSChE Journal edition in hard copy will be published twice annually – March/April Edition and September/October Edition.

6. REPRINT

Reprints are available on request at a moderate fee per page. Orders must be placed before the paper appears in Print.

7. READER'S INFORMATION

The papers are wholly the view of their author(s) and therefore the publisher and the editors bear no responsibility for such views.

8. SUBSCRIPTION INFORMATION

The subscription price per volume is as follows:

a. Individual Reader - N3,000.00
b. Institutions, Libraries, etc.- N5,000.00
c. Overseas Subscription - $100.00

Request for information or subscription should be sent to the Editor-in-Chief through the following emails addresses: nschejournal@yahoo.com and copy stevmomoh@yahoo.com.

9. COPYRIGHT NOTICE

By submitting your manuscript to the Journal, you have agreed that the copyright of the published material belongs to the journal.

10. PRIVACY STATEMENT

The names and email addresses entered in this journal site will be used exclusively for the stated purposes of this journal and will not be made available for any other purpose or to any other party.

.